



The hierarchy of incompressible fractional quantum Hall states

John J. Quinn^{a,*}, Arkadiusz Wójs^{b,a}, Kyung-So Yi^c, George Simion^a

^a Department of Physics and Astronomy, University of Tennessee, Knoxville, TN 37996, USA

^b Wrocław University of Technology, 50-370 Wrocław, Poland

^c Department of Physics, Pusan National University, Busan 609-735, Republic of Korea

ARTICLE INFO

Article history:

Accepted 5 June 2009

Available online 23 July 2009

editor: D.L. Mills

PACS:

71.10.Pm

73.43.-f

78.55.Bq

ABSTRACT

The correlations that give rise to incompressible quantum liquid (IQL) states in fractional quantum Hall systems are determined by the pseudopotential $V(\mathcal{R})$ describing the interaction of a pair of Fermions in a degenerate Landau level (LL) as a function of relative pair angular momentum \mathcal{R} . $V(\mathcal{R})$ is known for a number of different Fermion systems, e.g. electrons in the lowest Landau level (LL0) or the first excited Landau level (LL1), and for quasiparticles of Laughlin–Jain IQL states. Laughlin correlations, the avoidance of pair states with the smallest values of \mathcal{R} , occur only when $V(\mathcal{R})$ satisfies certain conditions. We show that Jain’s composite Fermion (CF) picture is valid only if the conditions necessary for Laughlin correlations are satisfied, and we present a rigorous justification of the CF picture without the need of introducing an “irrelevant” mean-field energy scale. Electrons in LL1 and quasielectrons in IQL states (e.g. QEs in CF LL1) do not necessarily support Laughlin correlations. Numerical diagonalization studies for small systems of Fermions (electrons in LL0 or in LL1, and QEs in CF LL1), with the use of appropriate pseudopotentials $V(\mathcal{R})$, show clear evidence for different types of correlations. The relation between LL degeneracy $g = 2\ell + 1$ and number of Fermions N at which IQL states are found is known for a limited range of N values. However, no simple intuitive models that we have tried satisfactorily describe all of the systems we have studied. Successes and shortcomings of some simple models are discussed, and suggestions for further investigation are made.

© 2009 Elsevier B.V. All rights reserved.

Contents

1. Introduction.....	30
2. Integral quantum Hall effect	31
3. Fractional quantum Hall effect	32
4. Numerical diagonalization	33
5. Chern–Simons gauge field and Jain’s composite Fermion picture.....	34
6. Beyond mean field	36
7. Adiabatic addition of CS flux	36
8. The composite Fermion hierarchy	37
9. Residual interactions	39
10. Pair angular momentum theorem and coefficients of fractional parentage.....	40
11. Harmonic pseudopotential and absence of correlations	41
12. The simplest anharmonicity and Laughlin correlations	41
13. Incompressible quantum liquids in the first excited Landau level.....	42

* Corresponding author. Tel.: +1 8659744089; fax: +1 8659747843.

E-mail address: jjquinn@utk.edu (J.J. Quinn).

13.1.	The $\nu = 5/2$ incompressible quantum liquid.....	42
13.2.	Heuristic picture of the $\nu = 5/2$ state.....	43
13.3.	Excitations of $\nu = 5/2$ state.....	44
13.4.	Other incompressible quantum liquid states in the first excited Landau level.....	44
13.5.	Other elementary excitations of IQLs of $\nu = 5/2$ IQL.....	46
13.6.	Generalized CF picture.....	47
14.	Model pseudopotentials and clusters of j particles.....	48
14.1.	Energy of clusters of j particles.....	48
14.2.	Model pseudopotentials.....	49
14.3.	Model three-body pseudopotential.....	49
15.	Spin polarized quasiparticles in a partially filled composite Fermion shell.....	50
15.1.	Heuristic picture.....	50
15.2.	Numerical studies of spin polarized QP states.....	52
15.3.	Numerical spectra.....	53
15.4.	Results from model interactions.....	56
15.5.	Unresolved questions.....	58
16.	Partially spin polarized systems.....	58
16.1.	Introduction and model.....	58
16.2.	Integral filling.....	59
16.3.	Fractional filling.....	59
16.4.	Spin-reversed quasielectrons.....	60
17.	Spin polarization transition of the $\nu = 4/11$ state.....	63
17.1.	Possible incompressible quantum liquid states.....	63
17.2.	Quasielectron energies.....	63
17.3.	Quasiparticle interactions and correlation energy.....	63
17.4.	Spin phase diagram for $\nu = 4/11$	65
18.	Electron system containing valence band holes.....	66
18.1.	Hidden symmetry and multiplicative states.....	66
18.2.	Numerical diagonalization.....	67
18.2.1.	Numerical results.....	67
18.2.2.	Binding energies.....	68
18.2.3.	Pseudopotentials $V_{AB}(L')$ of charged Fermions.....	68
18.3.	Generalized composite Fermion picture.....	69
18.4.	Low lying bands of N_e electron – N_h hole systems.....	69
18.4.1.	Condensed states of charged excitons.....	69
18.4.2.	Other charge configurations.....	70
18.5.	Spectra of N_e electron–single hole system.....	70
19.	Photoluminescence.....	72
19.1.	General considerations.....	72
19.2.	Singlet and triplet charged excitons: photoluminescence for dilute ($\nu \ll 1$) systems.....	72
19.3.	X^- in an incompressible quantum liquid of electrons: fractionally charged quasiexcitons.....	74
20.	Summary and conclusions.....	78
	Acknowledgments.....	79
	References.....	79

1. Introduction

Solid state theory has developed from the realization (Sommerfeld, 1928) that simple metals could be described in terms of free electrons that obeyed the Pauli exclusion principle (Pauli, 1925). Very early work on the effect of the periodic potential of the solid on the single-electron eigenstates (Bloch, 1928) led to the concept of energy bands and bandgaps (Wigner and Seitz, 1933), and to an understanding of why some solids were metals while others were insulators, semiconductors or semimetals (Wilson, 1931). The early decades of solid state physics were dominated by this “single-particle” description of electronic states.

In the middle of the last century scientists began to worry about why this single-particle picture worked so well, since the interaction between particles was not so small. Landau (1956, 1957) proposed the Fermi liquid theory to describe the effect of short range many-body interaction in liquid He³. The concept of quasiparticles (QPs), elementary excitations that satisfied Fermi–Dirac statistics and included a “self-energy” (due to interaction with the ground state) and a weak interaction with one another, became a critical new concept in solid state theory. Silin (1957) made use of Landau’s idea to study the properties of a “metallic” electron liquid with long range Coulomb interactions. In microscopic studies of the electron liquid many-electron interactions were treated via diagrammatic perturbation theory. The starting point, however, was still the single-electron eigenstates and the Fermi distribution function.

The BCS theory of superconductivity (Bardeen et al., 1957) demonstrates that perturbation theory was not always adequate, even when interactions were weak. However, even in BCS theory the noninteracting electron states served as the starting point for introduction of novel correlation effects via a generalized mean-field approximation.

During the past two decades novel systems have been discovered in which many-body interactions appear to dominate over single-particle energies. Transition metal oxides displaying a metal–insulator transition, magnetic phase transitions and high temperature superconductivity are one technologically important class of such “strongly interacting systems”. When interactions dominate, the standard technique of treating them as a perturbation on the single-particle spectrum is usually not adequate.

The paradigm for such systems is the fractional quantum Hall (FQH) system. At very high values of the applied magnetic field the massively degenerate single-particle Landau levels (LLs) disappear from the problem. The low energy spectrum is determined by a single energy scale e^2/λ , where $\lambda = (\hbar c/eB)^{1/2}$ is the magnetic length. The incompressible quantum liquid (IQL) states discovered by Tsui et al. (1982) result from the interaction alone.

In this paper we present a review of the families of FQH states observed experimentally and of how we understand them. Although a lot of theoretical methods have been developed, we would limit ourselves to those that are critical to our explanations, leaving out for example some work rooted in field theories (Balatsky and Fradkin, 1991; Fradkin and Schaposnik, 1991; Lopez and Fradkin, 1991, 1992, 1993, 1995) and the Hamiltonian method (Murthy and Shankar, 1999, 2002, 2003; Shankar and Murthy, 1997). Laughlin’s remarkable insight (Laughlin, 1983) into the nature of correlations giving rise to an IQL state and the fractionally charged excitations, quasielectrons (QEs) and quasiholes (QHs), are discussed. We consider Haldane’s idea (Haldane, 1983) that a hierarchy of IQL daughter states can be attributed to the fact that putting fractionally charged QPs into a QP Landau level is essentially the same problem as that of putting the original electrons in an electron Landau level. We review Jain’s remarkable composite Fermion (CF) picture (Jain, 1989). It predicts not only the filling factor ν at which the most prominent IQL states are observed, but the structure of the lowest band of energy states for any value of the applied magnetic field B . We emphasize the conditions under which the CF picture is valid and discuss why it’s valid. We give examples in which the CF picture is not valid. We suggest that a useful approach to many-Fermion systems dominated by the interaction between pairs is to study the antisymmetric eigenstates of a single pair and to use them to construct an appropriate product over all pairs. For the simplest case, this is exactly the Laughlin wavefunction, a better starting point for a many-Fermion system than a Slater determinant of single-particle wavefunctions. We propose novel correlations, different from Laughlin’s, when the pair interactions are different from the Coulomb interaction in the lowest Landau level (LL0).

Our objective is to give a deeper intuitive understanding of all FQH states in the hope that it may suggest novel ways to treat correlations in other strongly interacting systems.

2. Integral quantum Hall effect

The integral quantum Hall (IQH) effect was discovered by von Klitzing et al. (1980) who investigated the magnetotransport properties of a quasi-two-dimensional (2D) electron gas in a silicon surface inversion layer.

The Hamiltonian describing the motion of a single electron confined to the x - y plane in the presence of a dc magnetic field $\vec{B} = B\hat{z}$ is simply $H = (2\mu)^{-1}[\vec{p} + (e/c)\vec{A}(\vec{r})]^2$. The vector potential $\vec{A}(\vec{r})$ in the *symmetric* gauge is given by $\vec{A}(\vec{r}) = (1/2)B(-y\hat{x} + x\hat{y})$. We use \hat{x} , \hat{y} , and \hat{z} as unit vectors along the Cartesian axes. The Schrödinger equation $(H - E)\Psi(\vec{r}) = 0$ (Landau and Lifshitz, 1977) has eigenstates:

$$\Psi_{nm}(r, \phi) = e^{im\phi} u_{nm}(r) \quad (1)$$

$$E_{nm} = \frac{1}{2} \hbar \omega_c (2n + 1 + m + |m|). \quad (2)$$

The radial wavefunction $u_{nm}(r)$ can be written as

$$u_{nm}(r) = x^{|m|} \exp\left[-\frac{x^2}{2}\right] L_n^{|m|}(x^2), \quad (3)$$

where $x^2 = 1/2(r/\lambda)^2$, and $L_n^{|m|}$ is an associated Laguerre polynomial. $L_0^{|m|}$ is independent of x , and $L_1^{|m|}$ is proportional to $(|m| + 1 - x^2)$. From Eq. (2) it is apparent that the spectrum of single-particle energies consists of highly degenerate levels; the lowest LL has $n = 0$ and $m = 0, -1, -2, \dots$, and its wavefunction can be written $\Psi_{0m} = z^{|m|} \exp[-|z|^2/4\lambda^2]$, where z stands for $re^{-i\phi}$. For a finite-size sample of area \mathcal{A} , the number of single-particle states in the lowest LL is given by $N_\phi = B\mathcal{A}/\phi_0$, where $\phi_0 = hc/e$ is the quantum of flux. The filling factor ν is defined as N/N_ϕ , so that ν^{-1} is simply equal to the number of flux quanta of the magnetic field per electron.

When ν is equal to an integer, there is an energy gap (equal to $\hbar\omega_c$) between the filled states and the empty states. This makes the noninteracting electron system incompressible, because an infinitesimal decrease in the area \mathcal{A} can be accomplished only at the expense of promoting an electron across the energy gap and into the first unoccupied LL. This incompressibility is responsible for the integral quantum Hall effect (von Klitzing, 1986).

In Fig. 1 we display typical results for V_x , the voltage along the channel, and V_H , the Hall voltage. The former contains zeros at the integral values of the filling factor ν caused by the energy gap between the filled and empty LLs. Both localized and extended states occur in the LLs. When the chemical potential ζ resides in the localized states σ_{xx} vanishes (at $T = 0$), and since localized states make no contribution, the Hall conductivity σ_{xy} remains constant as ζ moves through the localized

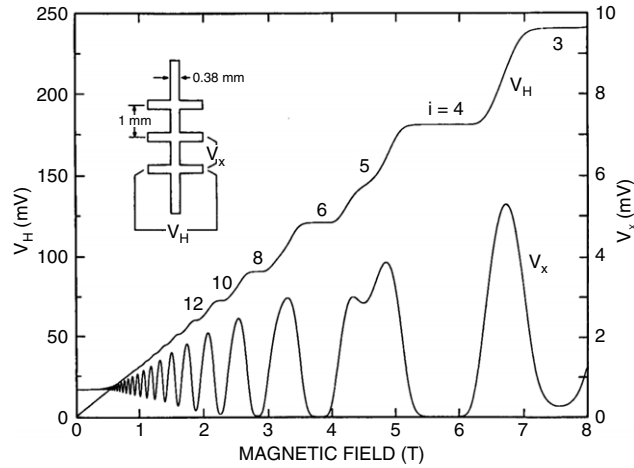


Fig. 1. V_H and V_x vs. B for a GaAs–AlGaAs heterostructure cooled to 1.2 K. The source–drain current $25.5 \mu\text{A}$ and $n = 5.6 \times 10^{11}$ electrons/ cm^2 (Cage, 1987; Cage et al., 1985).

states. The integral value of σ_{xy} in units of e^2/h is expected when ν is precisely equal to an integer. The Hall plateaus depend on the spectrum of the localized states which is related to the mobility of the sample.

3. Fractional quantum Hall effect

The observation of an incompressible quantum Hall liquid state in a fractionally filled 2D Landau level by Tsui et al. (1982) was quite unexpected. The behavior of ρ_{xx} and ρ_{xy} as a function of filling factor ν is displayed for a typical early measurement in Fig. 2. There are clear zeroes of ρ_{xx} at $\nu = 1/3$ and $2/3$ and corresponding plateaus in ρ_{xy} . At other fractions there are observable minima in ρ_{xx} and changes in slope in ρ_{xy} . The trace looks like a continuation of Fig. 1 to higher magnetic field or lower filling factor. Later, with significant improvement of the quality of the sample, other filling fractions have been observed in both lowest Landau level (Pan et al., 2003), and higher LL (Choi et al., 2008; Pan et al., 1999; Xia et al., 2004; Willett et al., 1987). Unlike the IQH effect, the FQH effect cannot be understood in terms of the single-particle spectrum. Coulomb correlations among electrons in the partially filled LL of degenerate single-particle states must be responsible for the incompressibility (and the energy gap associated with it). Clearly, this is a novel many-body state.

Laughlin (1983) correctly surmised that the FQH states observed at filling factors $\nu = m^{-1}$, with m being an odd integer, resulted when the electrons were able to avoid pair states with relative angular momentum smaller than m . These avoided pair states have the smallest pair separation and the largest Coulomb repulsion. Laughlin proposed a many-body wavefunction for the IQL state at filling factor $\nu = m^{-1}$ given by

$$\Psi_m(1, 2, \dots, N) = \prod_{i < j} z_{ij}^m \exp \left[-\frac{\sum_k |z_k|^2}{4\lambda^2} \right]. \quad (4)$$

Here $z_i = r_i e^{-i\phi_i}$ is a complex coordinate for the position of the i th electron, λ is the magnetic length and $z_{ij} = z_i - z_j$. Clearly, in going from the filled $\nu = 1$ state to the $\nu = 1/3$ state, the Laughlin wavefunction has introduced two additional zeroes as a function of pair separation $|z_{ij}|$. The relative pair angular momentum is simply m , the z -component of the relative angular momentum of particles i and j . Laughlin also showed that the elementary excitations of the IQL state could be described as fractionally charged QEs and QHs. Both localized and extended states of the quasiparticles were required to understand the observed behavior of ρ_{xx} and ρ_{xy} .

The first explanation of FQH states at values of $\nu = n(1 + 2p)^{-1}$ with $n > 1$ was given by Haldane (1983). He assumed that the dominant interaction between quasiparticles was the short range repulsive part of the pair interaction. Based on this assumption Haldane suggested that the problem of filling the degenerate states of the QP LL with N_{QP} Laughlin quasiparticles was similar to that of filling the original N_ϕ states of the electron LL with N electrons. Because the number of QP states could not exceed N , Haldane suggested the N took place of N_ϕ and N_{QP} the place of N in Laughlin's condition $N_\phi = (2p + 1)N$ for an IQL state. He proposed $N = 2pN_{QP}$ as the condition for new IQL states of the QPs. The even integer $2p$ was chosen because, according to Haldane, the QPs were Bosons. This ‘‘Haldane hierarchy’’ of IQL states contained all odd denominator fractions. Slightly different versions of Haldane's hierarchy were independently suggested by Laughlin (1984) and by Halperin (1984, 1983). The different versions differ in the definition of the relative angular momentum of QPs, resulting in different assignment of QP statistics. All of the versions depended on the residual interactions between QPs (which were not well-known) being sufficiently similar to the Coulomb interactions between electrons in LL0.

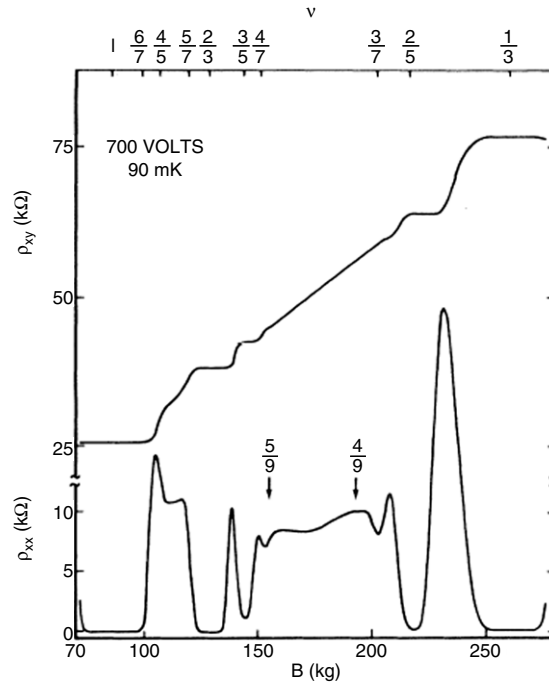


Fig. 2. ρ_{xx} and ρ_{xy} at 90 mK, for a sample which shows the fractional quantum Hall effect at $\nu = 1/3, 2/3, 2/5, 3/5, 3/7, 4/7, 4/9,$ and $5/9$ (Chang et al., 1984).

4. Numerical diagonalization

Confirmation of Laughlin's explanation of the correlations giving rise to FQH states at $\nu = 1/3, 1/5, \dots$ can be found through numerical diagonalization of the Coulomb interaction within the subspace of the lowest LL. Higher LLs play almost no role in the low energy spectrum if the cyclotron energy $\hbar\omega_c$ is much larger than the Coulomb energy e^2/λ . Exact numerical diagonalization is limited to small systems, but it must give qualitatively correct results as long as the correlation length is much smaller than the radius of the system. Restricting the area of the sample can be done in different ways, but probably the most useful is to make the 2D surface on which the electrons reside a sphere of radius R (Haldane, 1983; Haldane and Rezayi, 1985b). In this geometry a magnetic monopole of strength $2Q\phi_0$ (where $2Q$ is an integer) at the center of a sphere gives a radial magnetic field $B = 2Q\phi_0/4\pi R^2$. Boundary conditions are avoided and the rotational invariance replaces the translational invariance of an infinite plane.

The single-particle eigenstates (called monopole harmonics (Wu and Yang, 1976, 1977)) are denoted by $|Q, \ell, m\rangle$, where the angular momentum l and its z -component m must satisfy $|m| \leq l$. The single-particle eigenvalues are given by $E_l = (\hbar\omega_c/2Q)[\ell(\ell+1) - Q^2]$. Since E_l cannot be negative, the minimum allowed value of ℓ must be Q . We can write $\ell = Q + n$, with $n = 0, 1, \dots$ playing the role of LL index. For $\nu < 1$ only the lowest LL (with $\ell = Q$) is relevant at high magnetic fields. We can write N electron basis states as: $|m_1, m_2, \dots, m_N\rangle = c_{m_N}^\dagger \dots c_{m_2}^\dagger c_{m_1}^\dagger |vac\rangle$, where $|vac\rangle$ is the vacuum state and c_m^\dagger creates an electron in state $|Q, \ell, m\rangle$ with $\ell = Q$. Of course the allowed values of m must satisfy $|m| \leq \ell$. Although the two-body matrix elements of the Coulomb interaction $\langle m_1, m_2 | V | m_3, m_4 \rangle$ have a simple form in the lowest Landau level (Fano et al., 1986), the number of N -electron states $[N_\phi! / N!(N_\phi - N)!]$ grows rapidly with the system size. In the lowest LL where $\ell = Q$ the N -electron states can be written $|L, L_z, \alpha\rangle$ with L and L_z being the total angular momentum and its z component, and α is an index that distinguishes different multiplets with the same value of L . Because the Coulomb interaction Hamiltonian $H = \sum_{i < j} V(|\vec{r}_i - \vec{r}_j|)$ is spherically symmetric, the Wigner-Eckart theorem tells us that $\langle L', L'_z, \alpha' | H | L, L_z, \alpha \rangle = \delta(L', L)\delta(L'_z, L_z)V_{\alpha\alpha'}(L)$, and the reduced matrix element $V_{\alpha\alpha'}$ is independent of L_z . This fact can be used to reduce the size of matrices to be diagonalized (Quinn et al., 2004b; Wójs and Quinn, 1998a).

It is probably worth noting that on a plane (Wójs and Quinn, 1998a) the allowed values of m , the z -component of the single-particle angular momentum, are $0, 1, \dots, N_\phi - 1$. $M = \sum_i m_i$ is the total z -component of the angular momentum (the sum is over occupied states). It can be divided into $M_{CM} + M_R$, the center of mass and relative contributions. The connection between the planar and spherical geometries is $M = N\ell + L_z$, $M_R = N\ell - L$, and $M_{CM} = L + L_z$. The interactions depend only on M_R so $|M_R, M_{CM}\rangle$ acts just like $|L, L_z\rangle$. The absence of boundary conditions and the complete rotational symmetry make the spherical geometry attractive to theorists. Many experimentalists prefer using the $|M_R, M_{CM}\rangle$ states of the planar geometry.

Some exact diagonalization results (E vs. L) for the ten electron system are shown in Fig. 3. The Laughlin $L = 0$ incompressible ground state occurs at $2Q = 3(N - 1)$ for the $\nu = 1/3$ state. States with larger values of Q contain one or two

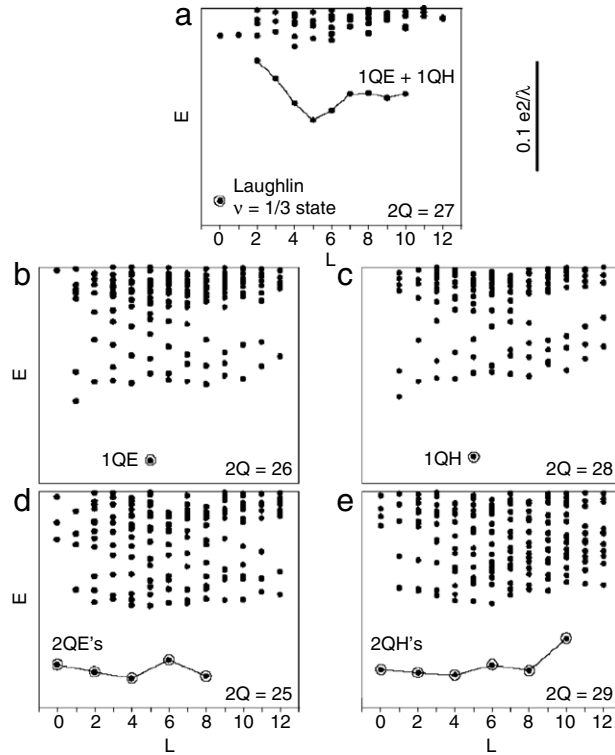


Fig. 3. The spectra of 10 electrons in the lowest Landau level calculated on a Haldane sphere with $2Q$ between 25 and 29. The open circles and solid lines mark the lowest energy bands with the fewest composite Fermion quasiparticles (Quinn and Wójs, 2000a).

QHs ($2Q = 28, 29$), and states with smaller values of Q contain QEs in the ground states (Quinn and Quinn, 2006; Quinn and Wójs, 2000a; Quinn et al., 2004b).

The energy of the multiplet $|\mathcal{L}\alpha\rangle$ can be expressed as

$$E_{\alpha}(L) = \binom{N}{2} \sum_{L'} P_{\mathcal{L}\alpha}(L') V(L'), \quad (5)$$

where $P_{\mathcal{L}\alpha}(L')$ is the probability that $|\mathcal{L}\alpha\rangle$ contains pairs with pair angular momentum L' , and $V(L')$ is the energy of interaction of a pair with angular momentum $L' = 2\ell - \mathcal{R}$. Here $\mathcal{R} = 1, 3, 5, \dots$ is referred to as the relative pair angular momentum. We will sometimes use the notation $V(\mathcal{R})$, understanding this to mean $V(2\ell - \mathcal{R})$ i.e. the function $V(L')$ with L' expressed as $2\ell - \mathcal{R}$.

It is straightforward to evaluate the pseudopotential $V(\mathcal{R})$ describing the interaction of a pair of electrons in a shell of angular momentum l in the Haldane spherical geometry (Fano et al., 1986). It depends on the radius of the sphere $R = (Q)^{1/2}\lambda$ and on the Landau level index $n = \ell - Q = 0, 1, 2, \dots$. Simple results for $V^{(n)}(\mathcal{R})$ are given in Fig. 4.

5. Chern–Simons gauge field and Jain’s composite Fermion picture

Jain (1989) made the remarkable observation that the most prominent IQL states observed experimentally could be understood in terms of a simple composite Fermion (CF) picture. This picture made use of a Chern–Simons (CS) transformation (Wilczek, 1982a,b) and a CS gauge field familiar to field theorists. The CS transformation can be described as attaching to the j th electron ($1 \leq j \leq N$) a flux tube carrying a magnetic field $\vec{b} = \alpha\phi_0\delta(\vec{r} - \vec{r}_j)\hat{z}$. Here $\phi_0 = (hc)/e$ is the quantum of flux, α is a constant, and \hat{z} a unit vector normal to the 2D layer. It is well-known that when this CS flux is added via a gauge transformation, no change in the classical equations of motion results. Only the phase of the quantum mechanical wavefunction is changed. However, the CS transformation results in a much more complicated many-body Hamiltonian that includes a CS vector potential $\vec{a}(\vec{r})$ given by

$$\vec{a}(\vec{r}) = \alpha\phi_0 \int d^2r_1 \frac{\hat{z} \times (\vec{r} - \vec{r}_1)}{(\vec{r} - \vec{r}_1)^2} \psi^\dagger(\vec{r}_1)\psi(\vec{r}_1), \quad (6)$$

in addition to the vector potential $\vec{A}(\vec{r})$ of the dc magnetic field. Simplification results only when the mean-field (MF) approximation is made. This is accomplished by replacing the density operator $\psi^\dagger(\vec{r})\psi(\vec{r})$ in the CS vector potential and in

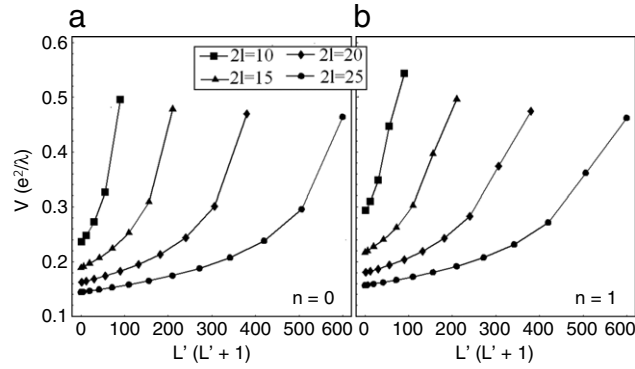


Fig. 4. Pseudopotential $V(L')$ of the Coulomb interaction in the lowest (a) and the first excited Landau level (b) as a function of squared pair angular momentum $L'(L'+1)$. Squares ($\ell = 5$), triangles ($\ell = 15/2$), diamonds ($\ell = 10$), and circles ($\ell = 25/2$) indicate data for different values of $Q = \ell + n$ (Quinn et al., 2004b).

Table 1

The effective CF monopole strength $2Q^*$, the number of CF quasiparticles (quasiholes n_{QH} and quasielectrons n_{QE}), the quasiparticle angular momenta and ℓ_{QH} , ℓ_{QE} and the angular momenta L of the lowest lying band of multiplets for a ten electron system at $2Q$ between 25 and 29.

$2Q$	29	28	27	26	25
$2Q^*$	11	10	9	8	7
n_{QH}	2	1	0	0	0
n_{QE}	0	0	0	1	2
ℓ_{QH}	5.5	5	4.5	4	3.5
ℓ_{QE}	6.5	6	5.5	5	4.5
L	10, 8, 6, 4, 2, 0	5	0	5	8, 6, 4, 2, 0

the Coulomb interaction by its MF value n_s , the uniform electron density. The resulting Hamiltonian is the sum of single-particle Hamiltonians in which an “effective” magnetic field $B^* = B - 2p\phi_0 n_s$ appears.

Jain introduced the idea of a CF to represent an electron with an attached flux tube which carried an even number α ($= 2p$) of flux quanta (Jain, 1990). In the MF approximation the CF filling factor ν^* is given by $\nu^* = \nu^{-1} - \alpha$, i.e. the number of flux quanta per electron of the dc field less the CS flux per electron. When ν^* is equal to an integer $n = \pm 1, \pm 2, \dots$, then $\nu = n(1 + \alpha n)^{-1}$ generates (for $\alpha=2$) quantum Hall states at $\nu = 1/3, 2/5, 3/7, \dots$, and $\nu = 1, 2/3, 3/5, \dots$. These are the most pronounced FQH states observed.

In the spherical geometry one can introduce an effective monopole strength seen by one CF (Chen and Quinn, 1994a). It is given by $2Q^* = 2Q - \alpha(N - 1)$ since the α flux quanta attached to every other CF must be subtracted from the original monopole strength $2Q$. Then $|Q^*| = \ell_0^*$ plays the role of the angular momentum of the lowest CF shell just as $Q = \ell_0$ is the angular momentum of the lowest electron shell. When $2Q$ is equal to an odd integer $(1 + \alpha)$ times $(N - 1)$, the CF shell ℓ_0^* is completely filled, and an $L = 0$ incompressible Laughlin state at filling factor $\nu = (1 + \alpha)^{-1}$ results. When $2|Q^*| + 1$ is smaller (larger) than N , QEs (QHs) appear in the shell $\ell_{QE} = \ell_0^* + 1$ ($\ell_{QH} = \ell_0^*$). The low energy sector of the energy spectrum consists of the states with the minimum number of QP excitations required by the value of $2Q^*$ and N . The first excited band of states will contain one additional QE–QH pair. The total angular momentum of these states in the lowest energy sector can be predicted by addition of the angular momenta (ℓ_{QH} or ℓ_{QE}) of the n_{QH} or n_{QE} quasiparticles treated as identical Fermions. In Table 1 we demonstrated how these allowed L values are found for a ten electron system with $2Q$ in the range $29 \geq 2Q \geq 25$. By comparing with numerical results presented in Fig. 3, we readily observe that the total angular momentum multiplets appearing in the lowest energy sector are always correctly predicted by this simple MF CS picture (Quinn and Quinn, 2006; Quinn and Wójs, 2000a; Quinn et al., 2004b).

For example, the Laughlin $L = 0$ ground state at $\nu = 1/3$ occurs when $2\ell_0^* = N - 1$, so that the N composite Fermions fill the lowest shell (with angular momentum ℓ_0^*). The CFQE and CFQH states occur at $2\ell_0^* = N - 1 \mp 1$ and have one too many (for QE) or one too few (for QH) particles to give integral filling. The single QPs have angular momentum $N/2$. The 2QE and 2QH states occur at $2\ell_0^* = N - 1 \mp 2$. They have $\ell_{QE} = (N - 1)/2$ and $\ell_{QH} = (N + 1)/2$. We expect, for example, $\ell_{QE} = 4.5$ and $\ell_{QH} = 5.5$ for a ten electron system, leading to low energy bands with $L = 0 \oplus 2 \oplus 4 \oplus 6 \oplus 8$ for 2 QEs and to $L = 0 \oplus 2 \oplus 4 \oplus 6 \oplus 8 \oplus 10$ for 2 QHs. In the MF picture, which neglects QP–QP interactions, these bands are degenerate. Of course, numerical results in Fig. 3 show that two QP states with different L have different energy. From this numerical data we obtain, up to an overall constant, V_{QP} the residual interaction of a QP pair as a function of the pair angular momentum L' (Quinn and Quinn, 2006; Quinn and Wójs, 2000a; Quinn et al., 2004b; Wójs and Quinn, 2000d).

In addition to the lowest energy band of multiplets, first excited bands which contain one additional QE–QH pair can be observed in Fig. 3. The “magnetoroton” band lying between the $L = 0$ Laughlin IQL ground state and a continuum of higher energy states can be observed in Fig. 3(a). This band contains one QH with $\ell_{QH} = 9/2$ and one QE with $\ell_{QE} = 11/2$. By adding the angular momenta of these distinguishable particles, a band with $1 = \ell_{QE} - \ell_{QH} \leq L \leq \ell_{QE} + \ell_{QH} = 10$ would

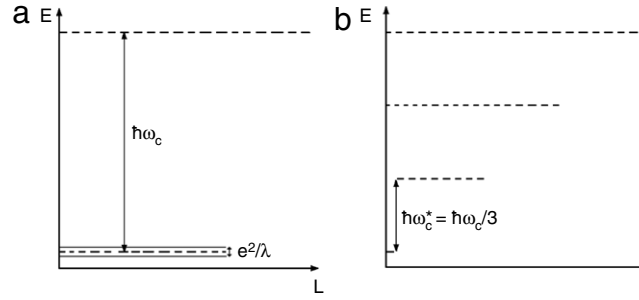


Fig. 5. Comparison of spectrum of N noninteracting electrons (a) with that of N noninteracting CFs (b), the electron Landau levels are separated by $\hbar\omega_c$; the CF levels $\hbar\omega_c^* = \nu\hbar\omega_c$. For $\hbar\omega_c \gg e^2/\lambda$, the Coulomb energy scale, the degenerate single-electron levels are split by the Coulomb energy. This splitting is much smaller than $\hbar\omega_c$ (or $\hbar\omega_c^*$). The higher electron LLs are not involved in determining the interacting spectrum, so $\hbar\omega_c$ and $\hbar\omega_c^*$, both proportional to B , are irrelevant.

be predicted. The state with $L = 1$ does not appear in Fig. 3(a) suggesting that QE–QH pairs with $L = 1$ are forbidden (or at least pushed into the higher energy continuum by interactions). Furthermore, the states in the band are not degenerate indicating residual interactions that depend on the angular momentum of the pair. Other bands that are not quite so clearly defined can be observed in other frames. For example, in frame (b) between the single QE state at $L = 5$ and the higher energy continuum, there is a 2QE–1QH band. The allowed L values can be estimated by taking $\ell_{QE} = 5$ and $\ell_{QH} = 4$ and adding angular momenta (treating the QEs as identical Fermions). Interactions cause the predicted multiplets to overlap the bottom of the continuum for $3 \leq L \leq 6$ but outside this range they are separate from it (Quinn and Quinn, 2006; Quinn et al., 2004b; Quinn and Wójs, 2000a).

6. Beyond mean field

Despite the satisfactory description of the allowed angular momentum multiplets, the magnitude of the MFCF energies is completely wrong. The magnetoroton energy does not occur at the effective cyclotron frequency $\hbar\omega_c^* = eB^*/mc$. This MF energy is irrelevant at large values of B (if we keep $m_{CF} = m_e$), so it is a puzzle why the CF picture does so well at predicting the structure of the energy spectrum. It is interesting to compare the energy spectrum of N noninteracting electrons with that of N noninteracting CFs as done in Fig. 5.

For large values of B the MF energy $\hbar\omega_c^*$ is much larger than the Coulomb scale e^2/λ . Therefore the low lying multiplets of interacting electrons will be contained in a band of width e^2/λ about the lowest electron LL. The noninteracting CF spectrum contains a number of bands separated by $\hbar\omega_c^*$. Interactions (Coulomb and CS gauge interactions) among fluctuations beyond the MF essentially have to restore the original noninteracting electron spectrum when $B \rightarrow \infty$. Halperin et al. (1993) and Lopez and Fradkin (1991, 1992, 1993) have used conventional many-body perturbation theory to treat fluctuations. However, there is no small parameter to guarantee convergence or to justify simple approximations like the random phase approximation (RPA). The standard many-body perturbation theory gives reasonable results probably because it can be thought of as a Silin–Landau theory (Landau, 1956; Silin, 1957) of an electron liquid. Long range correlations are handled by RPA; short range correlations by adding Landau Fermi liquid interactions (Simon and Halperin, 1993). What is clear is that the success of the CF picture does not result from a cancellation between CS gauge interactions and Coulomb interactions beyond MF.

Jain proposed a trial wavefunction which included a Jastrow factor $\prod_{i<j} z_{ij}^2$, and he projected it onto the lowest Landau level. He then diagonalized the Coulomb interaction using the projected trial function (Jain, 1990). Though the technique seems to give reasonably good results, it is not obvious why it works.

7. Adiabatic addition of CS flux

The CS magnetic field $\vec{b}(\vec{r}) = \alpha\phi_0 \sum_j \delta(\vec{r} - \vec{r}_j)\hat{z}$ is usually introduced via a gauge transformation. Then, it is a Bohm–Aharonov (Aharonov and Bohm, 1959) type field, having no effect on the classical equation of motion. The Lorentz force on the i th electron is given by $(-e/c)\vec{v}_i \times \vec{b}(\vec{r})$ with $\vec{r} = \vec{r}_i$. No electron senses its own CS flux, and since \vec{r}_i and \vec{r}_j cannot have the same value for a pair of Fermions, there is no effect from $\vec{b}(\vec{r})$ on the classical motion of the electrons. However, the CS flux does introduce a phase factor into the quantum mechanical wavefunction.

Let's define $\psi_m(\vec{r}) = \exp(im\phi)u_m(r)$ as the wavefunction for the relative coordinate $\vec{r} = \vec{r}_i - \vec{r}_j$ of pair electrons in the lowest LL. For Fermions m , the z -component of the relative angular momentum, must be odd so that under exchange ($\phi \rightarrow \phi + \pi$) the phase factor changes sign. If a CS flux $\phi = \alpha\phi_0$ is introduced on each electron via a gauge transformation, then $\psi_m \rightarrow \exp[i(m - \alpha)\phi]u_m(r)$. The phase factor is changed by $\exp(-i\alpha\pi)$ under exchange. If α is not an even integer this leads to the famous transmutation of statistics, since $\psi_m \rightarrow \exp(-i\alpha\pi)\psi_m$ under exchange (Leinaas and Myrheim, 1977; Wilczek, 1990).

A gauge transformation is not the only way by which CS flux can be introduced. We can start with some initial state of the relative coordinates of pair, e.g. one with $\alpha = 0$, and adiabatically increase the CS flux attached to each particle up to its final value. In this case ψ_m evolves adiabatically into $\exp(im\phi)u_{m+\alpha}(r)$. There is no change in phase (and therefore no change in statistics for any value of α). However, in the semiclassical orbit (described by a maximum in the density $\rho(r) = |\psi_m|^2$) $u_m(r)$ is replaced by $u_{m+\alpha}(r)$. The orbit size changes in such a way that the total flux (due to both the applied field B and the CS flux) is conserved. The change in orbit size results from the Faraday emf acting on the relative motion in the presence of a perpendicular magnetic field B . If the pair was initially in the smallest allowed pair orbit (with $m = -1$) and two CS flux quanta opposite to B were added ($\alpha = -2$), then the resulting new orbit will have $m = -3$. This is exactly what we mean by Laughlin correlations. The adiabatic addition of CS flux has altered the orbit to avoid the most repulsive pair state with $m = -1$. However, in the absence of Coulomb interactions all negative values of m belong to the lowest LL. No change in energy occurs without Coulomb repulsion. No MF approximation or MF energy scale is needed (Quinn and Quinn, 2003).

If we write the pair wavefunction as a product of center of mass (CM) and relative motion we find $\psi(\vec{r}_i, \vec{r}_j) = \exp(im\phi_{ij})u_m(r_{ij})u_0(R_{ij})$ can be written as $z_{ij}^{|m|} \exp[-(r_i^2 + r_j^2)/(4\lambda^2)]$. Here $z_i = r_i \exp(-i\phi_i)$ is the complex coordinate of the i th particle, and $\lambda^2 = \hbar c/eB = 2\lambda_{CM}^2 = \lambda_r^2/2$. For an N electron system the straightforward generalization of this pair function is the Laughlin wavefunction $\Phi_m(1, 2, \dots, N) = \prod_{i<j} z_{ij}^{|m|} \exp[-\sum_k r_k^2/(4\lambda^2)]$ where $|m|$ is an odd integer. Small values of $|m|$ correspond to small pair orbits, with $|m| = 1$ having the largest Coulomb repulsion. Adiabatic addition of CS flux to every electron forces each pair to be Laughlin correlated by avoiding pair orbits with $|m| = 1$. This is accomplished without the necessity of a MF approximation or the introduction of an MF energy scale.

From our previous discussion we know that we can form total angular momentum multiplets $|\ell^N; L\alpha\rangle$ by addition of the angular momenta $\hat{\ell}_i = \hat{\ell}$ ($i = 1, 2, \dots, N$) of N Fermions. In the absence of Coulomb repulsion, $E_\alpha(L)$ is the same for every value of L formed from N electrons, each with angular momentum ℓ in the lowest LL (with $\ell = Q$, the monopole strength in the Haldane spherical geometry). Let's define $G_{N\ell}(L)$ as the number of multiplets of total angular momentum L . If we adiabatically add two CS flux quanta to each electron, the N particle multiplets that can be formed belong to a subset $G_{N\ell}(L)$ with ℓ replaced by $\ell^* = \ell - (N - 1)$. The multiplets belonging to $G_{N\ell^*}(L)$ all avoid, to the maximum extent possible, pair states with $\mathcal{R} = 1$. This result is obviously true for a pair of Laughlin correlated electrons. The smallest allowed pair angular momentum would be $L' = 2\ell^* - 1 = 2\ell - 3$, completely avoiding $\mathcal{R} = 1$. In addition our numerical results, (Fig. 3), show that the allowed values of ℓ_{QE} and ℓ_{QH} [frames (b) and (c)] are $\ell_{QE} = \ell^* + 1 = 5$ and $\ell_{QH} = \ell^* = 5$. This was easily understood in terms of “effective monopole strength”, but the result does not depend on the MF approximation. From frame (e) it is clear that $L_{2QH} = 2\ell^* - j$ where j is an odd integer [and from (d) that $L_{2QE} = 2(\ell^* + 1) - j$]. Thus, the adiabatic addition of CS flux introduces Laughlin correlations (avoiding $\mathcal{R} = 1$) and selects (Benjamin et al., 2001; Quinn et al., 2001a) from $G_{N\ell}(L)$ the subset $G_{N\ell^*}(L)$ that avoids the smallest (and most repulsive) pair orbit with $\mathcal{R} = 1$. The proof that $G_{N\ell^*}(L)$ is a subset of $G_{N\ell}(L)$ has been given in Benjamin et al. (2001).

When $N > 2\ell^* + 1$, there are more particles than can be accommodated in the lowest CF LL. An integral number of filled CF levels occurs when $N = n(2\ell^* + n)$, where $n = 1, 2, \dots$. Then, the only state belonging to $G_{N\ell^*}(L)$ is the $L = 0$ incompressible Jain state with filling factor $\nu = n(2n \pm 1)^{-1}$. This completely explains the Jain sequences $1/3, 2/5, 3/7, \dots$ and $1, 2/3, 3/5, \dots$ (though for simplicity we have considered $p = 1$ instead of addition of $2p$ CS flux quanta). The gap between the lowest band of states (containing the minimum number of QPs required by the values of $2Q$ and N) and the first excited band is proportional to $V(\mathcal{R})$, the pseudopotential describing the interaction of a pair as a function of the relative pair angular momentum \mathcal{R} , for the value of \mathcal{R} avoided in the Laughlin correlated state. Note that the only energy scale is the Coulomb scale, and even though no extraneous MF energy has been introduced, the occurrence of Jain states, the form of the low energy spectrum, and the size of gaps has been determined qualitatively.

Fig. 6 is a simple illustration of this for a system of four electrons. If we start at $2\ell = 23$ [frame (d)] we find four bands. The highest band contains pairs with the largest values of L' (i.e. the largest pair repulsion). When we consider $2\ell^* = 2\ell - 2(N - 1) = 17$ [frame (c)] we eliminate the largest L' and there are only three bands. Ultimately at $2\ell^* = 2\ell - 6(N - 1) = 5$ [frame (a)] there is only a single band (with low L values and low pair repulsion). If we had chosen $2\ell = 21$ instead of 23, we would have had a Laughlin $L = 0$ IQL state for frame (a) since $2\ell^* = 21 - 6 \times 3 = 3$ and the level is filled by four electrons.

8. The composite Fermion hierarchy

Haldane (1983) introduced the idea of a hierarchy of condensed states in which Laughlin QPs of a condensed electron state could form daughter states. The new daughter states have their excitations (a second generation of QPs) which, in turn, could form new IQL daughter states with their own QPs, ad infinitum. Haldane assumed the problem of partial filling of a Landau level of QPs (or a QP angular momentum shell) was essentially the same as the original problem of putting N electrons into N_ϕ single-particle states of the lowest LL. Because the maximum allowed value of the number of QP states, was equal to N , the number of electrons in the Laughlin condensed state, he replaced the electron LL degeneracy N_ϕ by N , and replaced the number of electrons by N_{QP} in the Laughlin condition $N_\phi = (2p + 1)N$ for an IQL state. Because he treated the excitations as Bosons, Haldane's condition for a daughter state was taken as $N = 2pN_{QP}$, with the even integer $2p$ replacing Laughlin's odd integer $2p + 1$ appropriate to Fermions. This hierarchy picture implicitly assumed that residual interactions between QPs would give rise to Laughlin correlations among them.

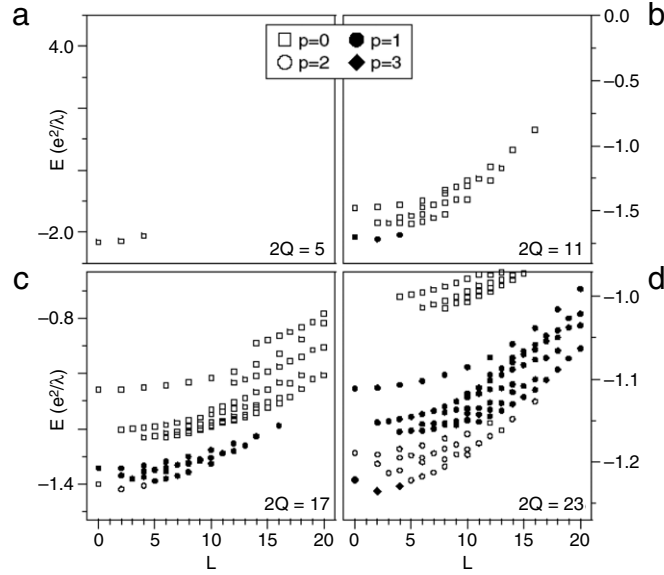


Fig. 6. The energy spectra of 4 electrons in the lowest Landau level at different monopole strength (a) $2Q = 5$, (b) $2Q = 11$, (c) $2Q = 17$, (d) $2Q = 23$. All those $2Q$ values are equivalent in mean-field CF picture (CS transformation with $p = 0, 1, 2$ and 3 , respectively). (Solid diamonds: states with $\mathcal{R} \geq 7$, that is $P(1) \approx P(3) \approx P(5) \approx 0$ and $P(7) > 0$; open circles: states with $\mathcal{R} \geq 5$, that is $P(1) \approx P(3) \approx 0$ and $P(5) > 0$; solid circles: states with $\mathcal{R} \geq 3$, that is $P(1) \approx 0$ and $P(3) > 0$; open squares: states with $\mathcal{R} \geq 1$, that is $P(1) > 0$) (Quinn and Wójs, 2000a).

Slightly different versions of the hierarchy were later independently proposed by Halperin (1984) and by Laughlin (1984, 1988). They differed primarily in the statistics (anyon, Fermion, Boson) satisfied by the QPs. These hierarchy schemes suggested that all odd denominator filling fractions should be IQL states.

Sitko et al. (1997, 1996) introduced a very simple CF hierarchy picture in an attempt to understand the connection between Haldane's hierarchy of Laughlin correlated QP daughter states and Jain's sequence of IQL states with integrally filled CF Landau levels. Jain's CF picture neglected interactions between QPs. The gaps causing incompressibility were energy separations between the single-particle CFLLs. Not all odd denominator fractions occurred in Jain's sequence $\nu = n(2pn \pm 1)^{-1}$ where n and p are integers. The missing IQL states, which occurred for partially filled QP shells (or CFQP Landau levels), had to depend on "residual interactions" between QPs, neglected in Jain's mean-field CF picture.

In the CF hierarchy picture (Sitko et al., 1997, 1996; Wójs and Quinn, 2000d; Yi and Quinn, 1997; Yi et al., 1996) an initial electron filling factor ν_0 was related to an effective CF filling factor ν_0^* by the relation

$$\nu_0^{*-1} = \nu_0^{-1} - 2p_0. \quad (7)$$

This says that the total number of flux quanta (of both the dc magnetic field and CS gauge field) seen by one CF was equal to the dc flux per electron minus the CS flux per electron subtracted in the CF transformation. If ν_0^* were an integer n , then the IQL state of the CFs would occur at $\nu_0 = n(2p_0n \pm 1)^{-1}$. This is the Jain sequence of integrally filled CF LLs.

What happens if ν_0^* is not equal to an integer? Sitko et al. (1997, 1996) suggested that one writes ν_0^* as $\nu_0^* = n_1 + \nu_1$, where n_1 was an integer and ν_1 represented the filling factor of the partially filled CFQP level. If, as Haldane (1983) suggested, the residual interactions between QPs were sufficiently similar to the Coulomb interaction between electrons in the lowest LL, one could assume Laughlin correlations among QPs. By reapplying the CF transformation to them and writing $\nu_1^{*-1} = \nu_1^{-1} - 2p_1$, ν_1^* could be an integer n_2 resulting in $\nu_1 = n_2(2p_1n_2 \pm 1)^{-1}$ and an IQL daughter state at

$$\frac{1}{\nu_0} = 2p_1 + [n_1 + n_2(2p_1n_2 + 1)^{-1}]^{-1}. \quad (8)$$

This is a new odd denominator fraction not belonging to the Jain sequence. If ν_1^* is not an integer, simply set $\nu_1^* = n_2 + \nu_2$ and reapply the CF transformation to the new QPs in the shell of filling factor ν_2 . In general one finds

$$\frac{1}{\nu_l} = 2p_l + \frac{1}{n_{l+1} + \nu_{l+1}} \quad (9)$$

at the l th level of the hierarchy. When $\nu_{l+1} = 0$, there is a filled shell of CFs at the l th level of the hierarchy. The procedure generates Haldane's continued fraction leading to IQL states at all odd denominator fractions. It gives the Jain sequence as a special case in which integral CF filling $\nu_0^* = n$ of the CFQP shell is found at the first level of the CF hierarchy. No residual interactions are needed to obtain the Laughlin–Jain sequence of IQL states; it arises from the gap between the last filled CF

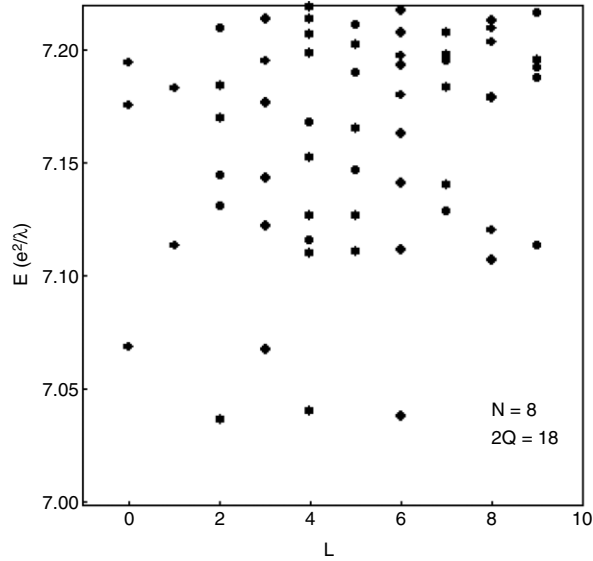


Fig. 7. Low energy spectrum of 8 electrons at $2\ell = 18$. The lowest band contains 3 QEs each with $\ell_{\text{QE}} = 3$. Reapplying the CS mean-field approximation to these QEs would predict an $L = 0$ daughter state corresponding to $\nu = 4/11$. The data makes it clear that this is not valid.

level and the empty ones. Haldane's result assumes QP interactions are responsible for the incompressibility gap, and that the interactions cause Laughlin correlations among the QPs.

It is not difficult to show by numerical diagonalization that the hierarchy picture can't be correct in general. The reason, as suggested by Sitko et al. (1996), has to do with the residual QP interactions. Consider, for example, the electron system with $(N, 2\ell)$ given by (8, 18). Applying the CF transformation with $2p_0 = 2$ gives $2\ell_1^* = 18 - 2(8 - 1) = 4$. Thus, the lowest CF shell has $\ell_1^* = 2$; it can accommodate five CFs. The remaining three CFs must go into the first excited CF shell with $\ell_{\text{QE}} = 3$. The five CFs in the lowest shell would give an IQL state if three CFQEs were not present. Only the CFs in the partially filled CF shell are considered to be QPs. Three Fermions each with $\ell_{\text{QE}} = 3$ give the multiplets $L = 0 \oplus 2 \oplus 3 \oplus 4 \oplus 6$. If the CF hierarchy were correct, applying a second CF transformation with $2p_1 = 2$ to the three CF QEs would give $2\ell_{\text{QE}}^* = 2\ell_{\text{QE}} - 2(N_{\text{QE}} - 1) = 2$. The new level of second generation CFs would exactly accommodate three QEs and give an $L = 0$ IQL ground state. Numerical diagonalization of the $(N, 2\ell) = (8, 18)$ system gives the spectrum shown in Fig. 7.

The low lying multiplets are exactly as predicted at the first CF level, giving three QEs each with $\ell_{\text{QE}} = 3$. However, the $L = 0$ multiplet is clearly not the ground state as predicted by reapplying the CF transformation. It should be emphasized that the numerical results are obtained for a spin polarized system (with total spin $S = N/2 = 4$). The reason for this failure [the "subharmonic" behavior of the CFQE pseudopotential (Wójs and Quinn, 2000d)] will be explained later (see Sections 9 and 15).

9. Residual interactions

The QEs and QHs have residual interactions that are more complicated than simple Coulomb interactions. They are difficult to calculate analytically, but if we look at an N electron system at a value of $2\ell = 3(N - 1) \pm 2$, we know that the lowest band of states in the spectrum will correspond to 2 QEs or 2 QHs for the minus and plus signs respectively. Fig. 3 gives the spectrum for $N = 10$ electrons at $2\ell = 25$ (2 QE case) and $2\ell = 29$ (2 QH case). It is clear that the low energy bands are not degenerate, but that the energy E depends on L , which (as we have seen) can be understood as the total angular momentum of the QP pair. For QEs, $E(L)$ has a maximum at $L = 2\ell_{\text{QE}} - 3$ and a minima at $L = 2\ell_{\text{QE}} - 1$ and $2\ell_{\text{QE}} - 5$. For QHs, $E(L)$ has a maximum at $L = 2\ell_{\text{QH}} - 1$ and $L = 2\ell_{\text{QH}} - 5$, and a minimum at $L = 2\ell_{\text{QH}} - 3$. This is quite different from the pseudopotentials for electrons (i.e. the energy of interaction as a function of total pair angular momentum), and it is undoubtedly the reason why the CF picture fails when it is reapplied to QEs.

More careful estimates of $V_{\text{QE}}(\mathcal{R})$ and $V_{\text{QH}}(\mathcal{R})$ (where $\mathcal{R} = 2\ell - L'$ and L' is the pair angular momentum) are shown for QPs of the Laughlin $\nu = 1/3$ and $\nu = 1/5$ IQL states in Fig. 8. The values of $V_{\text{QP}}(\mathcal{R})$ are determined (up to an overall constant) by diagonalization of N electron systems with $6 \leq N \leq 11$.

In Fig. 9 we display the pseudopotentials for electrons in LL0 and LL1 with that for QEs of the Laughlin $\nu = 1/3$ IQL state in CF LL1. The electron pseudopotentials are the same ones presented in Fig. 4 but are presented here as a function of $\mathcal{R} = 2\ell - L'$, the relative angular momentum of a pair, for large systems.

We define a pseudopotential to be harmonic if it increases with L' as $V_H(L') = A + BL'(L' + 1)$, where A and B are constants. The superharmonic behavior of $V^{(0)}(\mathcal{R})$ (i.e. it increases faster than $V_H(L')$ everywhere) is clear from the increasing slope with decreasing \mathcal{R} . For $V^{(1)}(\mathcal{R})$, only at $\mathcal{R} = 1$ is the pseudopotential harmonic (the slope for $1 < \mathcal{R} < 3$ is the same as

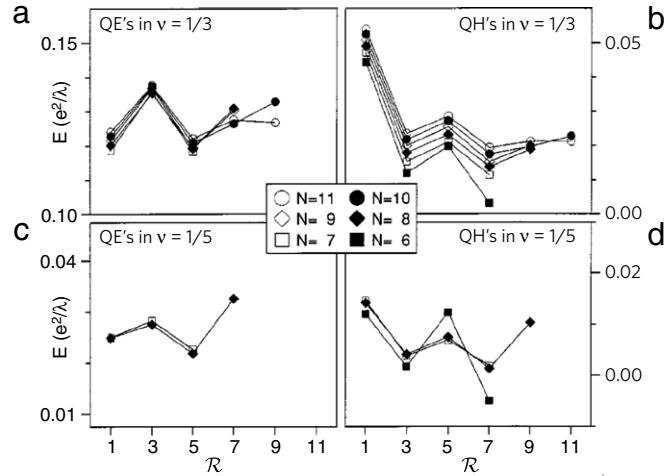


Fig. 8. The pseudopotentials of a pair of quasielectrons (left) and quasiholes (right) in Laughlin $\nu = 1/3$ (top) and $\nu = 1/5$ (bottom) states, as a function of relative angular momentum \mathcal{R} . Different symbols mark data obtained in the diagonalization of between 6 and 11 electrons (Wójs and Quinn, 2000d).

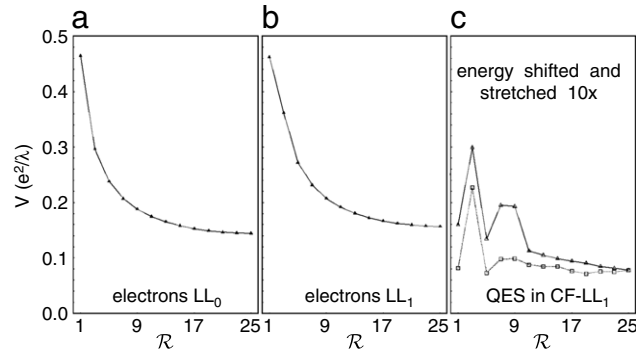


Fig. 9. Pair interaction pseudopotentials as a function of relative angular momentum \mathcal{R} for electrons in LL0 (a), LL1 (b) and for the QEs of the Laughlin $\nu = 1/3$ state calculated by Lee et al. (2001, 2002) (squares) and by Wójs et al. (2006b) (triangles).

that for $3 < \mathcal{R} < 5$). The QE pseudopotentials in frame (c) were taken from the calculations of Lee et al. (2001, 2002) and from the diagonalization of small electron systems done by Wójs et al. (2007, 2006b), and are known up to a constant. The magnitude of interaction of CFQEs is much smaller, and has a sharp maximum at $\mathcal{R} = 3$ and minima at $\mathcal{R} = 1$ and 5.

These pseudopotentials have been obtained for 2D electron layers of zero width. It is well-known (He et al., 1990; Peterson and Das Sarma, 2008; Wójs and Quinn, 2007) that the finite extent of the subband wavefunction in the direction perpendicular to the layer introduces a correction to the electron pseudopotentials. The QP pseudopotentials are also sensitive to the layer width since they are obtained from the energy of the two QP band obtained by exact diagonalization of the appropriate electron system and the specific form of the (lowest) subband wavefunction.

10. Pair angular momentum theorem and coefficients of fractional parentage

We can define the total angular momentum operator $L = \sum_i \hat{\ell}_i$ for an N electron system in a shell of angular momentum ℓ , and $\hat{L}_{ij} = \hat{\ell}_i + \hat{\ell}_j$, the angular momentum operator for the pair $\langle i, j \rangle$. The operator identity

$$\hat{L}^2 + N(N-1)\ell^2 - \sum_{(i,j)} \hat{L}_{ij}^2 = 0, \quad (10)$$

where the summation is over all pairs $\langle i, j \rangle$, can be obtained simply (Wójs and Quinn, 1999) by writing out \hat{L}^2 and $\sum_{(i,j)} \hat{L}_{ij}^2$, and eliminating $\hat{\ell}_i \cdot \hat{\ell}_j$. We consider the N electron multiplet $|\ell^N; L\alpha\rangle$ of total angular momentum L . The index α is used to distinguish independent multiplets with the same total angular momentum L . Taking the expectation value of Eq. (10) for the state $|\ell^N; L\alpha\rangle$ we obtain

$$L(L+1) + N(N-2)\ell(\ell+1) = \left\langle \sum_{(i,j)} \hat{L}_{ij}^2 \right\rangle. \quad (11)$$

This relates the expectation value of the sum over all pairs of the squared pair angular momenta to L and ℓ . The antisymmetric angular momentum multiplet $|\ell^N; L\alpha\rangle$ can be written

$$|\ell^N; L\alpha\rangle = \sum_{L_{12}} \sum_{L'\alpha'} G_{L\alpha L'\alpha'} |\ell^2, L_{12}; \ell^{N-2}, L'\alpha'; L\rangle. \quad (12)$$

Here $|\ell^2, L_{12}; \ell^{N-2}, L'\alpha'; L\rangle$ is an N electron multiplet of total angular momentum L formed from an $N - 2$ electron multiplet $|\ell^{N-2}; L'\alpha'\rangle$ and a pair wavefunction $|\ell^2; L_{12}\rangle$. It is antisymmetric with respect to the exchange of indices i, j when both i and j belong to the set $(1, 2)$ or when both belong to the set $(3, 4, \dots, N)$. It is not antisymmetric if i belongs to one set and j to the other. However, the coefficient $G_{L\alpha L'\alpha'}$, called the coefficient of fractional parentage, can be chosen so that $|\ell^N; L\alpha\rangle$ is totally antisymmetric. Fractional parentage has been widely used in atomic and nuclear physics (de Shalit and Talmi, 1963), but all that we need to know is that

$$\sum_{L'\alpha'} |G_{L\alpha, L'\alpha'}(L_{12})|^2 = P_{L\alpha}(L_{12}). \quad (13)$$

This says that the probability $P_{L\alpha}(L_{12})$ that the multiplet $|\ell^N, L\alpha\rangle$ has pairs with pair angular momentum L_{12} is equal to the sum over all $N - 2$ particle multiplets $|\ell^{N-2}; L'\alpha'\rangle$ of the square of the magnitude of $G_{L\alpha, L'\alpha'}(L_{12})$. Since $|\ell^N; L\alpha\rangle$ is totally antisymmetric, we can select a single pair $\langle i, j \rangle = \langle 1, 2 \rangle$ and multiply by the number of pairs. The right hand side of Eq. (12) is a linear combination of \hat{L}_{ij}^2 whose coefficients are $G_{L\alpha, L'\alpha'}(L_{12})$. The net result is that

$$\left\langle \sum_{(i,j)} \hat{L}_{ij}^2 \right\rangle = \frac{N(N-1)}{2} \sum_{L_{12}} L_{12}(L_{12}+1) P_{L\alpha}(L_{12}). \quad (14)$$

The summation on the right hand side is over all the allowed values of the pair angular momentum L_{12} , and $P_{L\alpha}(L_{12})$ was given in Eq. (13). This leads to two useful sum rules:

$$\sum_{L_{12}} P_{L\alpha}(L_{12}) = 1, \quad (15)$$

$$\frac{1}{2} N(N-1) \sum_{L_{12}} L_{12}(L_{12}+1) P_{L\alpha}(L_{12}) = L(L+1) + N(N-2)\ell(\ell+1). \quad (16)$$

It is interesting to note that the expectation value of $\sum_{(i,j)} \hat{L}_{ij}^2$ in the multiplet $|L, \alpha\rangle$ is independent of α since the right hand side of Eq. (16) is independent of α .

11. Harmonic pseudopotential and absence of correlations

The two sum rules allow us to make use of the concept of a harmonic pseudopotential. In Fig. 4 we plotted the pseudopotential for the Coulomb interaction of electrons in the LL0 and LL1 as a function of the eigenvalues of the square of the pair angular momentum L' . For LL0 $V^{(0)}(L')$ increases with increasing L' faster than $L'(L'+1)$; for LL1 this is true only for $L' < 2\ell - 5$. Between $L' = 2\ell - 5$ and $L' = 2\ell - 1$, $V^{(1)}(L')$ increases approximately as a linear function of $L'(L'+1)$. Let's define

$$V_H(L') = A + BL'(L'+1), \quad (17)$$

as a harmonic pseudopotential, with A and B being constants. From Eqs. (5) and (16), we can write, for a harmonic pseudopotential, the energy of the multiplet $|\ell^N; N\alpha\rangle$ as

$$E_\alpha(L) = N \left[\frac{1}{2} (N-1)A + B(N-2)\ell(\ell+1) \right] + BL(L+1). \quad (18)$$

We note that for a harmonic pseudopotential $E_\alpha(L)$ is totally independent of the multiplet index α . Every multiplet with the same angular momentum L has the same energy. As long as the constant B is positive, the energy increases with L as $BL(L+1)$, but the degeneracy of the myriad multiplets of a given value of L is not removed, implying the absence of correlations for the harmonic potential.

12. The simplest anharmonicity and Laughlin correlations

We define $\Delta V(L') = V(L') - V_H(L')$ as the anharmonic part of the pseudopotential. $\Delta V(L')$ is responsible for lifting the degeneracy of different multiplets having the same value of the total angular momentum L . We suggest that the simplest anharmonic contribution to the pseudopotential be taken as

$$\Delta V(L') = k\delta(L', 2\ell - 1). \quad (19)$$

If $k > 0$, it is apparent that the lowest energy multiplet for each value of L will be the one with the smallest value of $P_{L\alpha}(L' = 2\ell - 1)$ [or $P_{L\alpha}(\mathcal{R} = 1)$]. This is exactly what is meant by Laughlin correlations. Complete avoidance of $\mathcal{R} = 1$ pairs (or $m = 1$ pairs in the planar geometry) cannot occur unless $2\ell \geq 3(N - 1)$. In the limit of large systems this corresponds to a filling factor $\nu \geq 1/3$.

If $k < 0$ in Eq. (19), then the lowest energy state for each L will have the largest value of $P_{L\alpha}(\mathcal{R} = 1)$. This suggests a tendency to form $\mathcal{R} = 1$ pairs rather than Laughlin correlations.

It is important to emphasize that Laughlin correlations (e.g. maximum avoidance of pairs with $\mathcal{R} = 2\ell - L'$ equal to unity) occur only when $V(\mathcal{R})$ is “superharmonic” at $\mathcal{R} = 1$. From Fig. 9, we can see that electrons in LL0 (a) satisfy this condition, while QEs of the Laughlin $\nu = 1/3$ state (c) do not. This means that at $\nu_{\text{QE}} = 1/3$, the quasielectrons in CF LL1 will not be Laughlin correlated. This is in agreement with the numerical results of Sitko et al. (1996). Now, however, we understand why the CF hierarchy picture fails for a spin polarized system. The QE pseudopotential is subharmonic at $\mathcal{R} = 1$ and does not support Laughlin correlations. There have been a number of papers suggesting that the IQL states observed by Pan et al. (2003), like the $\nu = 4/11$ IQL, can be understood as a second generation of CFs (Goerbig et al., 2006, 2004; López and Fradkin, 2004; Smet, 2003). This suggestion cannot be correct. As previously shown in Section 8, the idea is not new (Sitko et al., 1997, 1996), and it had already been shown numerically to fail. The theorem on pair angular momentum and the harmonic potential make it clear (Quinn and Quinn, 2006; Quinn et al., 2001a, 2004a,b; Quinn and Wójs, 2000b; Wójs and Quinn, 2000d; Wójs et al., 2004) why the second generation of CFs can’t be correct for fully spin polarized states like $\nu = 4/11$: $V_{\text{QE}}(\mathcal{R})$ will not support Laughlin correlations at $\nu_{\text{QE}} = 1/3$.

If QEs of a spin polarized electron system can’t be Laughlin correlated at $\nu_{\text{QE}} = 1/3$, how will these QEs be correlated? Before considering this problem in detail, it is worthwhile looking at the problem of electrons in LL1. For electrons confined to a 2D surface, Fig. 9(b) shows that the pseudopotential is very close to harmonic for $\mathcal{R} < 3$. In such a case, Laughlin correlations (avoidance of $\mathcal{R} = 1$) will not produce the lowest energy state. There is no reason to avoid $\mathcal{R} = 1$ in favor of $\mathcal{R} = 3$ in the lowest band of energy states. Let’s study the problem by numerical diagonalization and attempt to understand the results in terms of simple intuitive pictures.

13. Incompressible quantum liquids in the first excited Landau level

13.1. The $\nu = 5/2$ incompressible quantum liquid

It has been known for some time (Eisenstein et al., 2002; Pan et al., 1999; Willett et al., 1987) that at filling factor $\nu = 2 + \nu_1 = 5/2$ (half-filling of one spin state of the LL1), an IQL state with a robust energy gap occurs. This is in stark contrast to the compressible state found at $\nu = 1/2$ (half filling of the lower spin state of LL0). The compressible state at $\nu = 1/2$ can be described in terms of CFs which experience a “mean magnetic field” B^* equal to $B - 2pn\phi_0$, where n is the electron concentration, and $\phi_0 = hc/e$ is the quantum of flux (Halperin et al., 1993). B^* vanishes at $\nu = 1/2$. Shubnikov–de Haas oscillations in the magnetoconductivity are observed as a function of B^* for small deviations away from filling factor $\nu = 1/2$ (Du et al., 1993; Mancoff et al., 1996). For $\hbar\omega_c \gg e^2/\lambda$, the difference between the behavior of electrons in LL0 and LL1 must be related to their pseudopotentials. In LL0 Laughlin correlations occur because $V_0(L')$ is “superharmonic”. Jain’s CF picture can be applied resulting in the Laughlin–Jain sequence of “filled CF” shells in the mean-field approximation. The Halperin, Lee, and Read (HLR) picture (Halperin et al., 1993) treats the interactions between the CFs beyond the mean-field approximation (both Coulomb and Chern–Simons gauge interactions) by standard many-body perturbation theory. HLR gives surprisingly good agreement with the qualitative features of the $\nu = 1/2$ state that are observed experimentally.

For the electrons in LL1 the pseudopotential $V_1(\mathcal{R})$ is not superharmonic at $\mathcal{R} = 2\ell - L_2 = 1$. Therefore, electrons in LL1 will not support Laughlin correlations and cannot be described in terms of weakly interacting CFs. Finite well width changes $V_1(\mathcal{R})$ through form factors associated with the subband wavefunction of the quantum well. It is possible that the effect can lead to a change in the ratio of $V_1(\mathcal{R} = 1)$ to $V_1(\mathcal{R} = 3)$ that will support Laughlin correlations within a certain range of well widths (Rezayi and Haldane, 2000). Only then can the $\nu = 5/2$ state be thought of as a CF state at $B^* = 0$, which might undergo a “Cooper pairing” instability and form the gapped IQL state observed in some experiments.

For the moment, let’s concentrate on the case of zero well width where $V_1(\mathcal{R})$ is given by Fig. 9(b). By standard numerical diagonalization within LL1 (i.e. neglecting Landau level mixing) we can obtain the energy spectra for N electrons in a shell of angular momentum ℓ interacting via the pseudopotential $V_1(\mathcal{R})$. We have carried out such diagonalizations for $N \leq 16$ and for different values of 2ℓ (Simion and Quinn, 2008; Wójs, 2001a; Wójs and Quinn, 2005, 2006). Incompressible $L = 0$ ground states are found to fall into families. The most prominent ones occur at $2\ell = 2N - 3$ for even values of N , and at $2\ell = 3N - 7$ (and by electron–hole symmetry at their e–h conjugate states $2\ell = 2N + 1$ and $2\ell = 3N/2 + 2$). The conjugate states are obtained with the replacement of N by $2\ell + 1 - N$. The energy gap for the $\nu_1 = 1/2$ state is less than 1/3 of the gap for the $\nu = 1/3$ state in LL0. The behavior of the gap with increasing particle number N suggests that this IQL state at $\nu_1 = 1/2$ will persist for macroscopic systems.

There has been a considerable amount of theoretical work on the $\nu = 5/2$ state (the half filled LL1 lower spin state). Moore and Read (1991) proposed a Pfaffian wavefunction for this state based on ideas from conformal field theory. Greiter et al. (1991, 1992) showed that the Pfaffian state is an exact solution to a special Hamiltonian which is large and repulsive when three electrons form a single droplet (with the total three-particle angular momentum $L_3 = 3\ell - 3$ or $\mathcal{R}_3 = 3\ell - L_3 = 3$)

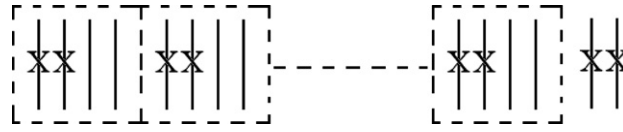


Fig. 10. Simple picture of the $\nu_1 = 1/2$ paired state. The vertical lines represent single-particle states of different ℓ_z , going from $-\ell$ to ℓ . Occupied states are marked by an X on the vertical line. The “unit cell” is shown by the dashed rectangles. Occupancy is chosen so that $L_z = 0$. The number of single-particle states satisfies the relation $2\ell + 1 = 4(N/2 - 1) + 2$, or $2\ell = 2N - 3$, corresponding to $\nu_1 = 1/2$ state (of LL1). Its conjugate state at $2\ell = 2N + 1$ should, by e-h symmetry, also be an IQL state.

and zero otherwise. For the Pfaffian state at $\nu_1 = 1/2$ in LL1, 2ℓ is given by $2N - 3$ (or its conjugate $2N + 1$) in agreement with numerical diagonalization.

It should be noted that Laughlin correlated states at $\nu = 1/m$ in LL0 occur at $2\ell = mN - m$, where m is an odd integer. States in the Jain sequence (Jain, 1990) $\nu = n(2pn \pm 1)^{-1}$, where n and p are positive integers, occur at $2\ell = \nu^{-1}N \pm n - 2p$ (and their e-h conjugate values). No even denominator fractional fillings are IQL states in the Laughlin–Jain sequence. How then can we understand the IQL state observed experimentally at $\nu_1 = \nu - 2 = 1/2$ in LL1 and found in numerical diagonalization of small systems at $2\ell = 2N - 3$?

13.2. Heuristic picture of the $\nu = 5/2$ state

As we have already noted, the pseudopotential $V_1(\mathcal{R})$ is not superharmonic at $\mathcal{R} = 1$, and the probability $P(\mathcal{R})$ of finding pairs with $\mathcal{R} = 1$ in the ground state will not be a minimum as it is for the Laughlin correlated case in LL0. Let’s make the assumption that $\mathcal{R} = 1$ pairs form. Of course, a state consisting of only $N/2$ pairs, each with pair angular momentum $L_2 = 2\ell - 1$ (or relative angular momentum $\mathcal{R} = 1$) is not an eigenstate of the interacting system. The electrons can scatter, breaking up the pairs, as long as both the total angular momentum of the system L and its z-component are conserved. However, we can think of this state as a “parent state” which will generate the exact ground state when Coulomb interactions admix different configurations with the same L and L_z .

A simple heuristic picture of the parent state with $L = 0$, containing $N/2$ pairs each with $\mathcal{R} = 1$ in an angular momentum $\ell = (2N - 3)/2$ is shown in Fig. 10. It corresponds to the maximum number of electrons in a $\nu_1 = 1/2$ filled state which has L_z , the z-component of the total angular momentum equal to zero. The $\mathcal{R} = 1$ pairs have total pair angular momentum $\ell_p = 2\ell - 1$. The pairs of electrons might normally be thought of as Bosons. However, in 2D, they can be treated as either Fermions of angular momentum ℓ_F , or as Bosons with $\ell_B = \ell_F - \frac{1}{2}(N - 1)$, where N is the number of particles (Benjamin et al., 2001; Quinn et al., 2001a; Xie et al., 1991). Let’s assume that N is even and that we form $N/2$ pairs. The pairs cannot approach one another too closely without violating the Pauli exclusion principle with respect to exchange of identical constituent Fermions belonging to different pairs. We can account for this effect by introducing an effective Fermion pair (FP) angular momentum defined by

$$2\ell_{FP} = 2(2\ell - 1) - \gamma_F(N_p - 1). \quad (20)$$

For a single pair $\ell_{FP} = 2\ell - 1$. As N_p increases, the allowed values of the total angular momentum of two pairs is restricted to the values less than or equal to $2\ell_{FP}$. The value of γ_F is determined by requiring that the FP filling factor ν_{FP} be equal to unity when the single Fermion filling factor has the electron filling factor corresponding to the appropriate FP filling. For the pair having $\ell_p = 2\ell - 1$, this corresponds to $\nu = 1$. (Wójs and Quinn, 2000d; Wójs et al., 2004). Remembering that $\nu_{FP}^{-1} = (2\ell_{FP} + 1)/N_p$ and that $\nu^{-1} = (2\ell + 1)/N$, then we find in the large N limit that $\gamma_F = 3$ and

$$\nu_{FP}^{-1} = 4\nu^{-1} - 3. \quad (21)$$

If we treated pairs as Bosons, γ_F would be replaced by $\gamma_B = \gamma_F + 1$. The factor of 4 in Eq. (21) results from having half as many pairs ($N_p = N/2$) filling twice as many states of the pair LL (since the pairs have charge $-2e$ giving the degeneracy of the pair Landau level $g_p = 2g$). The pairs form not because there is an attractive interaction between electrons, but because the anharmonic contribution to the pseudopotential, which determines the correlations, is attractive at $\mathcal{R} = 1$. By forming $N/2$ pairs that can be more widely separated than N electrons, the slightly stronger anharmonic part of the e-e repulsion at $\mathcal{R} = 3$ can be avoided. In fact, the pairs can become Laughlin correlated. For electrons in LL1 at filling factor $\nu = 1/2$, Eq. (21) gives $\nu_{FP} = 1/5$. Fermions in a Laughlin correlated $\nu_{FP} = 1/5$ state must have $2\ell_{FP} = 5(N_p - 1)$. This, together with Eq. (20) in which γ_F is set equal to 3, gives $2\ell = 2N - 3$, the relation between 2ℓ and N appropriate for the $\nu_1 = 1/2$ filling of LL1 (i.e. for the total filling factor $\nu = 2 + 1/2 = 5/2$).

It is worth noting that the heuristic picture of Fig. 10 has been used before for Laughlin–Jain states in LL0 (Giuliani and Quinn, 1985). For example, at $\nu = 3/7$, the unit cell contains seven single-particle states, the first three of which are filled. The number of unit cells is $(N/3) - 1$, three electrons being reserved to fill three states after the last unit cell to give an $L_z = 0$ state. This picture suggests that the “parent state” produces IQL states for $2\ell = (7/3)N - 5$. The minus five is the appropriate finite size correction for the Laughlin correlated $\nu = 3/7$ state. The finite size corrections obtained in the families of IQL states found in numerical studies appear to contain important information about correlations in the IQL state. It should be noted that our pair state is different from the Moore–Read Pfaffian state since the square of the overlap of the

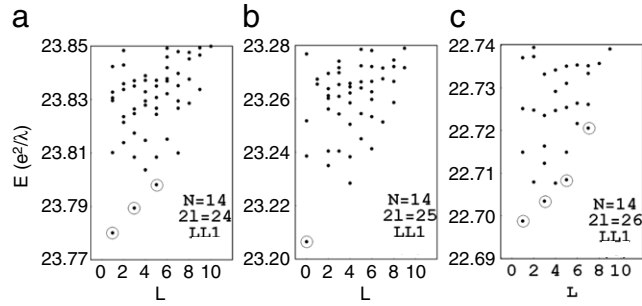


Fig. 11. Spectra of fourteen electrons in the first excited LL of a zero width quantum well. The values of 2ℓ are 24 (a), 25 (b) and 26 (c). Frame (b) has an $L = 0$ IQL ground state. Frames (a) and (c) contain at least two elementary excitations [two FP quasiparticles in (a) and two FP quasiholes in (b)] (Simon and Quinn, 2008).

two wavefunctions is not so close to unity for a 14-electron system. As a consequence, the wavefunctions describing the ground state and excited states are different from those predicted by Greiter et al. (1992), Töke and Jain (2006) and Töke et al. (2007). The work of Töke and Jain (2006) describes the IQL state at $\nu = 5/2$ as a result of residual CF interaction, showing that a realistic Coulomb interaction would produce a wavefunction which is somehow different from the Pfaffian one. A numerical study, made by Töke and Jain (2006) and Töke et al. (2007) shows that excited states of the $\nu = 5/2$ state in the presence of the Coulomb potential differ from those expected when a Pfaffian wavefunction is used. The absence of a degenerate band of quasiparticle states might suppress the expected non-Abelian behavior.

13.3. Excitations of $\nu = 5/2$ state

In Fig. 11 we display the spectra for 14 electrons in LL1 at values of 2ℓ equal to 24 (a), 25 (b), and 26 (c). In each case, the lowest band of states can be interpreted using a simple picture which assumes that the 14 electrons give rise to a “parent” state with seven pairs, each pair having pair angular momentum $\ell_p = 2\ell - 1$. We treat the pairs as Fermions with $2\ell_{FP} = 2\ell_p - 3(N_p - 1)$. For case (b) $\ell_p = 25$, giving $2\ell_{FP} = 30$. Then, by assuming that the seven pairs are Laughlin correlated with $2\ell_{FP}^* = 2\ell_{FP} - 2p(N_p - 1)$ and $p = 2$, we obtain $2\ell_{FP}^* = 6$. The shell of Laughlin correlated pairs (LCPs) can accommodate $2\ell_{FP}^* + 1 = 7$ pairs giving an $L = 0$ IQL ground state. For case (a) $\ell_p = 23$ giving $2\ell_{FP} = 28$ and $2\ell_{FP}^* = 4$. The lowest shell of FPs can accommodate only five pairs; the remaining two become FP quasiparticles with $\ell_{QP} = 3$. The allowed values of the total angular momentum L of two FP quasiparticles each with $\ell_{QP} = 3$ is $L = 2\ell_{QP} - j$, where j is an odd integer. This gives the band $1 \oplus 3 \oplus 5$ as seen in frame (a). For $2\ell = 26$, $2\ell_{FP}^* = 8$, and we find two FP quasiholes each with $\ell_{QH} = 4$ giving the band $1 \oplus 3 \oplus 5 \oplus 7$ as suggested in frame (c). The simple picture of $N_p (= N/2)$ pairs for even values of N correctly predicts the lowest band of excitations for all even N that we have tested at $2\ell = 2N - 3$ or $2\ell = 2N - 3 \pm 1$. In Fig. 12 we show $P(\mathcal{R})$, the probability of electron pairs with relative angular momentum \mathcal{R} for the $L = 0$ ground state in (b). Because $P(\mathcal{R})$ is a maximum for $\mathcal{R} = 1$ and a minimum for $\mathcal{R} = 3$, this IQL ground state is not a Laughlin correlated state of electrons.

In LL0, excitations of the $\nu = m^{-1}$ Laughlin IQL states obtained by changing $2\ell = m(N - 1)$ by one unit consist of single QPs of angular momentum $\ell_{QP} = N/2$. For LL1, changing 2ℓ from the $\nu_1 = 1/2$ value (of $2N - 3$) by unity must produce two QPs and a low lying band of excitations with angular momentum $L = 2\ell_{QP} - j$, where j is an odd integer. This is a very strong indication that the IQL state consists of pairs with pair angular momentum $\ell_p = 2\ell - 1$. The angular momentum of the pair changes by two units when the electron angular momentum ℓ changes by one. The variation with total angular momentum L of the energy in these bands can be interpreted as a pseudopotential $V_{QP}(L_2)$ describing the interaction of two Fermion pair QPs. Unfortunately, the dispersion of these bands is rather sensitive to the electron pseudopotential $V_1(\mathcal{R})$. Small changes like $\delta V_1(\mathcal{R}) = xV_1(\mathcal{R})\delta(\mathcal{R}, 1)$ have noticeable effect on $V_{QP}(L_2)$ even for $x \lesssim 0.1$. In addition, the bands (especially the QH bands) are not well separated from the quasicontinuum of higher excitations.

13.4. Other incompressible quantum liquid states in the first excited Landau level

In Fig. 13(a) we display the spectrum of an $N = 11$ electron system at $2\ell = 3N - 7 = 26$ in LL1. The $L = 0$ ground state is separated from higher states by a clearly observable energy gap. In frame (b) we show $P(\mathcal{R})$ versus \mathcal{R} for this ground state. Again $P(\mathcal{R})$ is neither a minimum at $\mathcal{R} = 1$ nor a maximum at $\mathcal{R} = 3$, indicating that it is not a Laughlin correlated electron state. Unfortunately, the energy gap of the $\nu_1 = 1/3$ state for $6 \leq N \leq 12$ electron system is not a smooth function of N^{-1} . Therefore we cannot extrapolate to the macroscopic limit with any certainty. In addition, no simple heuristic picture seems to describe the correlations at $\nu_1 = 1/3$ for all values of N . Mixed clusters (single electrons, pairs, triplets, etc.) treated by the generalized CF picture (Wójs et al., 1999b) may be necessary for an intuitive understanding of the correlations and elementary excitations at $\nu_1 = 1/3$.

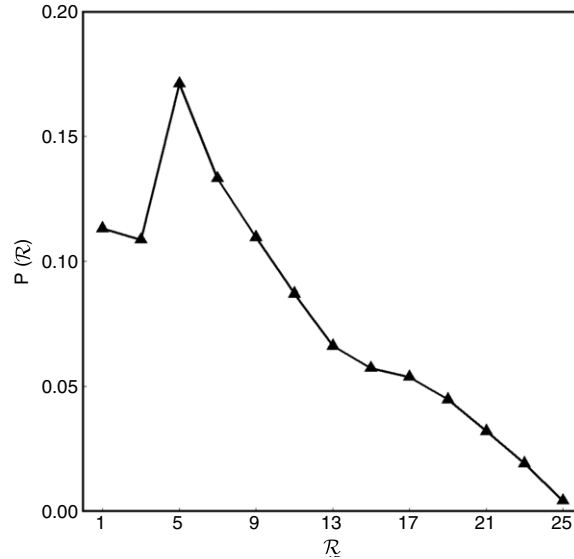


Fig. 12. $P(\mathcal{R})$ vs. \mathcal{R} for the $L = 0$ ground state of case (b) in Fig. 11. The profile is very different from that of a Laughlin correlated electron state in LL0 (Simion and Quinn, 2008).

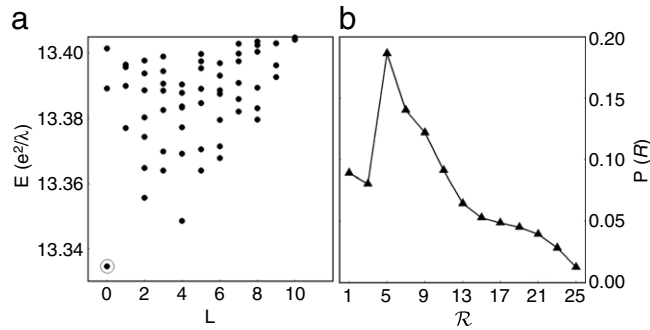


Fig. 13. (a) Spectrum of eleven electrons at $2\ell = 26$ in LL1. The ground state is an $L = 0$ IQL state. (b) $P(\mathcal{R})$ vs. \mathcal{R} for the IQL ground state. It is clearly not a Laughlin correlated electron state (Simion and Quinn, 2008).

Because $V_1(\mathcal{R})$ is not superharmonic at $\mathcal{R} = 1$, but it is at $\mathcal{R} = 3$, we do not expect Laughlin correlated electron (LCE) states for $1/2 \geq \nu_1 \geq 1/3$ where LCEs in LL0 can form Laughlin–Jain states with $\nu = n(1 + 2n)^{-1}$ and n an integer. However, we do expect LCE states for $1/3 > \nu_1 \geq 1/5$ where electrons will avoid pair states with $\mathcal{R} = 1$ and $\mathcal{R} = 3$, forming Laughlin–Jain states with $\nu_1 = n(1 + 4n)^{-1}$. In Fig. 14 we show spectra obtained using the pseudopotential $V_1(\mathcal{R})$ appropriate for a quantum well of zero width. The IQL states at $\nu_1 = 1/5$ and $\nu_1 = 2/7$ are LCE states that can be understood using Jain’s CF^4 picture. $P(\mathcal{R})$ is a minimum for $\mathcal{R} = 1$ and a maximum at $\mathcal{R} = 5$ for each of these states. For $\nu_1 = 2/5$ there is an extremely small gap between the $L = 0$ ground state and the lowest excited state. For this state $P(\mathcal{R})$ is a minimum at $\mathcal{R} = 3$ and a maximum at $\mathcal{R} = 1$ and $\mathcal{R} = 5$, implying ‘pairing’ rather than Laughlin correlation between electrons.

We have studied the $\nu_1 = 2/5$ state (in the case $N = 8$ and $2\ell = 16$) for the situation in which the pseudopotential $V_1(\mathcal{R})$ for a well of zero width is changed by an amount $\delta V_1(\mathcal{R}) = xV_1(\mathcal{R})\delta(\mathcal{R}, 1)$ (Simion and Quinn, 2008). As shown in Fig. 15(a), a very small gap Δ between $L = 0$ ground state and the lowest excited state is found for $x < -0.35$. The gap increases slightly with increasing x , but begins to decrease for $x > -0.1$. It disappears at $x \simeq +0.01$, but reappears at $x \gtrsim +0.08$ and then increases roughly linearly with x . A plot of $P(\mathcal{R})$ versus \mathcal{R} is shown in Fig. 15(b) for $x = -0.3$ (red) and $x = +0.15$ (green). Clearly the latter case is an LCE state, while the former must contain $\mathcal{R} = 1$ pairs. For $x = 0$, corresponding to the Coulomb pseudopotential in LL1, at most a very small gap (associated with Laughlin correlations among $\mathcal{R} = 1$ pairs) can occur.

Our simple picture suggests that when the pseudopotential is superharmonic at the value of relative pair angular momentum \mathcal{R} to be avoided in a Laughlin correlated electron state, Laughlin correlations occur and give rise to robust IQL ground states at special values of ν . When the pseudopotential is not superharmonic, LCE states do not occur. Other kinds of correlations (like formation of electron pairs or electron triplets) can occur, but they result in weaker IQL states than LCE states. It is well-known that Laughlin–Jain states at $\nu = n(1 \pm 2pn)^{-1}$ are the most robust FQH states in LL0, when $V_0(\mathcal{R})$ is superharmonic for $\mathcal{R} = 1, 3, 5 \dots$. For LL1, $V_1(\mathcal{R})$ is not superharmonic at $\mathcal{R} = 1$. FQH states at $\nu = 1/3, 1/2,$

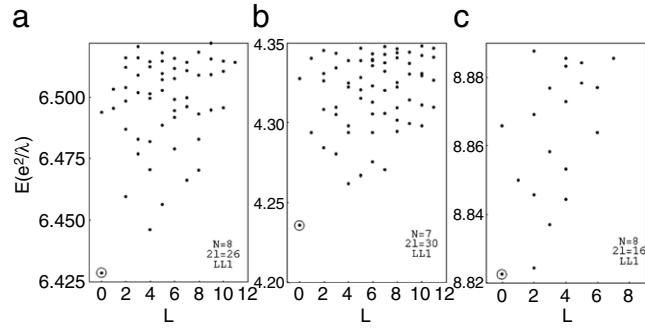


Fig. 14. Spectra for $\nu_1 = 2/7$ (a), $1/5$ (b), and $2/5$ (c) obtained using $(N, 2\ell) = (8, 26)$, $(7, 30)$, and $(8, 16)$ respectively. Case (c) has a very small gap and is not a robust IQL state. Cases (a) and (b) have bigger gaps and could persist in the macroscopic limit (Simion and Quinn, 2008).

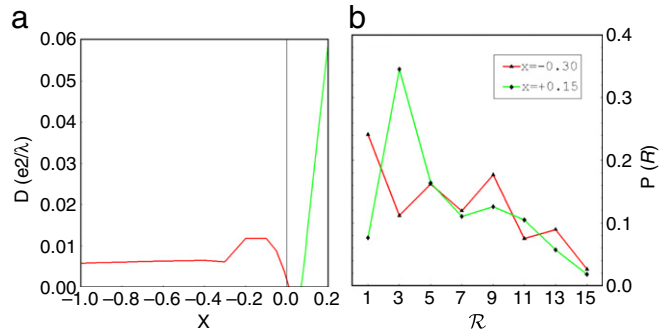


Fig. 15. (color online) (a) Energy gap vs. $\delta V_1/V_1 = x$. Remainder of pseudopotential $V_1(\mathcal{R})$ (for $\mathcal{R} = 3, 5, \dots$) is unchanged. (b) Sketch of pair probability for $x = -0.3$ (red) and $x = 0.15$ (green) (Simion and Quinn, 2008).

and $2/3$ can't be LCE states. They must involve formation of clusters (pairs, triplets, etc.) despite the repulsive nature of the Coulomb interaction. Gaps are smaller than for the LCE states. FQH states at $\nu_1 = 1/5$ and $2/7$ (and their e-h conjugates at $4/5$ and $5/7$) are LCE states quite similar to states of the same filling in LL0. The $\nu = 2/5$ state cannot be an LCE state. At most a very small gap, associated with correlations between pairs of electrons, can occur. This picture is in excellent qualitative agreement with the size of the energy gap determined from thermally activated conductivity of the IQL states in LL0 and LL1 (Choi et al., 2008).

13.5. Other elementary excitations of IQLs of $\nu = 5/2$ IQL

It is clear that the correlations and the elementary excitations are better understood for LL0 than for LL1 and higher Landau levels. In LL0 the CF picture allows us to introduce $\ell^* = |\ell - p(N - 1)|$, where p is an integer. Integral filling $\nu^* = n$ ($n = 1, 2, 3, \dots$) of the CF angular momentum shells gives $L = 0$ ground states at $\nu = n(2pn \pm 1)^{-1}$. The lowest band of states will contain the minimum number of QP excitations required by the values of N and 2ℓ (Chen and Quinn, 1993). The QHs reside in the angular momentum shell $\ell_{\text{QH}} = \ell^* + n$; the QEs are in the shell $\ell_{\text{QE}} = \ell_{\text{QH}} + 1$. The CF picture describes the lowest band of states for any value of the applied magnetic field. The band containing two QEs (or two QHs) can be used to determine (up to an overall constant) the pseudopotential $V_{\text{QP}}(L')$ describing the pairwise interaction between QPs of the Laughlin–Jain IQL states at $\nu = n(2pn \pm 1)^{-1}$. Higher bands of excitations contain one or more additional QE–QH pairs. They are not as well defined as the lowest band, overlapping at intermediate values of the allowed angular momentum. However, most of the states predicted by the simple CF picture are found via numerical diagonalization.

For LL1, we do understand the correlations for $\nu_1 = 1/2$. They can be described in terms of the formation of $N_p = N/2$ pairs when N is even. The pair Landau level has a degeneracy g_p twice that of the original electron LL. This increase in degeneracy and decrease in particle number can lead to Laughlin correlations among the pair giving rise to an IQL state of LCPs at $2\ell = 2N - 3$. This was illustrated in Fig. 11(a) and (c) where the lowest bands of states contain two QP excitations in a Fermion pair excited LL of angular momentum $\ell_{\text{FPQP}} = 3$ in frame (a) and two quasihole excitations in an FP Landau level with $\ell_{\text{FPQH}} = 4$ in frame (c). Some of these states were discussed by Greiter et al. (1991, 1992) but not in terms of a generalized CF picture capable of predicting the allowed values of L in the lowest band of energy levels.

Not all the elementary excitations are QP pairs (occupying an excited state FP LL) or QH pairs in the IQL state of Laughlin correlated FPs. We have attempted to interpret spectra which contain other kinds of excitations (e.g. unpaired electrons). In Fig. 16 we show the energy spectrum of a system containing ten electrons in a shell of angular momentum $\ell = 17/2$, interacting through the Coulomb pseudopotential appropriate for LL1 in an ideal quantum well. In addition to $L = 0$ ground state

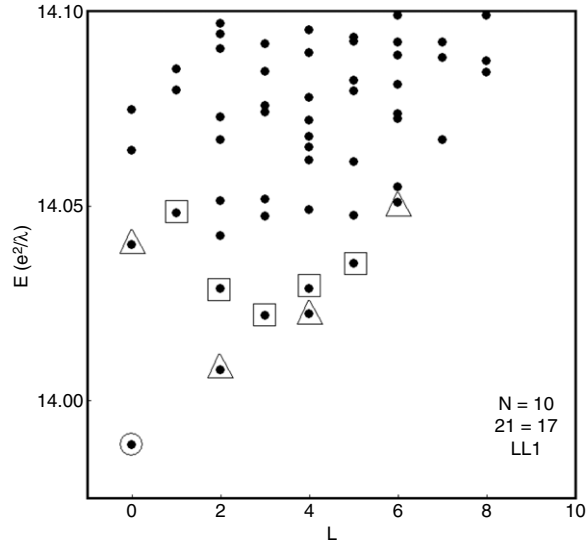


Fig. 16. Energy spectrum for $N = 10$ electrons and $2\ell = 17$ in LL1 for $V_1(\mathcal{R})$ corresponding to zero width quantum well.

corresponding to the IQL with $\nu = 5/2$, there appear to be two low lying bands with $L = 0 \oplus 2 \oplus 4 \oplus 6$ and $L = 1 \oplus 2 \oplus 3 \oplus 4 \oplus 5$ respectively. We suggest that these excitations can be identified using a slight generalization of the composite Fermion picture applied to an intuitive guess at the nature of excitations.

13.6. Generalized CF picture

As we discussed earlier, the ground state in Fig. 16 should contain $N_p = N/2$ pairs. In the absence of correlations the pairs have a charge of $-2e$. If we treat the pairs as Fermions, then the FP angular momentum is given by $\ell_{FP} = (2\ell - 1) - 3(N_p - 1)/2$. In low lying excited states it is possible that one of the ground state pairs breaks up into two unpaired electrons, each with charge $-e$ and angular momentum ℓ . We propose that the FPs and the unpaired electrons have correlations among themselves and with one another. We introduce the correlations in the standard CF way, by attaching CS flux quanta (opposite to the dc magnetic field) to each particle (both CF pairs and unpaired electrons).

We propose a generalized CF approximation to describe the correlations using the following equations:

$$2\ell_{FP}^* = 2\ell_{FP} - 2p_p(N_p - 1) - 2\gamma N_e. \quad (22)$$

$$2\ell_e^* = 2\ell_e - 2p_e(N_e - 1) - \gamma N_p. \quad (23)$$

It is straightforward to understand these correlations using the following simple picture.

1. The effective CS charge on the composite Fermion pairs is thought of as “red” in color and that on the unpaired electrons as “blue”.
2. In Eq. (22) $2p_p$ “red” and 2γ “blue” CS flux quanta are attached to each CF pair.
3. In Eq. (23) $2p_e$ “blue” and γ “red” CS flux quanta are attached to each unpaired electron.
4. The CS charge sense only the CS flux quanta of the same color, and no particle senses the flux attached to itself.

Thus Eq. (22) tells us that the effective angular momentum of one FP is decreased from ℓ_{FP} by p_p times the number of other FPs and by γ times the number of unpaired electrons. Eq. (23) tells us that the effective angular momentum of one unpaired electron is decreased by p_e times the number of other unpaired electrons and by $\gamma/2$ times the number of CF pairs.

We know that this generalization of Jain’s mean-field CF picture results in exactly the same correlations as the adiabatic addition of the CS flux, but that the latter approach needs no mean-field approximation. Note that $2p_{FP}$ and $2p_e$ are even, and that γ can be odd or even. Adding 2γ “blue” fluxes to the CF pair causes the unpaired electron of the “blue” charge to have exactly the same e -CF pair correlations as adding γ “red” fluxes sensed by the CF pair of “red” charge $-2e$ to the unpaired electron. The CS charge times the CS flux must be the same in steps (2) and (3) to obtain the same correlations. Eqs. (22) and (23) define the generalized CF picture in which different types of Fermions, distinguishable from one another, experience correlations which leave them as Fermions (since $2p$ is even) and give the same correlations between members of two different species since the product of CS charge and CS flux added are the same (i.e. $-e \cdot 2\gamma = -2e \cdot \gamma$).

If we apply the generalized composite Fermion (GCF) picture to Fig. 16 we know that the ground state has $N_p = 5$ and $N_e = 0$. Using the GCF equation with $2p_e = 4$ gives $2\ell_{FP}^* = 4$, so that the $N_p = 5$ FPs fill the $\ell_{FP}^* = 2$ shell giving $L = 0$ IQL ground state. We can think of two kinds of elementary excitations. First, one FP might be promoted from $\ell_{FP}^* = 2$ shell

(leaving an FP quasihole in this shell) into the $\ell_{\text{FP}}^* + 1$ shell (i.e. we can excite QEFP–QHFP with $\ell_{\text{QEFP}} = 3$ and $\ell_{\text{QHFP}} = 2$). This would produce a band of states with $1 \leq L \leq 5$. Second, we could have an excited state with $N_{\text{FP}} = 4$ and $N_e = 2$ (i.e. one broken FP). This gives $2\ell_{\text{FP}} = 23$, $2\ell_{\text{FP}}^* = 3$ and $2\ell_{\text{QE}} = 7$ (when $p_p = \gamma = 2$ and $p_e = 1$). The four FPs fill the shell $\ell_{\text{FP}}^* = 3/2$ giving $L_{\text{FP}} = 0$. The two QEs each with $\ell_{\text{QE}} = 7/2$ produce the band $L = 0 \oplus 2 \oplus 4 \oplus 6$. This band is marked by a triangle in Fig. 16, while the FPQE–FPQH band is marked by open squares going from $L = 1$ to $L = 5$. This interpretation is suggestive, but not completely certain because we know neither the QEFP–QHFP interaction nor the pseudopotential $V_{\text{QE}}(L')$ describing the interaction of a QE pair embedded in an IQL state of four FPs. However the assignment of L values fits the numerical results for the low energy excited states with $L \leq 6$.

It is worth noting that for the generalized CF picture (Wójs et al., 1999b) the correlations between a pair of particles can be thought of as resulting from adiabatic addition of fictitious CS flux quanta to one particle that is sensed by a fictitious charge on the other. The correlations among the particles cause pairs to avoid the smallest pair orbits by introducing an effective FP angular momentum ℓ_{FP}^* and an effective electron angular momentum ℓ_e^* given by Eqs. (22) and (23). The allowed values of the total angular momentum are obtained by addition of the angular momenta of N_p identical correlated FPs, each with angular momentum ℓ_{FP}^* to obtain L_{FP} , the total FP angular momentum, and of N_e identical correlated electrons, each with angular momentum ℓ_e^* to obtain the total electron angular momentum L_e . Then L_{FP} and L_e are added as the angular momenta of distinguishable systems to obtain the allowed total angular momentum values L of the system.

Our interpretation is an attempt to understand some of the low lying excitations of the $\nu_1 = 1/2$ state in a simple CF type picture. We present the ideas here, even though they are not firmly established, to motivate additional work on this important topic. We suggest investigating other values of N and 2ℓ , hoping that the generalized CF type picture might fit numerical data and give us better insight. The spectrum is more sensitive to small changes in the pseudopotential $V_1(\mathcal{R})$ than the spectrum in LL0 is to small changes in $V_0(\mathcal{R})$. Not understanding the correlations at $\nu_1 = 1/3$ gives us, at the moment, no hope of understanding the low energy excitations. We are still a long way from knowing anything about the interactions between the elementary excitations in that case.

14. Model pseudopotentials and clusters of j particles

14.1. Energy of clusters of j particles

Thus far we have used the actual Coulomb pseudopotential describing the interaction energy of a pair of electrons in the LL0 and LL1. The pseudopotentials depend on the total pair angular momentum L_2 (or on $\mathcal{R}_2 = 2\ell - L_2$, where ℓ is the angular momentum of the shell in which the electrons reside). They also depend on Landau level index since the antisymmetric wavefunction describing the relative motion of the pair is different for different Landau levels. We have already noted that the energy of the multiplet $|\ell^N; L\alpha\rangle$ is given by

$$E_\alpha(L) = \binom{N}{2} \sum_{L_2} V(L_2) P_{L\alpha}(L_2) \quad (24)$$

where $V(L_2)$ is the pair pseudopotential as a function of pair angular momentum L_2 , and $P_{L\alpha}(L_2)$ is the probability that $|\ell^N; L\alpha\rangle$ contains pairs with pair angular momentum L_2 . The sum in Eq. (24) is over all allowed values of $L_2 = 2\ell - \mathcal{R}_2$, where $\mathcal{R} = 1, 3, 5 \dots$.

For a cluster of j particles, we can define $V(L_j, \beta_j)$ as the interaction energy of the multiplet $|\ell^j; L_j \beta_j\rangle$. It is given by Eq. (24) with (N, L, α) replaced by (j, L_j, β_j) . Clearly one can write for the energy of $|\ell^N; L\alpha\rangle$

$$E_\alpha(L) = a_j \binom{N}{j} \sum_{L_j \beta_j} P_{L\alpha}(L_j, \beta_j) V(L_j, \beta_j). \quad (25)$$

Here $V(L_j, \beta_j)$ is the interaction energy of the electrons in the multiplet $|\ell^j; L_j \beta_j\rangle$ and $P_{L\alpha}(L_j \beta_j)$ is the probability that the multiplet $|\ell^j; L_j \beta_j\rangle$ appears in the eigenfunction $|\ell^N; L\alpha\rangle$ (Simon et al., 2007; Wójs and Quinn, 2005). The coefficient a_j is introduced to avoid overcounting of the number of pairs. We can use Eq. (24) for $V(E_j, \beta_j)$ with (N, L, α) replaced by (j, L_j, β_j) . Making use of identity $P_{L\alpha}(L_2) = \sum_{L_j \beta_j} P_{L_j \beta_j}(L_2) P_{L\alpha}(L_j \beta_j)$, and requiring Eq. (25) to reduce to the results given by (24) gives us the value of a_j ; $a_j = (N - j)!(j - 2)!/(N - 2)!$. Thus we find:

$$E_\alpha(L) = \frac{N(N - 1)}{j(j - 1)} \sum_{L_j \beta_j} P_{L\alpha}(L_j \beta_j) V(L_j, \beta_j). \quad (26)$$

This result gives us the energy of $|\ell^N; L\alpha\rangle$ in terms of the energies $V(L_j \beta_j)$ of j particle multiplets $|\ell^j; L_j \beta_j\rangle$.

It is worth recalling that when the pair pseudopotential $V(L_2)$ is “harmonic” (i.e. $V(L_2) = A + BL_2(L_2 + 1)$, where A and B are constants) the energies of the states $|\ell^j; L_j \beta_j\rangle$ are independent of the multiplet index β_j . Every state with the same value of the j particle angular momentum L_j has the same energy. In addition, the energy increases with L_j as $BL_j(L_j + 1)$. This means that a harmonic $V_H(L_2)$ leads to a harmonic $V_H(L_j)$ given by:

$$V_H(L_j) = A_j + BL_j(L_j + 1). \quad (27)$$

The coefficient B is independent of j , and the constant A_j gives an unimportant overall shift in the energy spectrum. Just as $V_H(L_2)$, the harmonic pair pseudopotential causes no correlations, $V_H(L_j)$, the harmonic pseudopotential of a j -particle cluster also causes no correlations.

14.2. Model pseudopotentials

Many authors (Greiter et al., 1991, 1992; Rezayi and Haldane, 2000; Wójs, 2001a; Wójs and Quinn, 2005) have noted that the most important pseudopotential coefficients are those with small values of \mathcal{R} ($\mathcal{R} = 1, 3, 5, \dots$) corresponding to small pair separations. For example, if the “superharmonic” pseudopotential for LL0 is approximated by $V_0(\mathcal{R}_2) = k\delta(\mathcal{R}_2, 1)$ where $k > 0$, the energy spectra obtained in numerical diagonalization for $1/2 > \nu \geq 1/3$ filling factors are in excellent qualitative agreement with those obtained using the full Coulomb pseudopotential (Quinn et al., 2004b; Wójs, 2001a). By this we mean that IQL states with gaps proportional to k occur at the values of 2ℓ predicted by Jain’s CF picture, in agreement with the numerical results for both Coulomb and model pseudopotentials.

This fact and the behavior of the leading pseudopotential coefficients for electrons in LL0 and LL1, and for CFQEs in CFL1 have led to the introduction of a model two-particle pseudopotential (Wójs, 2001a; Wójs and Quinn, 2005)

$$V_\alpha(\mathcal{R}) = (1 - \alpha)\delta(\mathcal{R}, 1) + \frac{\alpha}{2}\delta(\mathcal{R}, 3). \quad (28)$$

This model pseudopotential mimics the short range behavior of the Coulomb pseudopotential in LL0 if $\alpha = 0$, and in LL1 if α is approximately equal to $1/2$. It also mimics the QE–QE pseudopotential of QEs of the Laughlin $\nu = 1/3$ state (i.e. CFL1 where these QEs reside) if α is approximately equal to unity. Of course, any harmonic contribution to the model potential can be added to the Eq. (28) without any effect on the correlations.

Greiter et al. (1991, 1992) introduced a model three-particle pseudopotential that is equivalent to

$$V(\mathcal{R}_3) = \delta(\mathcal{R}_3, 3). \quad (29)$$

Here L_3 , the total angular momentum of a three-particle cluster, is given by $L_3 = 3\ell - \mathcal{R}_3$. \mathcal{R}_3 is called the three-particle relative angular momentum. GWW showed that their three-particle pseudopotential, which forbids occurrence of compact three-particle droplets with $\mathcal{R}_3 = 3$, had the Moore and Read (1991) Pfaffian state as an exact solution. MR proposed the Pfaffian wavefunctions based on correlation functions used in conformal field theory in order to look for an explanation for the IQL state observed at filling factor $\nu = 5/2$. The proposed Moore–Read Pfaffian wavefunction is to the GWW model pseudopotential exactly what the Laughlin $\nu = 1/3$ wavefunction is to the short range two-particle pseudopotential obtained by taking $\alpha = 0$ in Eq. (28). The $L = 0$ IQL ground state of the Moore–Read wavefunction occurs at $2\ell = 2N - 3$ (and its e–h conjugate $2\ell = 2N + 1$). If the value of 2ℓ is increased, QHs of zero excitation energy appear in the IQL state. When a number of degenerate QH states occur at the same value of total angular momentum L (e.g. if $N_{\text{QH}} = 4$ and $2\ell_{\text{QH}} = 5$ there will be 3 degenerate zero energy states at $L = 4 \oplus 2 \oplus 0$), any normalized linear combination of degenerate states of N_{QH} quasiholes is a perfectly good eigenstate. According to Read and Rezayi (1999) this can lead to new linear combinations of states under permutation of quasiholes that can give rise to non-Abelian statistics. Non-Abelian quasiparticles are of great current interest. Their existence appears to depend on the very special form of the GWW three-particle potential (or on similar pseudopotentials that vanish for relative angular momentum larger than some value). Neither the actual Coulomb pair pseudopotential nor the model pseudopotential given by (28) with α approximately equal to one half give rise to sets of zero energy eigenstates with the same total angular momentum. Although the idea of non-Abelian quasiparticles is very intriguing and of potential value in quantum computing, it isn’t yet clear that such quasiparticles occur in systems with realistic pseudopotentials.

14.3. Model three-body pseudopotential

We know that Eq. (28) mimics the behavior of the short range part of the two-particle pseudopotentials for the lowest Landau level when $\alpha = 0$, for the first excited Landau level when $\alpha \simeq 1/2$, and for the quasielectron of a Laughlin $\nu = 1/3$ state when $\alpha \simeq 1$. The energy spectra obtained using these short range pseudopotentials give reasonably good agreement with those obtained using the full pseudopotentials when filling factor ν is between $1/3$ and $1/2$.

According to Section 14.1

$$V(L_j, \beta_j) = \frac{j(j-1)}{2} \sum_{L_{12}} V(L_{12}) P_{L_j \beta_j}(L_{12}) \quad (30)$$

gives the energy of a j -particle cluster in the multiplet $|\ell^j; L_j \beta_j\rangle$ in terms of the pair pseudopotential and the probability that $|\ell^j; L_j \beta_j\rangle$ has pairs with pair angular momentum L_{12} . If short range interactions dominate in determining the correlations, then we can hope that the small values of $\mathcal{R}_3 = 2\ell - L_3$ in $V(L_3, \beta_3)$ are the important ones in determining the correlations. We have used Eq. (28), the model short range pair pseudopotential, to determine the $V(L_3, \beta_3)$ that it produces through Eq. (30). For $\mathcal{R} \leq 8$, there is only a single allowed multiplet for each value of $L_3 = 3\ell - \mathcal{R}_3$. For $\mathcal{R}_3 \leq 8$, we can think of $V(\mathcal{R}_3)$ as a short range three-particle pseudopotential produced by the pair potential given by Eq. (28). If short range

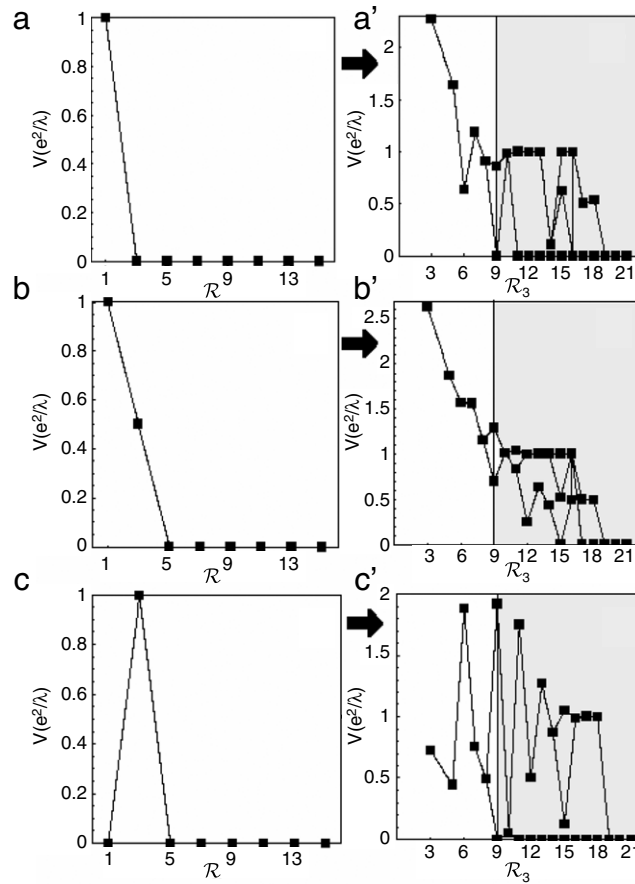


Fig. 17. The three-particle pseudopotentials $V(\mathcal{R}_3)$ (a', b', c') produced from the model pair pseudopotentials $V(\mathcal{R})$ (a, b, c).

interactions are the important ones for determining correlations, we can simply set $V(L_3) = 0$ for $\mathcal{R}_3 > 8$, expecting this portion of the interaction to have little effect on the correlations.

Fig. 17 shows the short range model pair potential for $\alpha = 0, 1/2$, and 1 (frames a, b, c respectively). Frames a', b', c' show the short range pseudopotential resulting from Eq. (30) with $j = 3$. It is worth noting that in the case b', $V(\mathcal{R}_3)$ is slightly superharmonic at $\mathcal{R}_3 = 3$ and has no strong maxima except at $\mathcal{R} = 3$ and no minima for $\mathcal{R} < 9$. In contrast, in c' $V(\mathcal{R}_3)$ has maxima at $\mathcal{R}_3 = 3$ and 6, and a deep minima at $\mathcal{R}_3 = 5$. These two three-body pseudopotentials are quite different, from one another and from frame a'. It seems unlikely that the electrons in LL1 and QEs of the Laughlin $\nu = 1/3$ state have the same correlations. The fact that frame b' has weak superharmonic behavior at $\mathcal{R}_3 = 3$ might support the idea of using the GWW pseudopotential as the simplest (one parameter $V(\mathcal{R}_3 = 3) \neq 0$) three-particle pseudopotential for LL1.

One can easily generalize the very special GWW three-particle pseudopotential to larger clusters. For j Fermions in a shell of angular momentum ℓ , the maximum allowed value of the total j particle angular momentum is $L_j^{\text{MAX}} = j(\ell - \frac{j-1}{2})$. This means that the minimum allowed value of $\mathcal{R}_j = j\ell - L_j$, the relative angular momentum of a j particle cluster is, $\mathcal{R}_j = j\ell - L_j^{\text{MAX}} = j(j-1)/2$. A model j particle pseudopotential given by $V(\mathcal{R}_j) = k\delta(\mathcal{R}_j, \mathcal{R}_j^{\text{MIN}})$ eliminates compact j particle clusters, just as the three-particle GWW pseudopotential eliminated three-particle compact droplets. The eigenstates of this model j particle pseudopotential are referred to as 'paraFermion' states (Read and Rezayi, 1999). It is not clear whether these simple paraFermion states give a reasonable approximation to those obtained with a realistic pseudopotential.

15. Spin polarized quasiparticles in a partially filled composite Fermion shell

15.1. Heuristic picture

In Section 12 we demonstrated that the simplest repulsive anharmonic pseudopotential $V(\mathcal{R}_2) = V_H(\mathcal{R}_2) + k\delta(\mathcal{R}_2, 1)$ caused the lowest energy state for each value of the total angular momentum L to be Laughlin correlated. For a spin polarized LL0 with $1/3 \leq \nu < 2/3$ such a potential (superharmonic at $\mathcal{R} = 1$) gives rise to the Laughlin–Jain sequence of integrally filled CF levels with $\nu_{\pm} = n(2n \pm 1)^{-1}$, where n is an integer. No interaction between the CFs is required. The gaps causing the IQL state are associated with the energy needed to create a QE–QH pair in the CF angular momentum shells. Haldane

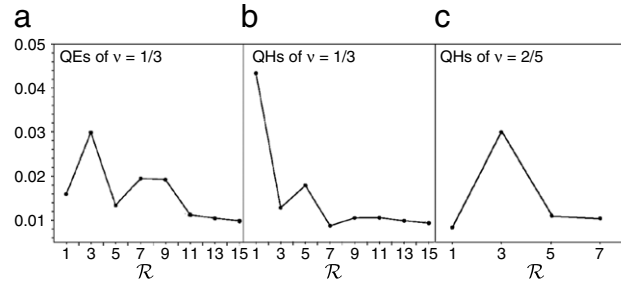


Fig. 18. $V_{QE}(\mathcal{R})$ and $V_{QH}(\mathcal{R})$ for (a) QEs of $\nu = 1/3$ state, (b) QHs of $\nu = 1/3$ state, and (c) QHs of $\nu = 2/5$ state.

Table 2

Values of $\nu_{FP} = m^{-1}$ for $m = 3, 5, 7,$ and 9 and the resulting values of ν_{QE}, ν_{QH} and the electron filling factor that they generate.

ν_{FP}^{-1}	3	5	7	9
ν_{QE}	2/3	1/2	2/5	1/3
ν	5/13	3/8	7/19	4/11
$\nu_{QH}(\text{CF LL1})$	2/3	1/2	2/5	1/3
ν	4/11	3/8	8/21	5/13

(1983) suggested that if the highest occupied CF level is only partially filled, a gap could result from the residual interactions between the QPs, in the same way that the original gap resulted from the electron interactions. However, this would require $V_{QP}(\mathcal{R})$ to be “superharmonic” at $\mathcal{R} = 1$ to give rise to Laughlin correlations. In Section 9 we showed that in a Laughlin $\nu = 1/3$ or $1/5$ state $V_{QE}(\mathcal{R})$ was not superharmonic at $\mathcal{R} = 1$ and $\mathcal{R} = 5$, and that V_{QH} was not at $\mathcal{R} = 3$. This means that many of the novel IQL states observed by Pan et al. (2003) have to result from correlations among the electrons that are quite different from the Laughlin correlations.

Just as electrons in LL1 tend to form clusters (pairs with pair angular momentum $\ell_p = 2\ell - 1$ or larger clusters), we expect QPs in CF LL1 to tend to form pairs or larger clusters. The major differences between electrons in LL1 and QPs in CF LL1 are: (i) the pseudopotential $V_1(L')$ for electrons in LL1 (shown in Fig. 9) is an increasing function of L' , but it is not superharmonic at $\mathcal{R} = 1$, while $V_{QE}(L')$ is strongly subharmonic having a maximum at $\mathcal{R} = 2\ell - L' = 3$ and minima at $\mathcal{R} = 1$ and 5 and (ii) the e–h symmetry of LL1 is not applicable to QEs and QHs in CF LL1 (Wójs, 2001b). The QEs are quasiparticles of the Laughlin $\nu = 1/3$ IQL state, while QHs in CF LL1 are actually quasiholes of the Jain $\nu = 2/5$ state. The QE and QH pseudopotentials in frames (a) and (c) are similar, but not identical as shown in Fig. 18. The QEs of $\nu = 1/3$ state and QHs of the $\nu = 2/5$ state reside in CF LL1. The QHs of the $\nu = 1/3$ state reside in CF LL0.

The experimental results of Pan et al. (2003) suggest that the novel $\nu = 4/11$ IQL ground state is fully spin polarized. In numerical studies testing their CF hierarchy picture, Sitko et al. (1996, 1997) found that this spin polarized IQL state did not occur at $\nu_{QE} = 1/3$. They suggested that the reason for this was related to the difference between $V_{QE}(L')$, the QE pseudopotential describing the residual interactions between the CFQEs, and $V_0(L')$, the pseudopotential describing the interactions between electrons in LL0. It was later shown that because $V_{QE}(L')$ is not superharmonic at $\mathcal{R}' \equiv 2\ell - L' = 1$, the CF picture could not be reapplied to interacting QEs in the partially filled CF shell (Wójs and Quinn, 2000d). This led to the suggestion (Park and Jain, 2000) that the QEs forming the daughter state had to be spin reversed and reside in CF LL0 as quasielectrons with reverse spin (QERs). Szlufarska et al. (2001) evaluated $V_{QER}(L')$, the pseudopotential of QERs. They showed that $V_{QER}(L')$ was superharmonic at $\mathcal{R} = 1$, so that unlike majority spin QEs, they could support Laughlin correlations at $\mathcal{R} = 1$.

This leaves at least two possible explanations of the $\nu = 4/11$ IQL state. It could be a Laughlin correlated daughter state of spin reversed QEs (i.e. QERs), or it could be a spin polarized state in which the QEs form pairs or larger clusters. In a later section we compare the energies of these two states. The total energies involve the QE (or QER) energies, the interaction energies of the QEs (or QERs), and the Zeeman energy. For the moment let’s look at the completely polarized case.

The simplest idea is exactly that used for electrons in LL1. There, the $\nu_1 = 1/2$ state could be attributed to the formation of pairs with $\ell_p = 2\ell - 1$, where ℓ is the angular momentum of the shell occupied by electrons. If we assume that the QEs form pairs and treat them as Fermions, then Eqs. (22) and (23) give us the relation between the “effective FP angular momentum” ℓ_{FP} , and the QE angular momentum ℓ , and the relation between the “effective FP filling factor” ν_{FP} , and the QE filling factor ν . If we take ν_{FP} equal to m^{-1} , where m is an odd integer, we can obtain the value of ν_{QE} corresponding to the Laughlin correlated state of FPs (pairs of quasielectrons with $\ell_p = 2\ell - 1$). Exactly the same procedure can be applied to QHs in CF LL1 since $V_{QE}(\mathcal{R})$ and $V_{QH}(\mathcal{R})$ are qualitatively similar at small values of \mathcal{R} . Here we are assuming that $V_{QE}(\mathcal{R})$ and $V_{QH}(\mathcal{R})$ are dominated by their short range behavior $\mathcal{R} \leq 5$. The QH pseudopotential is not as well determined for $\mathcal{R} > 5$ because it requires larger N electron systems than we can treat numerically. The electron filling factor is given by $\nu^{-1} = 2 + (1 + \nu_{QE})^{-1}$ or by $\nu^{-1} = 2 + (2 - \nu_{QH})^{-1}$. This results in the values of ν shown in Table 2 for $2/3 \geq \nu_{QP} \geq 1/3$.

The states generated at the values of ν_{QE} and ν_{QH} equal to $2/5$ have not been observed. Clear IQL states were observed by Pan et al. at $\nu = 3/8$ and $\nu = 4/11$. A somehow weaker IQL state at $\nu = 5/13$ is also observed.

Table 3

Values of ν_{QH} satisfying $1/3 > \nu_{\text{QH}} \geq 1/5$ and the resulting electron filling factors ν for LC QP₂s with $\nu_{\text{FP}}^{-1} = 7, 9, 11, 13$.

ν_{FP}^{-1}	7	9	11	13
ν_{QH}	2/7	1/4	2/9	1/5
ν	5/17	3/10	7/23	4/13

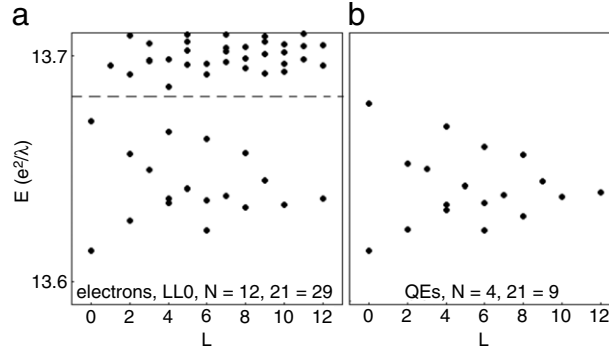


Fig. 19. Energy spectra for $N = 12$ electrons in the lowest LL with $2\ell = 29$ and for $N = 4$ QEs in the CF LL1 with $2\ell = 9$. The energy scales are the same, but the QE spectrum obtained using $V_{\text{QE}}(\mathcal{R})$ is determined only up to an arbitrary constant.

The daughter states generated by QPs in CF LL1 (QEs of the parent $\nu = 1/3$ Laughlin state or QHs of the parent $\nu = 2/5$ Jain state) give rise to filling factors for the electron system with $\nu > 1/3$. QHs of the $\nu = 1/3$ Laughlin state (residing in CF LL0) can also form daughter states, and they result in an electron filling factor ν in the range $1/3 > \nu \geq 1/5$. The pseudopotential for these QHs is superharmonic at $\mathcal{R} = 1$ and has a strong minimum at $\mathcal{R} = 3$. Because of this, if they form pairs, the pairs must have angular momentum $\ell_p = 2\ell - 3$ (instead of $\ell_p = 2\ell - 1$ for QE pairs). Eqs. (22) and (23) must be modified. We then replace $2\ell - 1$ in Eq. (22) by $2\ell - 3$, and γ_F by $\tilde{\gamma}_F$. The value of $\tilde{\gamma}_F$ is determined by requiring that $\nu_{\text{FP}} = 1$ when $\nu_{\text{QH}} = 1/2$. This condition results from the fact that the pairs are formed by two QHs separated by two filled CF states. The resulting value of $\tilde{\gamma}_F$ is 7, so Eq. (21) is replaced by:

$$\nu_{\text{FP}}^{-1} = 4\nu_{\text{QH}}^{-1} - 7. \quad (31)$$

The QH daughter states resulting from Laughlin correlated QH₂ (pairs of QHs of the $\nu = 1/3$ state) and the electron filling factor satisfying $\nu^{-1} = 2 + (1 - \nu_{\text{QH}})^{-1}$ are given in Table 3.

15.2. Numerical studies of spin polarized QP states

Standard numerical calculations for N_e electrons are not useful for studying such new states as $\nu = 4/11$, because convincing results require large values of N_e . Therefore we take advantage of the knowledge (Lee et al., 2001, 2002; Sitko et al., 1996; Wójs and Quinn, 2000d) of the dominant features of the pseudopotential $V_{\text{QE}}(\mathcal{R})$ of the QE–QE interaction (i.e., the QE–QE interaction energy V_{QE} as a function of relative pair angular momentum \mathcal{R}), and diagonalize the (much smaller) interaction Hamiltonian of N_{QE} systems. This procedure was earlier (Sitko et al., 1996) shown to reproduce accurately the low energy N_e -electron spectra at filling factors ν between $1/3$ and $2/5$. It was also used in a similar, many-QE calculation by Lee et al. (2001, 2002) (who, however, have not found support for QE clustering).

One might question whether using the pair pseudopotential for QPs obtained by diagonalization of a finite system of N electrons (containing two QEs or two QHs) gives a reasonable accurate description of systems containing more than a few QPs. We have attempted to account for finite size effects (Szufarska et al., 2001; Wójs, 2001b; Wójs and Quinn, 2000d; Wójs et al., 2006b) by plotting the values of $V_{\text{QP}}(\mathcal{R})$ for each value of \mathcal{R} as a function of N^{-1} , where N is the number of electrons in the system that produced the two CFQPs (Xie et al., 1993). We extrapolate $V_{\text{QP}}(\mathcal{R})$ to the macroscopic limit. In addition, the low energy spectra of an N electron system (obtained by diagonalization of $V_0(\mathcal{R})$) that contains N_{QP} quasiparticles is compared with the spectrum of N_{QP} quasiparticles [obtained by diagonalization of $V_{\text{QP}}(\mathcal{R})$]. The results for $(N, 2\ell) = (12, 29)$ and $(N_{\text{QE}}, 2\ell_{\text{QE}}) = (4, 9)$ are shown in Fig. 19.

A CF transformation on the $(N, 2\ell) = (12, 29)$ electron system gives an effective CF angular momentum ℓ^* satisfying $2\ell^* = 2\ell - 2(N - 1) = 7$. Eight of the 12 CFs fill the shell $\ell^* = 7/2$, leaving the four CFQEs in the shell of $\ell^* = 9/2$. Although the four QE spectrum is not identical to the low energy band of the 12 electron spectrum, it is clearly a rather good approximation. Both spectra have an $L = 0$ ground state, but the gaps are somewhat different in size. The fact that $(2\ell_{\text{QE}}, N_{\text{QE}})$ system has an $L = 0$ ground state at $2\ell_{\text{QE}} = 3N_{\text{QE}} - 3$ led a number of researchers (Chang and Jain, 2004; Goerbig et al., 2006, 2004; López and Fradkin, 2004) to suggest that it represented a second generation of CFs giving rise to a daughter state and resulting $\nu = 4/11$ spin polarized IQL state observed by Pan et al. (2003). This idea can't be correct

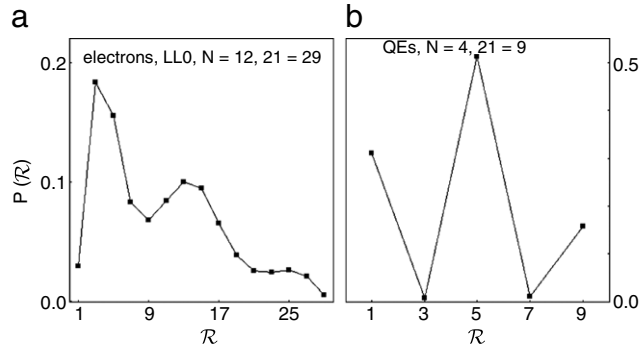


Fig. 20. Pair probability functions $P(\mathcal{R})$ for the two ground states shown in Fig. 19.

because $V_{\text{QE}}(L')$ is not superharmonic at $\mathcal{R} = 1$ and cannot cause a Laughlin correlated CF daughter state of spin polarized QEs. In Fig. 20, we show the pair probability $P(\mathcal{R})$ versus \mathcal{R} for the $(N, 2\ell) = (12, 29)$ electron ground state and for the $(N_{\text{QE}}, 2\ell_{\text{QE}}) = (4, 9)$ QE daughter state. Because the latter has $P(\mathcal{R})$ with maxima at $\mathcal{R} = 1$ and 5, and minima at $\mathcal{R} = 3$ and 7 it is certainly not a Laughlin correlated state of QEs. In fact it is a $\nu_{\text{QE}} = 1/2$ state at $2\ell_{\text{QE}} = 2N_{\text{QE}} + 1$ (the conjugate of $2\ell_{\text{QE}} = 2N_{\text{QE}} - 3$).

The fact that the magnitude of $V_{\text{QE}}(\mathcal{R})$ is only about one fifth as large as the energy necessary to create an additional QE–QH pair in a Laughlin correlated state permits diagonalization in the subspace of the partially filled QE Landau level with reasonably accurate results (see e.g., Fig. 19). For situations in which the width of the band of two QP states is closer to the energy needed to create a QE–QH pair, higher bands (or higher QP LL) cannot be neglected. In such cases the pseudopotential $V(L_j\beta_j)$, describing the interaction energy of a multiplet $|\ell^j; L_j\beta_j\rangle$ containing j particles in a state of total angular momentum L_j , may be useful in accounting for the large Hilbert space needed for a more accurate diagonalization (and more accurate description of correlations) of a many-particle system.

The value of 2ℓ at which the IQL state at filling factor ν occurs in the spherical geometry is given by $2\ell = \nu^{-1}N + \gamma(\nu)$, where N is the number of particles and $\gamma(\nu)$ is a finite size effect shift (Haldane, 1983). For Laughlin correlated electrons in LL0 at filling factor ν equal to the inverse of an odd integer, $\gamma(\nu) = -\nu^{-1}$, so that the $\nu = 1/3$ IQL states occur at $2\ell = 3N - 3$. For quasielectrons of Laughlin $\nu = 1/3$ state, an IQL state occurs at $(N, 2\ell) = (4, 9)$.

As mentioned earlier, we believe that because QEs will not support Laughlin correlations at $\nu = 1/3$, it is an “aliased” state (Morf, 1998; Morf et al., 2002) at $2\ell = 2N + 1$ (conjugate to $2\ell = 2N - 3$) that supports pairing correlations. By “aliased” states we mean two states with the same values of N and 2ℓ that belong to different sequences $2\ell = \nu^{(-1)}N + \gamma(\nu)$. Different values of $\gamma(\nu)$ for IQL states of electrons in LL0 and QEs in CFLL1 suggest that the QE correlations are different from the Laughlin correlations for electrons in LL0. It also gives emphasis to how important it is to carry out numerical calculations for many different values of 2ℓ for each value of the particle number N , instead of assuming the value of $\gamma(\nu)$ at which the IQL state is expected.

The essential information about the interaction of particles confined to some Hilbert space can be obtained by defining the value of interaction energy for all allowed pair states. For charged particles confined to an LL in the presence of a magnetic field, the relative motion is strongly quantized. The orbital pair eigenstates can be labeled with a single discrete quantum number, relative angular momentum \mathcal{R} . This number is a non-negative integer; it must be odd (even) for a pair of identical Fermions (Bosons), and it increases with increasing average distance $\sqrt{\langle r^2 \rangle}$ between the two particles.

The pair interaction energy of two QPs, the QP pseudopotential $V_{\text{QP}}(\mathcal{R})$, determines the correlations between QPs. On a spherical surface, $\mathcal{R} \leq 2\ell$, where ℓ is the angular momentum of the QP shell. Thus the number of pseudopotential parameters is finite. However, even in an infinite (planar) system, only those few leading parameters at the values of \mathcal{R} corresponding to the average distance not exceeding the correlation length ξ are of significance (provided that the correlations are indeed characterized by finite $\xi \sim \lambda$).

15.3. Numerical spectra

We begin with numerical results for the spectrum $E_\alpha(L)$ and the ground state pair probability $P(\mathcal{R})$ of a system of N quasielectrons in a shell of angular momentum $\ell = 17/2$. \mathcal{R} is the relative angular momentum of a pair $\mathcal{R} = 2\ell - L'$, where L' is the total angular momentum of the pair. We observe in Fig. 21(a) that there is an $L = 0$ ground state separated by a gap from the lowest excited states.

The spectrum is obtained by exact diagonalization (within the subspace of CF LL1) of the N quasielectron system interacting through the pseudopotential coefficients $V_{\text{QE}}(\mathcal{R})$ represented in Fig. 9(c) by triangles. The solid circles in Fig. 21 show $P(\mathcal{R})$ the probability that a QE pair has relative angular momentum \mathcal{R} in the $L = 0$ ground state. The solid circles in Fig. 21 (b) show $P(\mathcal{R})$, the probability that a QE pair has relative angular momentum \mathcal{R} in the $L = 0$ ground state. The open circles in Fig. 21(b) show, for contrast, $P(\mathcal{R})$ for ten electrons in LL0 interacting via the Coulomb interaction. The maxima in

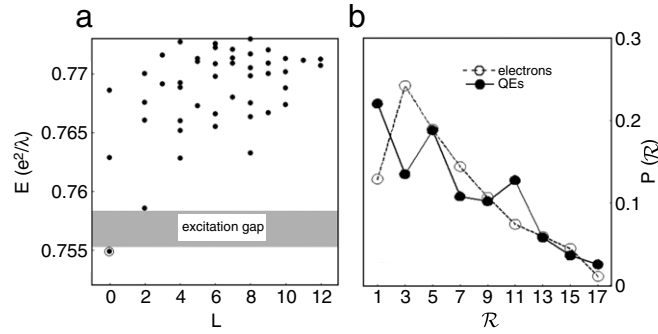


Fig. 21. (a) Energy spectrum as a function of total angular momentum L of 10 QEs at $2\ell = 2N - 3 = 17$ corresponding to $\nu_{\text{QE}} = 1/2$ and $\nu = 3/8$. It is obtained in exact diagonalization in terms of individual QEs interacting through the pseudopotential shown in Fig. 9(c) (triangles) (b) Coefficient of $P(\mathcal{R})$, the probability associated with pair states of relative angular momentum \mathcal{R} , for the lowest $L = 0$ state. The solid dots are for 10 QEs of the $\nu_{\text{QE}} = 1/2$ state in a shell of angular momentum $\ell = 17/2$. The open circles are for 10 electrons in the LL0 at $\ell_0 = 17/2$ (Quinn et al., 2004b).

$P(\mathcal{R})$ at $\mathcal{R} = 1$ and 5 and the minimum at $\mathcal{R} = 3$ for the QE system are in sharp contrast to the Laughlin correlated $P(\mathcal{R})$ of the ten electron system in LL0. The QE maximum at $\mathcal{R} = 1$ and minimum at $\mathcal{R} = 3$ suggests formation of QE pairs with $\ell_p = 2\ell - 1$ and the avoidance of pairs with $\mathcal{R} = 2\ell - L' = 3$, the pair state with the largest repulsion. This IQL ground state occurs at $2\ell = 2N - 3$ and corresponds to $\nu_{\text{QE}} = 1/2$ and $\nu = 3/8$.

For $\nu_{\text{QP}} = 1/2$ an IQL ground state should occur at the conjugate value of 2ℓ given by $2\ell = 2N - 3$ and $2N + 1$. Thus Fig. 21 can be thought of as $N_{\text{QP}} = 10$ or $N_{\text{QP}} = 8$, the former corresponding to $2\ell = 2N - 3$ and the latter to $2\ell = 2N + 1$. We have already mentioned that QEs in the CFLL1 are Laughlin QEs of the $\nu = 1/3$ IQL, while QHs in the CFLL1 are QHs of the Jain $\nu = 2/5$ state. It seems reasonable to diagonalize $V_{\text{QP}}(\mathcal{R})$ for QHs when CFLL1 is more than half filled and for QEs when it is less than half filled. If only $V_{\text{QP}}(\mathcal{R})$ for $\mathcal{R} \leq 5$ is important, $V_{\text{QE}}(\mathcal{R})$ and $V_{\text{QH}}(\mathcal{R})$ are qualitatively similar (but not identical). We should then expect the same correlations independent of which $V_{\text{QP}}(\mathcal{R})$ is used in the numerical diagonalization. This would suggest that Fig. 21 be interpreted as containing $N_{\text{QH}} = 8$ and $2\ell = 2N_{\text{QH}} + 1 = 17$ instead of as $N_{\text{QE}} = 10$ and $2\ell = 2N - 3 = 17$.

In Fig. 22 we display spectra for $N = 10, 12$, and 14 QEs in angular momentum shells with various values of ℓ ($2\ell = 21, 23, 25$, and 27). In frames (a) and (c) the ground states occur at total angular momentum $L = 6$ and $L = 8$ respectively. They are not IQL ground states. Frames (b) and (d) have $L = 0$ ground states separated from the low energy excitations by a substantial gap. For frame (b) $2\ell = 3N - 7$, and for frame (d) $2\ell = 2N - 3$. These are the values for which we find QE daughter states with $\nu_{\text{QE}} = 1/3$ and $\nu_{\text{QE}} = 1/2$ respectively. Using $\nu^{-1} = 2 + (1 + \nu_{\text{QE}})^{-1}$ gives the value $\nu = 4/11$ and $\nu = 3/8$ for these two states. It is worth mentioning that the N_{QE} quasielectron systems used in studying the energy spectra in Fig. 22 arise from much larger electron systems after a CF transformation was applied. For example it can be seen that frame (d) results for $(N_e, 2\ell_e) = (38, 97)$ by noting that $2\ell^* = 2\ell_e - 2(N_e - 1) = 23$. This lowest CF shell can hold $2\ell^* + 1 = 24$ of the CFs; the remaining 14 become CFQEs in CF LL1 with angular momentum $2\ell_{\text{QE}}^* = 2(\ell^* + 1) = 25$. This $(N_e, 2\ell_e) = (38, 97)$ is far too large to study numerically, but $(2\ell_{\text{QE}}, N_{\text{QE}}) = (25, 14)$ can be handled without difficulty.

We have calculated similar $(2\ell, N)$ spectra for up to 14 QEs at filling factors $\nu_{\text{QE}} \sim N/(2\ell + 1)$ between 1/2 and 1/3. Note that the assignment of the filling factor to a finite system $(2\ell, N)$ is not trivial, and it depends on the form of correlations. As discussed earlier, the $(2\ell, N)$ sequences that correspond in the thermodynamic limit to a filling factor ν are described by a linear relation,

$$2\ell = \nu^{-1}N - \gamma(\nu), \quad (32)$$

where the “shift” $\gamma(\nu)$ depends on the microscopic nature of the many-body state causing incompressibility at this ν . For example, the sequence of finite-size nondegenerate ($L = 0$) ground states that extrapolates to $\nu = 1/3$ occurs at $2\ell = 3N - 3$ for the Laughlin state, at $2\ell = 3N - 5$ for the Laughlin correlated state of Fermion pairs (Quinn et al., 2003b; Wójs, 2001b; Wójs and Quinn, 2002a; Wójs et al., 2003) and at $2\ell = 3N - 7$ for the incompressible QE state identified below.

In Table 4 we present the excitation gaps obtained for the QE systems with various values of N and 2ℓ . The table should be symmetric under the replacement of N by $2\ell + 1 - N$ which reflects the particle–hole symmetry in a partially filled QP shell (i.e., in CF LL1). This symmetry is only approximate in real systems. The largest of the gaps Δ (those shown in boldface) occur for the following two sequences: $2\ell = 3N - 7, 2N - 3$ (and its e - h conjugate $2\ell = 2N + 1$), corresponding to $\nu_{\text{QE}} = 1/3$ and 1/2. Using Eq. (9), these values can be converted to the electron filling factors $\nu = 3/8, 4/11$, and 5/13.

The dependence of the excitation gaps Δ on the QE number N for the $\nu_{\text{QE}} = 1/3$ series at $2\ell = 3N - 7$ (full dots) and for the $\nu_{\text{QE}} = 1/2$ series at $2\ell = 2N - 3$ (open circles) is plotted in Fig. 23. It is difficult to extrapolate accurately our finite-size data to the thermodynamic limit to predict the magnitude of Δ in an infinite (planar) system. However, we believe that the series of finite-size nondegenerate ground states occurring at $2\ell = 2N + 1$ (or $2\ell = 2N - 3$) describe the FQH state observed experimentally at $\nu = 3/8$. The series at $2\ell = 3N - 7$ is less certain. It shows large oscillations over the limited range of N values for which we can calculate, and we do not know if this series persists to the thermodynamic limit.

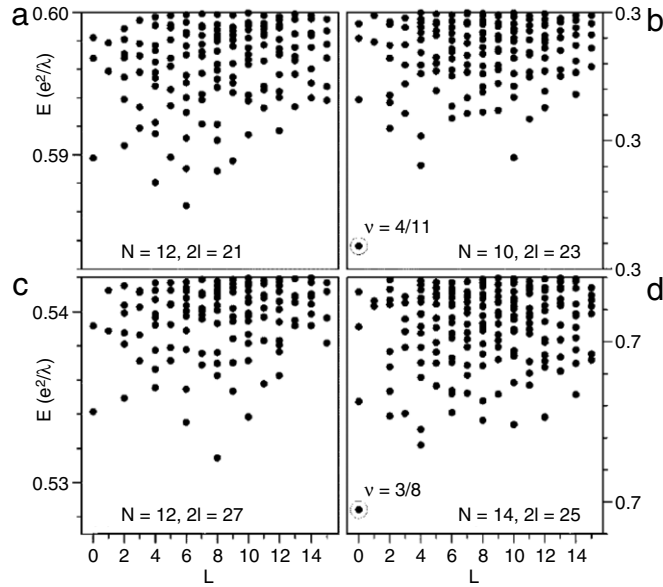


Fig. 22. Energy spectra of up to $N = 14$ QEs in LL shells with various degeneracies $2\ell + 1$, calculated using the pseudopotentials shown in Fig. 9(c) (Wójs et al., 2004).

Table 4

Excitation gaps Δ in units of $10^{-3}e^2/\lambda$, above the nondegenerate ($L = 0$) ground state of N QEs each with angular momentum ℓ , interacting through pseudopotential in Fig. 9(c). Circles \circ mark degenerate ($L \neq 0$) ground states. The values in boldface are the largest; they all belong to the three $(N, 2\ell)$ sequences corresponding to $\nu_{QE} = \frac{1}{2}, \frac{1}{3}$, and $\frac{2}{3}$.

$N^{2\ell}$	17	18	19	20	21	22	23	24	25	26	27	28	29
8	4.71	\circ	\circ	\circ	0.01								
9	\circ	\circ	\circ	5.47	\circ	\circ	\circ	1.18					
10	4.71	\circ	\circ	\circ	\circ	\circ	6.29	\circ	0.81	\circ	\circ	\circ	\circ
11	\circ	\circ	\circ	\circ	\circ	\circ	\circ	\circ	\circ	6.07	\circ	\circ	\circ
12		\circ	\circ	5.47	\circ	\circ	0.37	\circ	4.02	\circ	\circ	\circ	5.28
13			\circ	\circ	\circ	\circ	\circ	\circ	\circ	\circ	\circ	\circ	\circ
14				0.01	\circ	\circ	6.29	\circ	4.02	\circ	\circ	\circ	\circ
15							\circ	\circ	\circ	\circ	\circ	\circ	\circ
16								1.18	0.81	6.07	\circ	\circ	\circ
17										\circ	\circ	\circ	\circ
18											\circ	\circ	5.28

In our numerical studies the $\nu_{QP} = 1/2$ state occurs only when the number of QPs is even, suggesting that QP pairs are formed. However, IQL states are formed only when the number of minority QPs in CFLL1 is 8 or 12, but not when it is 10 or 14. This could indicate that the CF pairs form quartets (i.e. pairs of CF pairs) in the IQL state. This is completely speculative since we have very little knowledge of the pseudopotential describing the interaction between CF pairs. For $\nu_{QE} = 1/3$, a gap occurs at all values of N between 6 and 12. Even values of N can be made up of pairs; $N = 8$ and 12 can give states containing quartets (pairs of pairs); $N = 6, 9$, and 12 could contain triplets. We have not yet attempted to explore IQL states containing clusters of different sizes (single QEs, CF pairs, triplets, etc.) that would be needed to obtain IQLs at $N = 7$ and 11. The effect of different cluster sizes might be responsible for large variations in the gap for $\nu_{QE} = 1/3$ with N .

The “shift” defined by Eq. (32) and describing the $2\ell = 3N - 7$ sequence identified here ($\gamma = 7$) is different not only from $\gamma = 3$ describing a Laughlin state, but also from $\gamma = 5$ that results for a Laughlin state of Fermion pairs. This precludes the interpretation of these finite-size $\nu_{QE} = 1/3$ ground states found numerically (and also of the experimentally observed $\nu = 4/11$ FQH state) as a state of Laughlin correlated pairs of QEs (i.e., particles in the partially filled CF LL1). However, it is far more surprising that paired state of QEs turns out as an invalid description for these states as well. Clearly, the correlations between the pairs of QEs at $\nu_{QE} = 1/3$ must be of a different, non-Laughlin type, and we do not have an alternative explanation for the incompressibility of this state.

While we do not completely understand the correlations between QEs at $\nu_{QE} = 1/3$, it may be noteworthy that the value of $\gamma = 7$ appropriate for the series of incompressible states found here can be obtained for the Laughlin state of QE triplets (QE_3 s), each with the maximum allowed angular momentum, $L = 3\ell - 3$, or of quartets (made up of pairs of pairs) with maximum allowed angular momentum of the quartet $\ell_Q = 4\ell - 10$. The quartet state can be thought of as consisting of

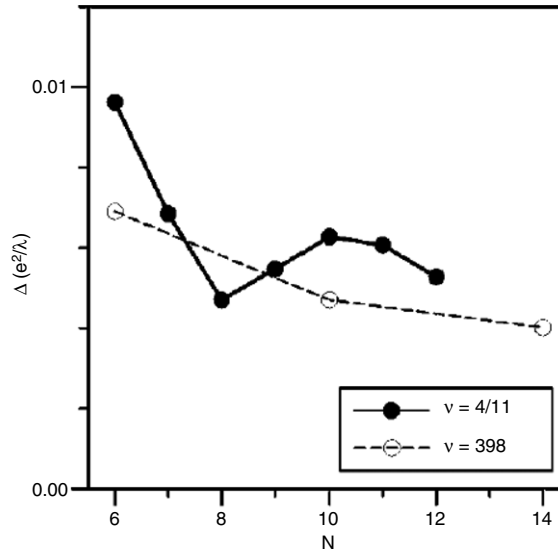


Fig. 23. Excitation gap Δ for the $\nu_{\text{QE}} = \frac{1}{3}$ series of N QE ground states at $2\ell = 3N - 7$ (full dots) and for the $\nu_{\text{QE}} = \frac{1}{2}$ series at $2\ell = 2N - 3$ (open circles), plotted as a function of the QE number, N (Wójs et al., 2004).

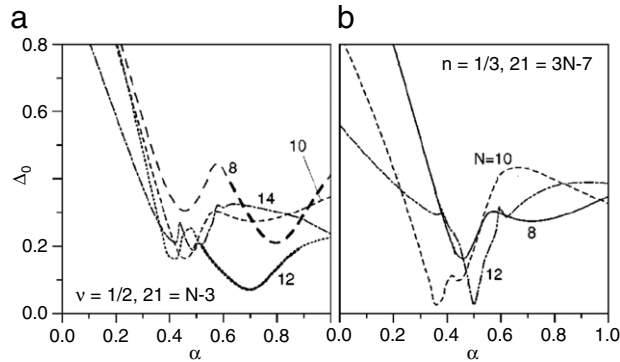


Fig. 24. The excitation gap Δ_0 between the lowest and the first excited states in the $L = 0$ subspace of N particles on Haldane sphere with the values of 2ℓ corresponding to $\nu = \frac{1}{2}$ (a) and $\nu = \frac{1}{3}$ (b), plotted as a function of the interaction of parameter α defined by Eq. (28) (Wójs et al., 2004).

four filled states ($\ell, \ell - 1, \ell - 4, \ell - 5$) separated by two empty states ($\ell - 2, \ell - 3$). Both of these heuristic pictures give $2\ell = 3N - 7$ for the $\nu = 1/3$ state.

15.4. Results from model interactions

In this section we present the results of similar calculations, obtained using the model pseudopotential given by Eq. (28). It is known (Wójs, 2001b; Wójs and Quinn, 2002a) that the correlations characteristic of electrons in the partially filled LL0 and LL1 are accurately reproduced by $V(\mathcal{R}_2)$ given by Eq. (28) with $\alpha \approx 0$ and $1/2$, respectively. Similarly, by the comparison of pair amplitudes, we have confirmed that this model pseudopotential with $\alpha \approx 1$ causes correlations characteristic of QEs in their partially filled LL. We have repeated the diagonalization of a few finite systems with $2\ell = 2N - 3$ (or $2N + 1$) and $3N - 7$, for α varying between 0 and 1, in order to answer the following two questions. First, to what extent is the stability of the identified $\nu = 3/8$ and $4/11$ states affected by the (quantum well width dependent) details of the QE–QE interaction? And second, does a phase transition occur for values of α between $1/2$ and 1, indicating a different origin of the incompressibility of the $\nu = 3/8$ and $4/11$ states and their electron counterparts (in LL1) at $\nu = 5/2$ and $7/3$? The latter question is naturally motivated by our observation that the $2\ell = 2N + 1$ sequence of nondegenerate ground states occurs only for $N = 8$ and 12 , in contrast to the situation in LL1 where they occurred for any integral value of $N/2$.

In Fig. 24 we plot the $L = 0$ excitation energy gap Δ_0 (difference between the two lowest energy levels at $L = 0$), as a function of α . A minimum in $\Delta_0(\alpha)$ suggests a (forbidden) level crossing, i.e., a phase transition in the $L = 0$ subspace. Such minima occur near $\alpha = 1/2$ for all values of N and for both $2\ell = 2N - 3$ and $3N - 7$. They reveal destruction of Laughlin correlations that occur for small α (e.g., for electrons in LL0) and formation of incompressible $\nu = 1/2$ and $1/3$

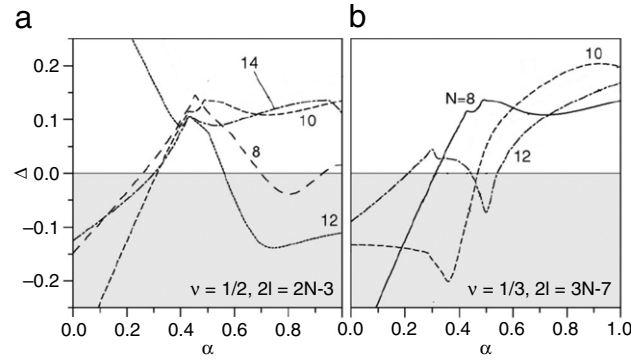


Fig. 25. The excitation gap Δ from the lowest state with $L = 0$ to the lowest state with $L \neq 0$ for N particles on Haldane sphere with values of 2ℓ corresponding to $\nu = \frac{1}{2}$ (a) and $\nu = \frac{1}{3}$ (b), plotted as a function of the interaction of parameter α defined by Eq. (28) (Wójs et al., 2004).

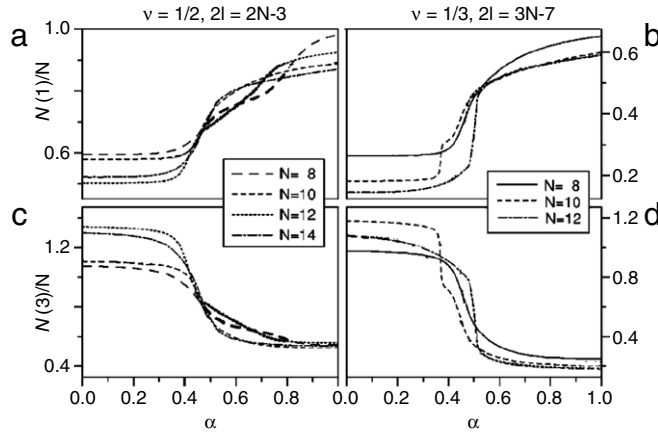


Fig. 26. The average number of pairs with relative angular momentum $\mathcal{R} = 1$ (a, b), and $\mathcal{R} = 3$ (c, d) per particle, $\mathcal{N}(\mathcal{R})/N$, calculated for the lowest state in the $L = 0$ subspace of N particles on Haldane sphere with values of 2ℓ corresponding to $\nu = 1/2$ (a, c), and $\nu = 1/3$ (b, d) plotted as a function of the interaction of parameter α defined by Eq. (28) (Wójs et al., 2004).

states of a different (paired) character that occur for $\alpha \approx 1/2$ (e.g., for electrons in LL1). In Fig. 24(a), similar strong minima occur at $\alpha \approx 0.7$ for $N = 8$ and 12 (marked with thick lines). This is consistent with our observation that the correlations between the QEs and between the electrons in LL1 (both at the half filling) are different. In Fig. 24(a) and (b), additional weaker minima between $\alpha = 1/2$ and 1 appear also for other combinations of N and 2ℓ . This confirms that the $\nu = 1/2$ and $1/3$ incompressible states of QEs are generally different from those of the electrons in LL1, despite the fact that they both usually occur at the same values of $2\ell = 2N + 1$ and $3N - 7$ in the finite systems.

The absolute excitation gaps $\Delta(\alpha)$ of the $L = 0$ ground states (difference between the lowest energies at $L \neq 0$ and $L = 0$) are shown in Fig. 25. The negative value of Δ means that the absolute ground state is degenerate (i.e., $L \neq 0$), and the abrupt changes in the slope of $\Delta(\alpha)$ occur whenever level crossings occur for the lowest $L \neq 0$ state. Clearly, except for $N = 8$ and 12 with $2\ell = 2N - 3$, the lowest $L = 0$ states remain the absolute ground states of the system in the whole range of α between $1/2$ and 1. This shows that the incompressibility of the $\nu_{\text{QE}} = 1/2$ and $1/3$ ground states will not be easily destroyed in experimental systems by a minor deviation from the model QE–QE pseudopotential used here in the numerical diagonalization.

Let us finally examine the dependence of the leading pair amplitudes, $P(1)$ and $P(3)$, on α . In Fig. 26 we plot the number of pairs, $\mathcal{N}(\mathcal{R}) = \frac{1}{2}N(N-1)P(\mathcal{R})$ divided by N . A transition from Laughlin correlations at $\alpha = 0$ to pairing at $\alpha = 1/2$ and possibly grouping into larger clusters at $\alpha \sim 1$ is clearly visible in each curve. It is also confirmed that just as the Laughlin ground state remains virtually insensitive to the exact form of the interaction pseudopotential V_ℓ as long as it is strongly superharmonic at short range, the correlations in the $\nu_{\text{QE}} = 1/2$ and $1/3$ states are quite independent of the details of the QE–QE interaction, as long as V_{QE} is strongly subharmonic at short range. This result supports our expectation that the incompressible QE ground states found here numerically indeed describe the FQH $\nu = 3/8$ and $4/11$ electron states observed in experiment. On the other hand, correlations at $\alpha \approx 1/2$ (electrons in LL1), characterized by having $P(1) \approx P(3)$, are quite different from those at $\alpha \sim 1$ (QEs), characterized by having the minimum possible $P(3)$, much smaller than $P(1)$. Finally, with thick lines in Fig. 26(a) we have marked the curves for $N = 8$ and 12 in the vicinity of $\alpha = 0.7$ at which the forbidden crossings were found in Fig. 24(a). A different behavior of $\mathcal{N}(1)/N$ and $\mathcal{N}(3)/N$ for these two values of N is clearly visible.

15.5. Unresolved questions

We have demonstrated by direct calculation of the pair amplitudes $P(\mathcal{R})$ that, at sufficiently large filling factor ($\nu_{\text{QE}} \geq 1/3$), the QEs form pairs or larger clusters, with a significant occupation of the minimum relative pair angular momentum, $\mathcal{R} = 1$. The QE (and analogous QH) clustering is an opposite behavior to Laughlin correlations characterizing, e.g., electrons partially filling LL0. Therefore it invalidates the reapplication of the CF picture to the individual QEs or QHs (and thus also the equivalent multiflavor CF model) and precludes the simple hierarchy interpretation of any incompressible states at $1/3 \leq \nu_{\text{QP}} \leq 2/3$. The series of finite-size nondegenerate ground states at QE filling factors $\nu_{\text{QE}} = 1/2, 1/3$, and $2/3$ have been identified. These values correspond to the electronic filling factors $\nu = 3/8, 4/11$, and $5/13$, at which the FQH effect has been experimentally discovered (Pan et al., 2003). Due to a discussed similarity between the QE–QE and QH–QH interactions, these three QE states have their QH counterparts at $\nu_{\text{QH}} = 1/4, 1/5$, and $2/7$, corresponding to $\nu = 3/10, 4/13$, and $5/17$, all of which have also been experimentally observed (Pan et al., 2003).

The finite-size $\nu_{\text{QE}} = 1/2$ states of QEs (CFs in LL1) are found at the same values of $2\ell = 2N - 3$ (and its conjugate) as the $\nu = 5/2$ (Greiter et al., 1991, 1992; Moore and Read, 1991; Morf and d’Ambrumenil, 1995; Morf, 1998; Morf et al., 2002; Rezayi and Haldane, 2000), despite the different electron and CF pseudopotentials. This is also true for the $\nu_{\text{QE}} = 1/3$ state at $2\ell = 3N - 7$ and the $\nu = 7/3$ IQL in LL1. Therefore we have studied the dependence of the wavefunctions and stability of the novel FQH states on the exact form of interaction at short range. We found several indications that the novel QE states are distinctly different from the electron states in LL1: (i) the $\nu_{\text{QE}} = 1/2$ state appears incompressible only for the even values of $N/2$, where N is the number of minority QPs; (ii) the pair-correlation functions $P(\mathcal{R})$ are quite different; (iii) although they remain incompressible, the ground states appear to undergo phase transitions when the QE–QE pseudopotential is continuously transformed into that of electrons in LL1. However, further studies are needed to understand these transitions. On the other hand, weak dependence of the wavefunctions and excitation gaps of the novel FQH states on the details of the QE–QE interaction, as long as it remains strongly subharmonic at short range, justifies the use of a model pseudopotential in the realistic numerical calculation.

We have also explored an idea (Halperin, 1983; Quinn et al., 2003b; Wójs et al., 2004) of the formation of Laughlin states of QE pairs (QE₂s). An appropriate composite Fermion model has been formulated and shown to predict a family of novel FQH states at a series of fractions including all those observed in experiment. However, several observations strongly point against this simple model: (i) our best estimate of the QE₂–QE₂ interaction pseudopotential is not superharmonic to support Laughlin correlations of QE₂ (except possibly for $\nu_{\text{QE}} = 1/2$); (ii) the values of 2ℓ predicted for finite N are different from these obtained from the numerical diagonalization (except for $\nu_{\text{QE}} = 1/2$); (iii) the numerical results do not confirm the significance of parity of the number of QEs in finite systems (the $\nu_{\text{QE}} = 1/2$ states occur only for $N = 8$ and 12 at $2\ell = 2N - 3$, and the $\nu_{\text{QE}} = 1/3$ states occur for both even and odd values of N).

16. Partially spin polarized systems

16.1. Introduction and model

The experiment of Pan et al. (2003) has suggested some of the novel IQL states (e.g. $\nu = 4/11$) are fully spin polarized and that other states could be partially spin polarized. Sitko et al. (1997, 1996) found that the $\nu = 4/11$ state did not occur in the CF hierarchy of spin polarized IQL states. They suggested that the reason for this was that the pseudopotential $V_{\text{QE}}(L')$ was not sufficiently similar to $V_0(L')$, the pseudopotential for electrons in LL0, to support the same kind of correlations. It was shown (Quinn and Wójs, 2000a; Wójs, 2001a) that because $V_{\text{QE}}(L')$ was not “superharmonic” at $\mathcal{R} = 2\ell - L' = 1$, the QEs could not support Laughlin correlations and no second generation of CFs could occur at $\nu_{\text{QE}} = 1/3$ producing a completely spin polarized IQL state at $\nu^{-1} = 2 + (1 + \nu_{\text{QE}})^{-1} = 11/4$ (although an IQL with some other, non-Laughlin, form of QE–QE correlations was not excluded by this argument). This led to the suggestion (Park and Jain, 2000) that the QE excitations would have to have reversed spin in order to produce a daughter state at $\nu_{\text{QE}} = 1/3$.

Until now, we have concentrated on fully spin polarized systems with total spin $S = N/2$ (each electron having projection $s_z = -1/2$). In this section we describe the numerical calculations for systems with total spin $S = N/2 - K$, where K is the number of electrons with reversed spin. The spin excitations of a fully spin polarized system are evaluated for both integral (Rezayi, 1987) and fractional IQL states. Reversed spin quasielectrons (QERs), skyrmions (SK) (Sondhi et al., 1993), and spin waves are found, and their properties are discussed. The goal of this section is to present enough information about spin excitations to be able to compare fully spin polarized and partially spin polarized states in the FQH hierarchy.

We perform numerical diagonalization of the Coulomb interaction for a system of N electrons in a shell of angular momentum ℓ , specifying the total z-component of angular momentum for $N - K$ electrons of spin \downarrow and K electrons of spin \uparrow . There are four conserved quantum numbers: L , the total angular momentum; S , the total spin, and their projections L_z and S_z . The energy eigenvalues depend only on L and S , and they are therefore $(2L + 1)(2S + 1)$ -fold degenerate. For more realistic results, finite well width effects are accounted for by replacing e^2/r (where r is in-plane separation) by $V_{\xi}(r) = e^2 \int dz dz' \xi^2(z) \xi^2(z') [r^2 + (z - z')^2]^{-1/2}$, where $\xi(r)$ is the envelope function for the lowest subband. The basis functions $|m_1\sigma_1, m_2\sigma_2, \dots, m_N\sigma_N\rangle = c_{m_1\sigma_1}^\dagger \dots c_{m_N\sigma_N}^\dagger |vac\rangle$, where $|vac\rangle$ stands for the vacuum state, have $L_z = \sum_i m_i$ and $S_z = \sum_i \sigma_i$ as good quantum numbers. The total angular momentum L and total spin S are resolved numerically in the diagonalization of each appropriate (L_z, S_z) Hilbert subspace.

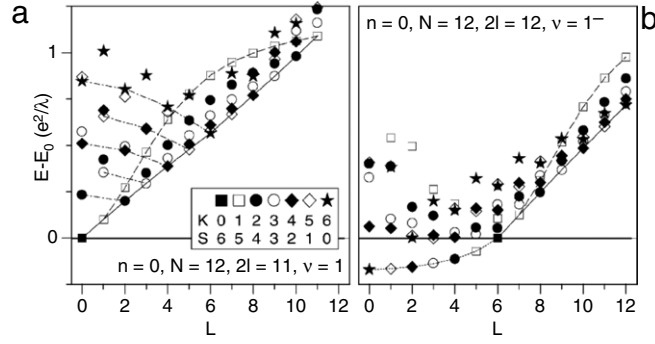


Fig. 27. The energy spectra of 12 electrons in the LL0 calculated on Haldane sphere with $2\ell = 11$ (a) and 12 (b) (Wójs and Quinn, 2002b).

16.2. Integral filling

In Fig. 27(a) and (b) we present the low energy spectra of the $\nu = 1$ and 1^- (a single hole in $\nu = 1$) states, respectively. In this and all other spectra, only the lowest state at each L and S is shown. E_0 is the energy of the lowest maximally polarized state ($K = 0$), and the Zeeman energy E_Z is omitted. The ferromagnetic ground state of Fig. 27(a) at $L = 0$ and $S = N/2 = 6$ results from the Coulomb interaction even when $E_Z = 0$. States with different values of S are indicated by the different symbols shown in the inset. The lowest excited state is a spin wave (SW) (Kallin and Halperin, 1984) consisting of a hole in the spin \downarrow level and an electron in the spin \uparrow level with $L = K = 1$. A dashed line marks the entire single SW band at $1 \leq L \leq 11$ (resulting from $\vec{L} = \vec{\ell}_e + \vec{\ell}_h$ with $\ell_e = \ell_h = \ell = 11/2$). The lowest energy excitation for a given value of either L or K occurs at $L = K$ where $K = (1/2)N - S$ is the number of spin flips away from the fully polarized ground state. The (near) linearity of $E(K)$ for this band of states (denoted by W_K) suggests that it consists of K SWs, each with $L = 1$; which are (nearly) noninteracting. As shown with the dot-dash lines connecting different states of the same number K of $L = 1$ SWs, only the $L = K$ state (in which the SWs have parallel angular momenta) is noninteracting, and all others (at $L < K$) are repulsive.

We have compared the linear W_K energy bands calculated for different electron numbers $N \leq 14$, and found that they all have the same slope $u \approx 1.15e^2/\lambda$ when plotted as a function of the “relative” spin polarization $\zeta = K/N$. The fact that $E - E_0 = u\zeta$ for the W_K band for every value of N has two noteworthy consequences in the $N \rightarrow \infty$ limit. (i) For any value of $E_Z \neq 0$, the interaction energy of each W_K state, $E - E_0 \propto K/N$, is negligible compared to its total Zeeman energy, KE_Z . (ii) The gap for spin excitations at $\nu = 1$ equals E_Z ; if this gap can be closed (e.g. by applying hydrostatic pressure), the $\nu = 1$ ferromagnet becomes gapless and the density of states for the W_K excitations becomes continuous.

Because of the exact particle-hole symmetry in the lowest LL, the $\nu = 1^-$ state whose spectrum appears in Fig. 27(b) can be viewed as containing either one hole or one reversed spin electron in a $\nu = 1$ ground state. The band of states with $0 \leq L \leq 5$ and $S = L$ (dotted line) is the skyrmion band denoted by S_K . Its energy increases monotonically with S and L . For $6 \leq L \leq 12$, the single SW band (dashed line) and band of K SWs each with $L = 1$ (solid line) resemble similar bands in Fig. 27(a), except that their angular momenta are added to that of the hole which has $\ell_h = \ell = 6$.

Fig. 27 completely ignores the Zeeman energy. The total Zeeman energy measured from the fully polarized state is proportional to K . The total energy of the skyrmion band is $E(K) = E_S(K) + KE_Z$ and the lowest S_K state occurs when $E(K)$ has its minimum. If we very roughly approximate the skyrmion energy in a finite system by $E_S(K) \approx E_S(N/2) + \beta S^2$, where $\beta \geq 0$ is a constant, this minimum occurs at $K = 1/(N - E_Z/\beta)$ spin flips. This vanishes when $E_Z = \beta N$, defining the critical value, \tilde{E}_Z , and it reaches its maximum value $K = N/2$ (or complete depolarization) when $E_Z = 0$. At such E_Z the ground state at $\nu = 1^\pm$ is a finite size skyrmion, its gap for spin excitations (“internal” spin excitations introduced by Fertig et al. (1996)) is much smaller than (and largely independent of) E_Z . This is in contrast to the exact $\nu = 1$ filling and allows spin coupling of the electron system to the magnetic ions, nuclei, or charged excitons.

The only difference between the filling factors $\nu = 3, 5, \dots$ and 1 is that the monopole harmonics $|Q; \ell = Q + n, m\rangle$ correspond to the excited LL instead of the lowest. Matrix elements of the Coulomb interaction e^2/r between these higher monopole harmonics give a different pseudopotential $V_n(\mathcal{R})$ from that for $n = 0$. Though one might expect skyrmions to be the lowest energy charged excitations in this case, the change in the pseudopotential from $V_0(\mathcal{R})$ to $V_n(\mathcal{R})$ with $n \geq 1$ causes the charged spin flip excitations to have higher energy than the single hole or reversed spin electron (Wu and Jain, 1994).

16.3. Fractional filling

Since the CF picture (Jain, 1989) describes the FQH effect in terms of integral filling of effective CF levels, it is interesting to ask (Kamilla et al., 1996) if spin excitations analogous to the SWs and SKs occur at Laughlin fractional fillings $\nu = (2p + 1)^{-1}$ (where $p = 1, 2, \dots$). In Fig. 28 we display numerical results for $\nu \approx 1/3$.

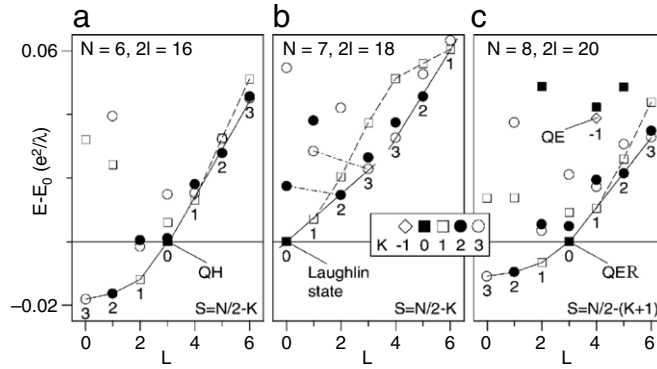


Fig. 28. The energy spectra of $N = 6 - 8$ electrons on Haldane sphere at values of 2ℓ corresponding to $\nu = (1/3)^-$ (a), $\nu = 1/3$ (b), and $\nu = (1/3)^+$ (c) (Wójs and Quinn, 2002b).

The values of N and 2ℓ in frames (b), (a), and (c) correspond to a Laughlin $\nu = 1/3$ condensed state, Laughlin quasihole (QH), and Laughlin quasielectron (QE) or reversed spin quasielectron (QER), respectively. For each of these cases, the lowest CF LL has a degeneracy of seven. Clearly the single SW dispersion (dashed line) and the linear W_K band (solid line) both appear in Fig. 28(b). The SK bands beginning at $L = 0$ lie below the single QH state (a) and below the single QE_R state (c). The solid and dashed lines at $3 \leq L \leq 6$ in Fig. 28(a) and (c) are completely analogous to those in Fig. 27 (b), and correspond to the single SW band and the W_K band, except that their angular momenta are added to $\ell_{QH} = 3$ or $\ell_{QER} = 3$. What is clearly different from the $\nu = 1$ case is the smaller energy scale, and a noticeable difference between the $\nu = (1/3)^-$ (QH) and $\nu = (1/3)^+$ (QER) spectra. Since the QH–QH and QER–QER interactions are known to be different (Szulufarska et al., 2001), this lack of QH–QER symmetry is not unexpected. It implies a lack of symmetry between the CF skyrmion (QER + K SW) and CF antiskyrmion (QH + K SW) states in contrast to the skyrmion–antiskyrmion symmetry of $\nu = 1$. Because the CF skyrmion energy scale is so much smaller than E_C at $\nu = 1$, the critical E_Z at which skyrmions are stable is correspondingly smaller (Leadley et al., 1997).

16.4. Spin-reversed quasielectrons

It is well known that even in the absence of the Zeeman energy gap, $E_Z = 0$, the ground state of the 2DEG in the lowest LL is completely spin-polarized at the precise values of the Laughlin filling factor $\nu = (2p + 1)^{-1}$, with $p = 0, 1, 2, \dots$. There are two types of elementary charge-neutral excitations of Laughlin $\nu = (2p + 1)^{-1}$ ground states, carrying spin $S = 0$ or 1, respectively. Their dispersion curves $E_S(k)$ have been studied for all combinations of p and S . In Fig. 29 we present the exact numerical results for $\nu = 1/3$ obtained from our exact diagonalization of up to $N = 11$ electrons on Haldane sphere (Szulufarska et al., 2001). As an example, in Fig. 29 (a), we show the entire low-energy spectrum of an $N = 9$ system with all spins polarized and with one reversed spin (Hilbert subspaces of total spin $S = N/2 - K = 9/2$ and $7/2$ for $K = 0$ and 1, respectively), from which the dispersion curves $E_S(k)$ are obtained. The energy E is plotted as a function of angular momentum L , and $2Q = 3(N - 1) = 24$ is the strength of the magnetic monopole inside Haldane sphere corresponding to the LL degeneracy $g = 2Q + 1 = 25$ and the Laughlin filling factor $\nu = (N - 1)/(g - 1) = 1/3$ (for the details of Haldane spherical geometry see Refs. Fano et al. (1986), Haldane (1983), Wójs and Quinn (2007), Wu and Yang (1976, 1977) and Section 4. The energy E does not include the Zeeman term E_Z , which scales differently from the plotted Coulomb energy with the magnetic field B . The excitation energies $\mathcal{E}_K = E - E_0$ (where E_0 is the Laughlin ground state energy) have been calculated for the states identified in the finite-size spectra as the $S = 0$ charge-density wave and the $K = 1$ spin-density wave. These states are marked with dotted lines in Fig. 29 (a). The values of \mathcal{E}_K obtained for different $N \leq 11$ have been plotted together in Fig. 29 (b) as a function of the wave vector $k = L/R = (L/\sqrt{S})\lambda^{-1}$. Clearly, using the appropriate units of λ^{-1} for wave vector and e^2/λ for excitation energy in Fig. 29 (b) results in the quick convergence of the curves with increasing N , and allows an accurate prediction of the dispersion curves in an infinite system, as marked with thick lines. The most significant features of these curves are (i) the finite gap $\Delta_0 \approx 0.076e^2/\lambda$ and the magnetoroton minimum $k = 1.5\lambda^{-1}$ in $E_0(k)$ and (ii) the vanishing of $\mathcal{E}_1(k)$ in the $k \rightarrow 0$ limit (for $E_Z = 0$).

The similar nature of the charge and spin waves in the $\nu = 1/3$ state to those at $\nu = 1$ lies at the heart of the composite Fermion picture (Halperin et al., 1993; Jain, 1989; Lopez and Fradkin, 1991) in which these excitations correspond to promoting one CF from a completely filled lowest ($n = 0$) spin \downarrow CF LL either to the first excited ($n = 1$) CF LL of the same spin (\downarrow) or to the same CF LL ($n = 0$) but with the reversed spin (\uparrow). The three constituent QPs of which the charge and spin waves are composed (a hole in the $n = 0$ spin \downarrow CFFL and particles in the $n = 1$ spin \downarrow and $n = 0$ spin \uparrow CFFLs) are analogous to those in the electron LLs from which the charge and spin waves at $\nu = 1$ are built. Independently of the CF picture, one can define three types of QPs (elementary excitations) of the Laughlin $\nu = 1/3$ fluid. They are Laughlin quasiholes and quasielectrons and Rezayi spin-reversed quasielectrons (QER). The excitations in Fig. 29 are more complex in a sense that

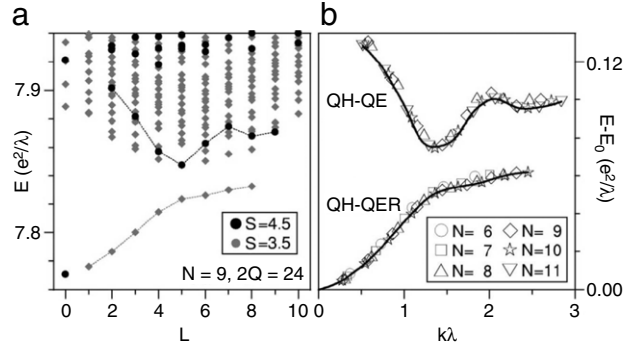


Fig. 29. (a) The energy spectrum of the system of $N = 9$ electrons on Haldane sphere at monopole strength $2Q = 3(N - 1) = 24$. Black dots and gray diamonds mark states with the total spin $S = \frac{N}{2} = \frac{9}{2}$ (maximum polarization) and $S = \frac{N}{2} - 1 = \frac{7}{2}$ (one reversed spin), respectively. Ground state is the Laughlin $\nu = \frac{1}{3}$ state. Lines connect states containing one QE–QH ($S = \frac{9}{2}$) or QER–QH ($S = \frac{7}{2}$) pair. (b) The dispersion curves (excitation energy $\varepsilon_k = E - E_0$ vs. wavevector k) for the $K = 0$ charge-density wave (QE–QH pair) and the $K = 1$ spin-density wave (QH–QER pair) in the Laughlin $\nu = \frac{1}{3}$ ground state, calculated in the systems of $N \leq 11$ electrons on Haldane sphere (Szlufarska et al., 2001).

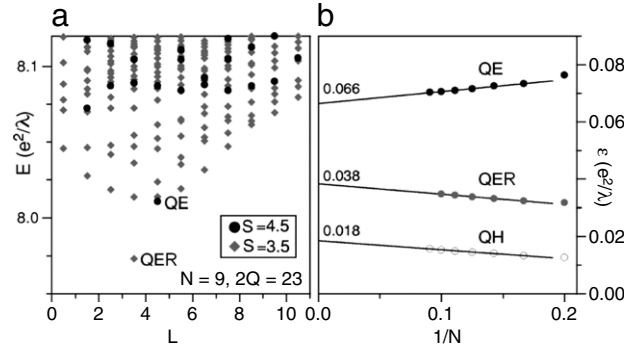


Fig. 30. (a) The energy spectrum of the system of $N = 9$ electrons on Haldane sphere at monopole strength $2Q = 3(N - 1) - 1 = 23$. Black dots and gray diamonds mark states with the total spin $S = \frac{N}{2} = \frac{9}{2}$ (maximum polarization) and $S = \frac{N}{2} - 1 = \frac{7}{2}$ (one reversed spin), respectively. Ground state at $S = \frac{7}{2}$ is the QER of the Laughlin $\nu = \frac{1}{3}$ state and the lowest energy state at $S = \frac{9}{2}$ is the Laughlin QE. (b) The energies ε of all three types of quasiparticles of Laughlin $\nu = \frac{1}{3}$ ground state (QH, QE, and QER) in the systems of $N \leq 11$ electrons on Haldane sphere and plotted as a function of N^{-1} . The numbers give the results of linear extrapolation to an infinite (planar) system.

they consist of a (neutral) pair of QH and either QE ($K = 0$) or QER ($K = 1$). Each of the QPs is characterized by such single-particle quantities as (fractional) electric charge ($\mathcal{Q}_{\text{QH}} = +e/3$ and $\mathcal{Q}_{\text{QE}} = \mathcal{Q}_{\text{QER}} = -e/3$), energy ε_{QP} , or degeneracy g_{QP} of the single-particle Hilbert space. On Haldane sphere, the degeneracy g_{QP} is related to the angular momentum ℓ_{QP} by $g_{\text{QP}} = 2\ell_{\text{QP}} + 1$, with $\ell_{\text{QH}} = \ell_{\text{QER}} = Q^*$ and $\ell_{\text{QE}} = Q^* + 1$ and $2Q^* = 2Q - 2(N - 1)$ being the effective monopole strength in the CF model.

The energies ε_{QP} to create an isolated QP of each type in the Laughlin ground state have been previously estimated in a number of ways. Here, we present our results of exact diagonalization for $N \leq 11$ (ε_{QE} and ε_{QH}) and $N \leq 10$ (ε_{QER}) (Szlufarska et al., 2001). In Fig. 30(a) we show an example of the numerical energy spectrum for the system of $N = 9$ electrons, in which an isolated QE or QER occurs at $2Q = 3(N - 1) - 1 = 23$ in the subspace of $S = N/2 = 9/2$ and $S = N/2 - 1 = 7/2$, respectively. Both of these states have been identified in Fig. 30(a). To estimate ε_{QE} and ε_{QER} , we use the standard procedure (Fano et al., 1986; Haldane, 1987; Haldane and Rezayi, 1985a; Wójs and Quinn, 2000a,d) to take into account the finite-size effects (the dependence of λ on $2Q$, $Q\lambda^2 = R^2$), and express the energies E of Fig. 30(a) in units of e^2/λ with λ appropriate for $\nu = 1/3$, before subtracting from them the Laughlin ground state energy of Fig. 29(a). Plotting the results for different values of N in Fig. 30(b) as a function of N^{-1} allows the extrapolation to an infinite system, with the limiting values of $\varepsilon_{\text{QE}} = 0.0664e^2/\lambda$ and $\varepsilon_{\text{QER}} = 0.0383e^2/\lambda$ (with the difference $\varepsilon_{\text{QE}} - \varepsilon_{\text{QER}} = 0.0281e^2/\lambda$ in remarkable agreement with Rezayi’s original estimate (Rezayi, 1987, 1991) based on his numerics for $N \leq 6$). For completeness, we have also plotted the QH energies, which extrapolate to $\varepsilon_{\text{QH}} = 0.0185e^2/\lambda$. Note that to obtain the so-called “proper” QP energies $\tilde{\varepsilon}_{\text{QP}}(N)$ in a finite system (Fano et al., 1986; Haldane and Rezayi, 1985a; Wójs and Quinn, 2000a), the term $\mathcal{Q}_{\text{QP}}^2/2R$ must be added to each value in Fig. 30(b). The linear extrapolation of $\tilde{\varepsilon}_{\text{QP}}(N)$ to $N^{-1} \rightarrow 0$ gives $\tilde{\varepsilon}_{\text{QE}} = 0.0737e^2/\lambda$, $\tilde{\varepsilon}_{\text{QER}} = 0.0457e^2/\lambda$, and $\tilde{\varepsilon}_{\text{QH}} = 0.0258e^2/\lambda$. The energies of spatially separated QE–QH and QER–QH pairs (activation energies in transport experiments) are hence equal to $E_0(\infty) = \tilde{\varepsilon}_{\text{QE}} + \tilde{\varepsilon}_{\text{QH}} = 0.0995e^2/\lambda$ and $E_1(\infty) = \tilde{\varepsilon}_{\text{QER}} + \tilde{\varepsilon}_{\text{QH}} = 0.0715e^2/\lambda$. While the QHs are the only types of QPs that occur in low-energy states at $\nu < (2p + 1)^{-1}$, the QEs and QERs are two competing excitations

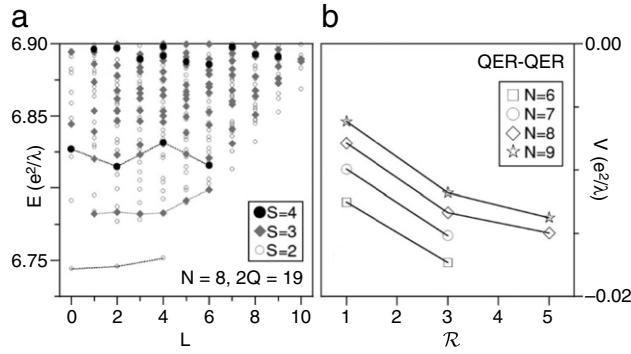


Fig. 31. (a) The energy spectrum of the system of $N = 8$ electrons on Haldane sphere at monopole strength $2Q = 3(N - 1) - 2 = 19$. Black dots and gray diamonds mark states with the total spin $S = \frac{N}{2} = 4$ (maximum polarization), $S = \frac{N}{2} - 1 = 3$ (one reversed spin), and $S = \frac{N}{2} - 2 = 2$ (two reversed spins), respectively. Lines connect states containing one QE-QE ($S = 4$), QE_R-QE ($S = 3$), or QE_R-QE_R ($S = 2$) pair. (b) The pseudopotential (pair energy V vs. relative angular momentum \mathcal{R}) of the QER-QER interaction calculated in the systems of $N \leq 9$ electrons on Haldane sphere (Szlufarska et al., 2001).

at $\nu > (2p + 1)^{-1}$. As pointed out by Rezayi (1987, 1991) and Chakraborty et al. (1986), whether QEs or QERs will occur at low energy depends on the relation between their energies including the Zeeman term, ε_{QE} and $\varepsilon_{\text{QER}} + E_z$. Although it is difficult to accurately estimate the value of E_z in an experimental sample because of its dependence on a number of factors (material parameters, well width w , density ρ , magnetic field B , etc.), it seems that both scenarios with QEs and QERs being lowest-energy QPs are possible. For example, using the bulk value for the effective g^* factor in GaAs ($dE_z/dB = 0.03$ meV/T) results in the QER-QE crossing at $B = 18T$, while including the dependence of g^* on w and B as described by Wójs et al. (2000b) makes QER more stable than QE up to $B \sim 100T$.

Once it is established which of the QPs occur at low energy in a particular system (defined by ρ , w , B , ν , etc.), their correlations can be understood by studying the appropriate pair interaction pseudopotentials (Haldane, 1987; Quinn and Wójs, 2000a; Wójs, 2001a; Wójs and Quinn, 2000a). The pseudopotential $V(\mathcal{R})$ is defined (Haldane, 1987) as the dependence of pair interaction energy V on relative orbital angular momentum \mathcal{R} . On a plane, \mathcal{R} for a pair of particles ab is the angular momentum associated with the (complex) relative coordinate $z = z_a - z_b$. On Haldane sphere, the compatible definition of \mathcal{R} depends on the sign of $Q_a Q_b$: for a pair of opposite charges, \mathcal{R} is the length of total pair angular momentum, $L = |\vec{\ell}_a + \vec{\ell}_b|$, while for two charges of the same sign, $\mathcal{R} = |\ell_a + \ell_b - L|$. In all cases, $\mathcal{R} > 0$ and larger \mathcal{R} corresponds to a larger average ab separation (Quinn and Wójs, 2000a; Wójs and Quinn, 2000a). Furthermore, only odd values of \mathcal{R} are allowed for indistinguishable ($a = b$) Fermions.

Since the QE-QH and QER-QH pseudopotentials have been plotted in Fig. 29 ($V_{\text{QE-QH}} = E_0$ and $V_{\text{QER-QH}} = E_1$), and the QE-QE and QH-QH pseudopotentials can be found, for example, in Wójs and Quinn (2000d), we only need to discuss $V_{\text{QER-QER}}$ and $V_{\text{QE-QER}}$. Two QERs occur in an N -electron system with at least two reversed spins ($S < (N/2) - 1$) and at $2Q = 3(N - 1) - 2$ (i.e., at $g = g_0 - 2$ where g_0 corresponds to the Laughlin state). An example of the energy spectrum is shown in Fig. 31(a) for $N = 8$ at $2Q = 19$. The lowest-energy states in the subspaces of $S = N/2 = 4$, $N/2 - 1 = 3$, and $N/2 - 2 = 2$ are connected with dashed lines and contain a QE-QE, QE-QER, and QER-QER pair, respectively. The angular momenta L that occur in these bands result from addition of $\vec{\ell}_{\text{QE}}$ and/or $\vec{\ell}_{\text{QER}}$ (with $\ell_{\text{QE}} = Q^* + 1 = 7/2$ and $\ell_{\text{QER}} = Q^* = 5/2$). For identical Fermions, the addition must be followed by antisymmetrization that picks out only odd values of \mathcal{R} for the QE-QE and QER-QER pairs. An immediate conclusion from Fig. 31(a) is that the maximally spin-polarized ($S = N/2$) system is unstable at the filling factor close but not equal to the Laughlin value of $\nu = 1/3$ (the actual spin polarization decreases with decreasing E_z , and $S = 0$ for $E_z = 0$). This was first pointed out by Rezayi (1987, 1991) and interpreted in terms of an effective attraction between $S = 1$ spin waves; in this paper we prefer to use charged QPs as the most elementary excitations and explain the observed ordering of different S bands by the fact that $\varepsilon_{\text{QE}} \neq \varepsilon_{\text{QER}}$ (at $E_z = 0$, $\varepsilon_{\text{QE}} - \varepsilon_{\text{QER}} = 0.0281e^2/\lambda$) and the particular form of involved interaction pseudopotentials.

We have calculated the QE-QER and QER-QER pseudopotentials from the energy spectra as that in Fig. 31 (a) by converting L into \mathcal{R} and subtracting the Laughlin ground state energy and the energy of two appropriate QPs from the total N -electron energy, $V_{AB}(\mathcal{R}) = E(L) - E_0 - \varepsilon_A - \varepsilon_B$. To minimize the finite-size effects, all subtracted energies are given in the same units of e^2/λ_0 , where $\lambda_0 = R/\sqrt{Q_0}$ corresponds to $2Q_0 = 3(N - 1)$, i.e., to $\nu = 1/3$. The result for $V_{\text{QER-QER}}$ and $N \leq 9$ is shown in Fig. 31(b). Clearly, obtained values of $V_{\text{QER-QER}}(\mathcal{R})$ still depend on N and, for example, the positive sign characteristic of repulsion between equally charged particles is only restored in the $N^{-1} \rightarrow 0$ limit with $V_{\text{QER-QER}}(1)$ of the order of $0.01e^2/\lambda$ (compare with discussion of the signs of $V_{\text{QE-QE}}$ and $V_{\text{QH-QH}}$ in Wójs (2001b) and Section 9). However, it seems that the monotonic character of $V_{\text{QER-QER}}(\mathcal{R})$ is independent of N . More importantly, $V_{\text{QER-QER}}(\mathcal{R})$ is also a superlinear function of $L(L + 1)$. This implies (Quinn and Wójs, 2000a; Wójs and Quinn, 2000a; Wójs, 2001a) Laughlin correlations and incompressibility at $\nu_{\text{QER}} = (2p + 1)^{-1}$, in analogy to the spin-polarized Laughlin states of QEs or QHs in Haldane's hierarchy picture (Haldane, 1983; Wójs and Quinn, 2000d). The most prominent of QER Laughlin states, $\nu_{\text{QER}} = 1/3$, corresponds to the electronic filling factor of $\nu = 4/11$ and the 75% spin polarization ($S = N/4$). This state has been first suggested by Béran and

Morf (1991). The expected critical dependence of the excitation gap at $\nu = 4/11$ on the Zeeman gap E_Z might be revealed in tilted-field experiments. This dependence will be very different from that at some other fractions.

17. Spin polarization transition of the $\nu = 4/11$ state

17.1. Possible incompressible quantum liquid states

In Section 15 we mentioned that there were at least two candidates for the $\nu = 4/11$ state observed by Pan et al. (2003). The fully spin polarized state (for which there is some experimental support) cannot be a second generation CF state resulting from Laughlin correlated QEs at filling factor $\nu_{\text{QE}} = 1/3$. The QE pseudopotentials $V_{\text{QE}}(\mathcal{R})$ are strongly subharmonic at $\mathcal{R} = 1$ and cannot support Laughlin correlations. A state with pairs of electrons of total angular momentum $\ell_p = 2\ell - 1$ (where ℓ is the QE angular momentum), or with larger clusters can cause a totally spin polarized state at $\nu = 4/11$. However, a partially spin polarized state in which CF quasielectrons have reversed spin (QERs) relative to those in the IQL state above which they reside, could give rise to an IQL state with $\nu_{\text{QER}} = 1/3$ (Park and Jain, 2000). This is possible because $V_{\text{QER}}(\mathcal{R})$ is superharmonic at $\mathcal{R} = 1$ (Szlufarska et al., 2001) allowing the QERs to form a Laughlin state.

Which of these has a lower energy? The total energy depends on (i) the energies of the quasielectrons, ε_{QE} and ε_{QER} , (ii) the interaction energy of these quasiparticles, which depends on their pseudopotentials $V_{\text{QE}}(\mathcal{R})$ and $V_{\text{QER}}(\mathcal{R})$, and finally on (iii) the Zeeman energy E_Z due to the total spin S in the applied magnetic field B . In real samples each of these energies depends upon the width of the quantum well in which the electrons are confined. The QE energies and their interactions depend on well width primarily because the interactions of the electrons in the systems that give rise to QEs involve form factors resulting from integration over squares of the subband wavefunctions $\chi(z)$ for the quantum well. The Zeeman energy $E_Z = g^* \mu_B B$ depends on the effective g -factor of the electrons, observed experimentally to increase from $g^* = -0.44$ for wide wells to zero for a well width of roughly 6 nm.

17.2. Quasielectron energies

As we have seen in earlier sections, in the mean-field CF transformation, the liquid of correlated electrons at filling factor $\nu_e = 4/11$, is converted to the system of CFs with an effective filling factor $\nu_{\text{CF}} = 4/3$. Approximately $3N_e/4$ of the CFs fill the lowest CF energy level CF LLO \uparrow , with angular momentum $\ell^* = \ell - (N_e - 1)$. The remaining $N \sim N_e/4$ CFs go into the lowest ($\simeq 1/3$ -filled) excited CF energy level (either CF LLO \downarrow or CF LL1 \uparrow) depending on the relative magnitude of electron Zeeman energy E_Z and the “effective” CF cyclotron gap (proportional to e^2/λ). Each CF in the partially filled $1 \uparrow$ or $0 \downarrow$ CF LLs represent a “normal” QE (Laughlin, 1983) or QER (Rezayi, 1987, 1991) of the underlying incompressible Laughlin liquid, respectively.

The Coulomb energies ε_{QE} and ε_{QER} of these two QPs can be extracted (Fano et al., 1986; Szlufarska et al., 2001) from exact diagonalization of finite systems of N_e electrons in the lowest LL with the appropriate degeneracy g . The Laughlin ground state occurs at $g = 3N_e - 2 \equiv g_L$; it is nondegenerate ($L = 0$) and spin-polarized ($S = N_e/2$). A single QE or QER appears in the Laughlin liquid in the lowest states at $g = g_L - 1$ and either $S = N_e/2$ or $(N_e/2) - 1$, respectively. The QE and QER energies defined relative to the underlying Laughlin liquid are obtained from the comparison of the N_e -electron energies at $g = g_L$ and $g_L - 1$. The numerical procedure and the result for an ideal 2D electron layer (Szlufarska et al., 2001; Wójs, 2001b) were presented earlier in Sections 9 and 16. In Fig. 32, we compare the QE/QER energies calculated for quasi-2D layers of finite width w . Here, w is the effective width of the electron wavefunction in the normal z direction, approximated by $\chi(z) \propto \cos(z\pi/w)$ (Wójs et al., 2007). It is slightly larger than the quantum well width W ; e.g., for symmetric GaAs/Al_{0.35}Ga_{0.65}As wells, $w = W + 3$ nm over a wide range of $W \geq 10$ nm. The regular dependence on system size in Fig. 32 (a) allows reliable extrapolation to ($N_e^{-1} \rightarrow 0$) planar geometry. From the comparison of $\varepsilon_{\text{QE}}(w)$ and $\varepsilon_{\text{QER}}(w)$ in Fig. 32 (b), it is clear that their difference is less sensitive to the width than any of the $\varepsilon_{\text{QER}}(w)$ or $\varepsilon_{\text{QE}}(w)$. To put the shown width range in some perspective, let us note that a (fairly narrow) $W = 12$ nm well in a (fairly low) field $B = 10$ T corresponds to $w/\lambda = 1.9$ and $\Delta\varepsilon(w)/\Delta\varepsilon(0) = 0.9$, justifying the 2D approximation. On the other hand, a wide $W = 40$ nm well in a high field $B = 23$ T gives $w/\lambda = 8.1$ and $\Delta\varepsilon(w)/\Delta\varepsilon(0) = 0.5$, i.e., a significant width effect.

17.3. Quasiparticle interactions and correlation energy

The weak effective CF–CF interactions are known with some accuracy from earlier studies (Lee et al., 2001, 2002; Sitko et al., 1997; Szlufarska et al., 2001; Wójs and Quinn, 2000d; Wójs et al., 2006b). At least at sufficiently low CF fillings factors $\nu \leq 1/3$, they can be well approximated by fixed Haldane pseudopotentials independent of the CF LL filling or spin polarization. The short-range QE–QE, QER–QER, and QE–QER pseudopotentials can be obtained from finite-size diagonalization for N_e electrons with up to two reversed spins $S = N_e/2 - 2$ at $g = g_L - 2$.

The result is a reliable account of the relative values $\Delta V_{\mathcal{R}\mathcal{R}'} = V_{\mathcal{R}} - V_{\mathcal{R}'}$ at small neighboring \mathcal{R} and \mathcal{R}' , but the absolute values are not estimated very accurately. Fortunately, since vertical correction of $V(\mathcal{R})$ by a constant does not affect the many-CF wavefunctions and only rigidly shifts the entire energy spectrum (Wójs and Quinn, 2000d), a few leading values of ΔV completely determine the short-range CF correlations at a given ν . Therefore, the knowledge of those few approximate

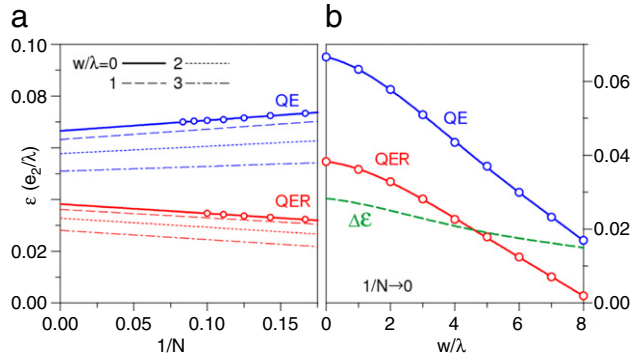


Fig. 32. (Color online) Dependence of the QE and QER energies ε on (a) the inverse electron number N_e^{-1} in a finite-size calculation and (b) the electron layer effective width w . λ is the magnetic length (Wójs et al., 2007).

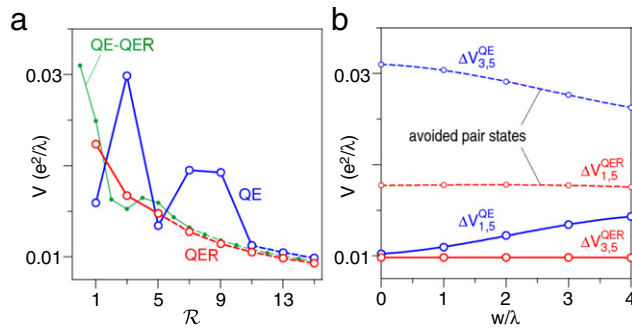


Fig. 33. (Color online) (a) Haldane pseudopotential pair interaction energy V as a function of relative angular momentum \mathcal{R} for QEs and QERs in an ideal 2D ($w = 0$) electron layer. (b) Dependence of pseudopotential increments $\Delta V_{\mathcal{R},\mathcal{R}'} = V_{\mathcal{R}} - V_{\mathcal{R}'}$ on the electron layer effective width w . λ is the magnetic length (Wójs et al., 2007).

values of ΔV_{QER} and ΔV_{QE} was sufficient to establish that: (i) the QERs form a Laughlin $\nu = 1/3$ liquid (Mandal and Jain, 2002; Park and Jain, 2000; Wójs and Quinn, 2002c) which in finite N – QER systems on a sphere occurs at $g = 3N - 2$, and (ii) in contrast, the QEs form a different (probably paired) state (Wójs et al., 2005, 2006b, 2004) at the same $\nu = 1/3$, which, on a sphere, occurs at $g = 3N - 6$.

However, the relative strength of QE–QE and QER–QER pseudopotentials V_{QE} and V_{QER} must also be known in addition to ΔV to compare the energies of many-QER and many-QE states (i.e., of the spin-polarized and unpolarized electron states at $\nu_e = 4/11$). The absolute values of V_{QER} and V_{QE} can be obtained by matching (Haldane, 1987) the short-range behavior from exact diagonalization of small systems with the long-range behavior predicted for a pair of charges $q = -e/3$. Specifically, the short-range part of $V_{QER}(\mathcal{R})$, which describes a pair of CFs in the $1 \downarrow$ CF LL, is shifted to match $\eta V_0(\mathcal{R})$, the electron pseudopotential in the lowest LL rescaled by $\eta \equiv (q^2 \lambda_q^{-1}) / (e^2 \lambda_e^{-1}) = (q/e)^{5/2}$. Similarly, the short-range part of V_{QE} , related to the $1 \uparrow$ CF LL, is shifted to match $\eta V_1(\mathcal{R})$.

The result in Fig. 33(a) for an ideal 2D layer was reported earlier (Szufarska et al., 2001). In Fig. 33(b), the width dependence of the leading parameters ΔV has been plotted. It is noteworthy that V_{QE} is much more sensitive to the electron layer width w than V_{QER} . This is explained by stronger oscillations in $V_{QE}(\mathcal{R})$ at $w = 0$, which tend to weaken in wider wells (when the characteristic in-plane distances decrease relative to w). The curves involving $V_{QER}(1)$ and $V_{QE}(3)$ have been drawn with dashed lines, since the QER–QER and QE–QE pair states associated with these dominant pseudopotential parameters will be avoided (Wójs et al., 2005, 2004) in the unpolarized and polarized $\nu = 1/3$ CF ground states, respectively.

As mentioned above, due to the strong QER–QER repulsion at short range ($\mathcal{R} = 1$), the QERs form a Laughlin $\nu = 1/3$ state similar to the electrons in LL0 at $\nu_e = 1/3$. The corresponding series of nondegenerate N – QER ground states on a sphere occurs at the Laughlin sequence of $g = 3N - 2$. In Fig. 34(a), we plot the size dependence of their correlation energy u (per particle), defined as

$$u = \frac{E + U_{\text{bckg}}}{N} \zeta. \quad (33)$$

Here, E is the interaction energy of the ground state of N QERs and $U_{\text{bckg}} = -(Nq)^2/2R$ is a correction due to interaction with the charge-compensating background with the sphere radius $R = \lambda\sqrt{Q}$ taken for $2Q + 1 = g$, in analogy to the relation for electrons in the lowest LL. Factor $\zeta = \sqrt{Q(Q-1)^{-1}}$ is used to rescale the energy unit $e^2/\lambda = \sqrt{Q}e^2/R$ from that corresponding to $g_{QER} = 3N - 2$ to that of an average $\bar{g} = 1/2(g_{QER} + g_{QE}) = 3N - 4$, to allow for a later comparison

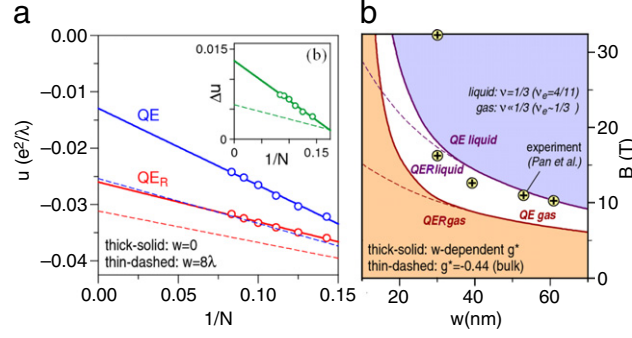


Fig. 34. (Color online) (a) Correlation energy u in the $\nu = 1/3$ incompressible liquid of QE or QER as a function of their inverse number N^{-1} for two different widths w of the quasi-2D electron layer; λ is the magnetic length. (b) Difference $\Delta u = u_{\text{QE}} - u_{\text{QER}}$ as a function of N^{-1} . (c) Phase diagram critical layer width w vs magnetic field B for the QE–QER spin transition at $\nu = 1/3$ i.e., at $\nu_e = 4/11$, assuming the effective electron Landé g^* factor for GaAs. Dashed line is for the bulk value $g^* = -0.44$, ignoring dependence on the layer width w . The experimental points were taken after Pan et al. (2003).

of u calculated for QERs and QEs at different values of g and thus at different magnetic lengths corresponding to the same area $4\pi R^2$. The correlation energies u were calculated for $N \leq 12$ and extrapolated to $N^{-1} \rightarrow 0$ to eliminate the finite-size effects.

Let us turn to the QEs. The dominant QE–QE repulsion at $\mathcal{R} = 3$ causes the QEs to form pairs (Wójs et al., 2006b) rather than a Laughlin state at $\nu = 1/3$ although the exact wavefunction of this incompressible state is still unknown. The corresponding series of nondegenerate N -QE ground states on a sphere was identified (Wójs et al., 2005, 2004) at $g = 3N - 6$, different from the Laughlin sequence. The QE correlation energy u was calculated from the same Eq. (33) but with a different $\zeta = \sqrt{Q(Q+1)^{-1}}$ (where $g = 2Q + 1$) also. By using different ζ_{QER} and ζ_{QE} , we removed the discrepancy between λ/R of finite N -QER and N -QE systems, in order to improve size convergence of $\Delta u = u_{\text{QE}} - u_{\text{QER}}$. In an ideal 2D system $w = 0$, the extrapolated value at $N^{-1} = 0$ is $u_{\text{QE}} = -0.013e^2/\lambda$, twice as small in the absolute value than u_{QER} of a Laughlin state. The difference is $\Delta u = 0.013e^2/\lambda$. The accuracy of this estimate can be judged from the extrapolation plot in Fig. 34(b).

The $u_{\text{QER}} - u_{\text{QE}}$ difference can be explained from the comparison (Wójs et al., 2006b) of QER and QE charge-density profiles $\rho(r)$. The roughly Gaussian QER is (up to normalization) very similar to ρ_0 of an electron in the lowest LL, yielding similar QER and electron pseudopotentials $V(\mathcal{R})$ and correlation energies u (in the η -rescaled units). The ring-like ρ_{QE} is more complicated and has a bigger radius, causing stronger (on average) QE–QE repulsion. The difference between u_{QER} and u_{QE} appears to result primarily from the difference between QE and QER charge densities.

17.4. Spin phase diagram for $\nu = 4/11$

Whether QEs or QERs will form a $\nu = 1/3$ state at $\nu_e = 4/11$ depends on the competition of Coulomb and Zeeman energies. The condition for the QE \leftrightarrow QER transition is:

$$\Delta\varepsilon + \Delta u = E_Z. \quad (34)$$

The competing phases differ in electron-spin polarization. They are both incompressible but probably have different excitation gaps (and thus might not show equally strong FQH effect). In an ideal 2D electron layer, the excitation gap for neutral excitations of the polarized state can be expected (Wójs et al., 2005, 2004) below $0.005e^2/\lambda$, and, for the Laughlin state of QERs, it is estimated at $0.06\eta e^2/\lambda = 0.004e^2/\lambda$. The nature of charged excitations and the corresponding transport gaps (especially in more realistic conditions, i.e., for $w > 0$, including LL mixing and disorder, etc.) are not known, and their prediction should require a much more extensive calculation.

Let us concentrate on the question of stability of either QERs or QEs at $\nu_e = 4/11$. In order to draw the phase diagram for GaAs heterostructures in Fig. 34(c), we combined the estimated dependences of $\Delta\varepsilon/(e^2\lambda^{-1})$ and $\Delta u/(e^2\lambda^{-1})$ on w/λ (where $e^2\lambda^{-1}/\sqrt{B} = 4.49$ meV/T $^{1/2}$ and $\lambda\sqrt{B} = 25.6$ nmT $^{1/2}$) with published data (Wójs, 2001a) on width dependence of the effective Landé factor g^* , governing the Zeeman splitting $E_Z = g^*\mu_B B$ (for $W \geq 30$ nm, it is $g^* = -0.44$ and $E_Z/B = 0.03$ meV/T; in narrower wells, g^* increases, passing through zero at $W \approx 5.5$ nm; recall that $w \approx W + 3$ nm).

The most important phase boundary drawn in Fig. 34(c) divides the polarized and unpolarized $\nu_e = 4/11$ states, i.e., the correlated QE and QER liquids at a finite $\nu = 1/3$. In the experiment of Pan et al. (2003), the polarized $\nu_e = 4/11$ state was observed in a symmetric $W = 50$ nm GaAs quantum well at $B = 11$ T. The corresponding experimental point (w, B) marked with a plus lies very close to the predicted phase boundary, suggesting that the experimentally detected polarization depended critically on the choice of a very wide well. Pan et al. (2003) report identification of an incompressible $\nu_e = 4/11$ state at a very high field $B = 33$ T, taken as an argument for spin polarization. Indeed, the corresponding data point marked with a cross $W = 30$ nm lies deep inside the predicted “QE liquid” phase area. However, no clear evidence for an unpolarized $\nu_e = 4/11$ has yet been reported. It is clear from Fig. 34(c) that the spin transition in narrower wells shifts quickly to higher magnetic fields (i.e., to higher electron concentrations $\rho_e = \nu_e(2\pi\lambda^2)^{-1}$), especially when the width dependence of g^* is

taken into account. This suggests that the spin transition at $\nu_e = 4/11$ might be confirmed in a similar experiment, carried out in a sample with the same W and ρ_e but with the layer width w tuned by the electric gates inducing a controlled well asymmetry. The role of QP interaction in stabilizing the QER phase is clear from the comparison of boundaries dividing correlated QE/QER liquids and noninteracting QE/QER gases (the gas occurs at $\nu \ll 1/3$, with the critical equation $\Delta\varepsilon = E_Z$; the CF gas \leftrightarrow liquid transition was recently demonstrated by inelastic light scattering (Gallais et al., 2006). Additional boundaries (not shown here, but see Figure 13(b) in Wójs and Quinn (2002d)) appear at even smaller B , defining the areas of stability for a gas of CF skyrmions of different sizes (Kamilla et al., 1996; Leadley et al., 1997; MacDonald and Palacios, 1998; Wójs and Quinn, 2002d). Note also that $\Delta\varepsilon$ is determined more accurately than Δu , possibly explaining the incorrect position of the experimental point inside the predicted QE gas and/or QER liquid area.

The spin polarization transition results from a competition between the Zeeman energy which is proportional to B and the interaction energy which is proportional to $B^{1/2}$ (or e^2/λ). Large Zeeman energy favors the totally spin polarized state. Large quantum well width decreases the interaction energy relative to the Zeeman energy, so that wide wells and large total magnetic field (the perpendicular component of B is fixed by the electron density and the filling factor $\nu = 4/11$) favor a fully spin polarized state. Our phase diagram is clearly qualitatively correct, but the evaluation of the energy of each state involves a number of approximations. The phase transition lines in the w - B (well width–applied magnetic field) plane is only approximate. Our suggestion of using a back gate to change the quantum well size in a single sample offers a conceptually simple way to test our simple model. It should be noted that we have considered only the two extreme polarizations $P = (n_\uparrow - n_\downarrow)/(n_\uparrow + n_\downarrow)$ equal to 1 and 1/2, omitting the possibility of intermediate P .

18. Electron system containing valence band holes

The first observations of both the integral and fractional quantum Hall effects were made in magnetotransport studies (von Klitzing et al., 1980; Tsui et al., 1982). Deep minima in the longitudinal conductivity, σ_{xx} , and flat plateaus in the transverse conductivity σ_{xy} , at special filling factors ν were the signatures of the IQL states. Magnetotransport has continued to be a very important technique for studying quantum Hall systems. However, optical measurements, including infrared spectroscopy, inelastic light scattering, and photoluminescence have been valuable probes of quantum Hall systems (Byszewski et al., 2006; Heiman et al., 1988; Kukushkin et al., 1994; Pinczuk et al., 1993). Many of the optical processes involve valence band holes interacting with the electrons confined in a quasi-2D system. A valence band hole can bind one or two electrons to form a neutral or a negatively charged exciton (X or X^-). In this section we study the properties of a quasi-2D system containing N_e electrons interacting with N_h valence band holes.

The electron–hole systems are of interest for several reasons. In quasi-2D systems, neutral excitons and negatively charged excitonic complexes can form in relatively stable bound states. The negatively charged excitonic complexes are charged Fermions with LL structure of their own. They have correlations with one another and with electrons, just as unbound electrons have with one another. The correlations between unbound electrons and negatively charged excitonic complexes is another example of the usefulness of the generalized CF picture. In some ways it is a simpler example because the constituents ($e, X^- = e^2h, X_2^- = e^3h^2, \dots$) all have the same total charge. However, it is more complicated because more than two different kinds of Fermion can occur.

18.1. Hidden symmetry and multiplicative states

If the electrons and the valence band holes are confined to the same 2D plane, and if the magnetic field is sufficiently large that the Landau level separations are large compared to the Coulomb interaction energy of a pair of particles, only a single LL for electrons and a single LL for holes need be considered. In such a case, the magnitude of the interaction between a pair of particles ($e - e, e - h, h - h$) is the same. Then a “hidden symmetry” (Dzyubenko and Lozovik, 1983; Lerner and Lozovik, 1981; MacDonald and Rezayi, 1990; MacDonald et al., 1992; Paquet et al., 1985) results from the fact that the commutator of the Hamiltonian \hat{H} with the operator $d^\dagger(0) = N_\phi^{-1/2} \sum_{\vec{k}'} c_{\vec{k}'}^\dagger d_{-\vec{k}'}^\dagger$, which creates a neutral exciton with wavevector $k = 0$, satisfies the relation:

$$\left[\hat{H}, d^\dagger(0) \right] = E_X(0) d^\dagger(0). \quad (35)$$

Here $E_X(0)$ is the energy of the exciton; $N_\phi = 2Q + 1$ is the LL degeneracy, and $c_{\vec{k}'}^\dagger$ (or $d_{\vec{k}'}^\dagger$) creates an electron (or hole) in LL0 with wavenumber (in y -direction for the Landau gauge) equal to k . Because of Eq. (35), if $|\Phi\rangle$ is an eigenstate of \hat{H} with energy E_Φ , then $d^\dagger(0)|\Phi\rangle$ is an eigenstate of \hat{H} with energy $E_\Phi + E_X$. The neutral $k = 0$ exciton is essentially uncoupled from the electron system. States containing N_X such neutral excitons and N_e free unbound electrons are referred to as “multiplicative states” (Dzyubenko and Lozovik, 1983; Lerner and Lozovik, 1981; MacDonald and Rezayi, 1990; MacDonald et al., 1992; Paquet et al., 1985). These low energy multiplicative states are not necessarily the ground states of a system of N_h holes and N_e ($>N_h$) electrons. For multiplicative states, the photoluminescence (PL) results from the recombination of the electron–hole pair bound in the “uncoupled” exciton (X). Since X is not coupled to the background 2D system, this PL spectrum contains no information about the correlations in the fluid of free electrons. To obtain information about those correlations, it is necessary to break the “hidden symmetry”. In real systems, this does occur as a result of: (i) finite well width

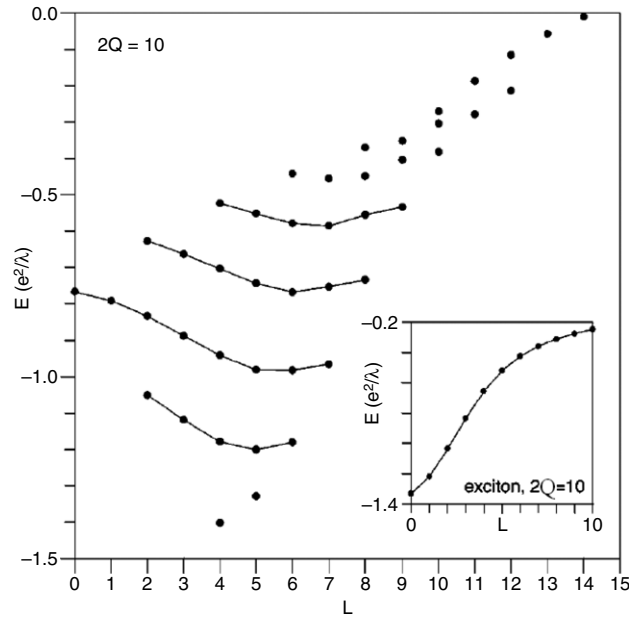


Fig. 35. The energy spectrum of two electrons and one hole at $2Q = 10$. Inset: the energy spectrum of an electron–hole pair (Quinn et al., 2003a).

giving different subband wavefunction for electrons and holes and different e – e and e – h pseudopotentials, (ii) separation of the centers of mass of the electron and hole layers due to asymmetry of the quantum well (e.g. not symmetrically modulation doped), and (iii) admixing of higher LLs when the Coulomb interaction is not very small compared to the LL separations. For understanding the qualitative aspects of the PL spectrum, it is sufficient to remove the “hidden symmetry” by introducing a separation d between the 2D planes on which the electrons and holes reside. Then $V_{e-h} = e^2(r^2 + d^2)^{-1/2}$ and $|V_{e-e}| = e^2/r$. This breaks the hidden symmetry without the need of including subband wavefunction or admixing higher LLs. For comparison with real experiments, a more careful treatment of the e – e and e – h interactions and the admixing of higher LLs is necessary.

In the next subsection we present spectra obtained by numerical diagonalization of systems containing up to four electrons and two valence holes. From the results we obtain binding energies and angular momenta of the neutral exciton (X), the negatively charged exciton ($X^- = e + X$), and the negatively charged biexciton ($X_2^- = X + X^-$). We also obtain the pseudopotentials describing the interaction V_{AB} of charged Fermion pairs where A and B can be e^- , X^- , X_2^- , etc. Many of the results in the remainder of this section have been summarized in Quinn et al. (2003a).

18.2. Numerical diagonalization

18.2.1. Numerical results

In Fig. 35, we show the spectrum (in magnetic units) of a system with two electrons and one hole at $2Q = 10$ as a function of the total angular momentum L (Wójs et al., 1999b). The lowest energy state at $L = Q$ is the multiplicative state with one neutral exciton in its $\ell_X = 0$ ground state and one electron of angular momentum $\ell_e = Q$. Only one state of lower energy occurs in the spectrum. It appears at $L = Q - 1$ and corresponds to the only bound state of the negatively charged exciton X^- . The value of the X^- angular momentum $\ell_{X^-} = Q - 1$, can be understood by noticing that the lowest energy single-particle configuration of the two electrons and one hole is the “compact droplet”, in which the two electrons have z -component of angular momentum $m = Q$ and $m = Q - 1$, and the hole has $m = -Q$ giving $M = Q - 1$. As marked with lines in Fig. 35 unbound states above the multiplicative state form bands, which arise from the e – h interaction and are separated by gaps associated with the characteristic excitation energies of an e – h pair. (The e – h pseudopotential, i.e., the energy spectrum of an exciton, is shown in the inset). These bands are rather well approximated by the expectation values of the total (e – e and e – h) interaction energy, calculated in the eigenstates of the e – h interaction alone without e – e interaction.

In Fig. 36, we display the energy spectrum obtained by numerical diagonalization of the Coulomb interaction of a system of four electrons and two holes at $2Q = 15$ (Wójs et al., 1999b). The states marked by open and solid circles are multiplicative (containing one or more decoupled X s) and non-multiplicative states, respectively. For $L < 10$ there are four rather well defined low lying bands. Two of them begin at $L = 0$. The lower of these consists of two X^- ions interacting through a pseudopotential $V_{X^-X^-}(L)$. The upper band consists of states containing two decoupled X s plus two electrons interacting through $V_{e-e}(L)$. The band that begins at $L = 1$ consists of one X plus an X^- and an electron interacting through $V_{e-X^-}(L)$, while the band which starts at $L = 2$ consists of an X_2^- interacting with a free electron.

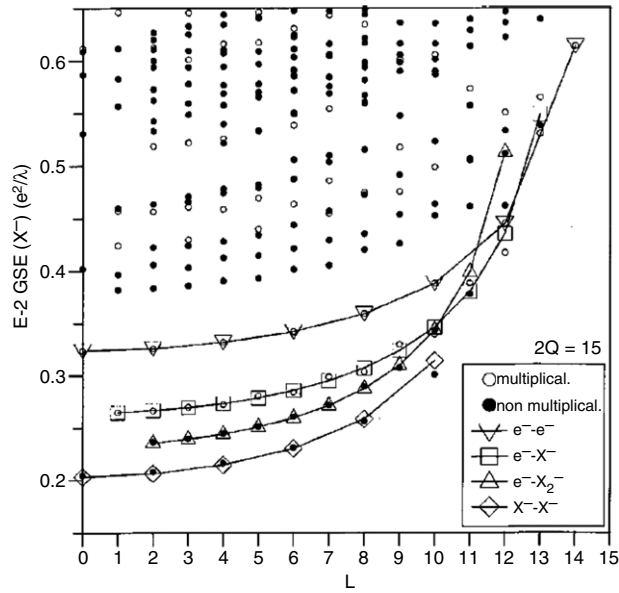


Fig. 36. The energy spectrum of four electrons and two holes at $2Q = 15$. Open circles: multiplicative states; solid circles: non-multiplicative states; triangles, squares and diamonds: approximate pseudopotentials (Quinn et al., 2003a).

Table 5

Binding energies $\varepsilon_0, \varepsilon_1, \varepsilon_2, \varepsilon_3$ of $X, X^-, X_2^-,$ and X_3^- , respectively, in units of e^2/λ .

$2Q$	ε_0	ε_1	ε_2	ε_3
10	1.3295043	0.0728357	0.0411069	0.0252268
15	1.3045679	0.0677108	0.0395282	0.0262927
20	1.2919313	0.0647886	0.0381324	0.0260328

Knowing that the angular momentum of an electron is $\ell_e = Q$, we can see that $\ell_{X_k^-} = Q - k$, and that decoupled excitons do not carry angular momentum ($\ell_X = 0$). For a pair of identical Fermions of angular momentum ℓ the allowed values of the pair angular momentum are $L' = 2\ell - j$, where j is an odd integer. For a pair of distinguishable particles with angular momenta ℓ_A and ℓ_B , the total angular momentum satisfies $|\ell_A - \ell_B| \leq L' \leq \ell_A + \ell_B$. The states containing two free electrons and two decoupled neutral excitons fit exactly the pseudopotential for a pair of electrons at $2Q = 15$; the maximum pair angular momentum is $L'^{\text{MAX}} = 14$ as expected. By comparing this band of states with the band containing two X^- s, we can obtain the binding energy of the neutral exciton to the electron to form the X^- . The other binding energy, that of a neutral exciton to an X^- to form an X_2^- can be obtained in a similar way.

18.2.2. Binding energies

We define ε_0 as the binding energy of a neutral exciton, ε_1 as the binding energy of an X to an electron to form an X^- , and ε_k as the binding energy of an X to an X_{k-1}^- to form an X_k^- . An estimate of these binding energies (in magnetic energy units e^2/λ , where λ is the magnetic length) as a function of $2Q$ are given in Table 5. We note clearly that $\varepsilon_0 > \varepsilon_1 > \varepsilon_2 > \varepsilon_3$.

18.2.3. Pseudopotentials $V_{AB}(L')$ of charged Fermions

In Fig. 36 the band of states containing two X^- s terminates at $L' = 10$. Since the X^- s are Fermions, one would have expected a state at $L'^{\text{MAX}} = 2\ell_{X^-} - 1 = 12$. This state is missing in Fig. 36. We surmise that the state with $L' = L'^{\text{MAX}}$ does not occur because of the finite size of the X^- . Large pair angular momentum corresponds to the small average separation, and two X^- s in the state with L'^{MAX} would be too close to one another for the bound X^- to remain stable. We can think of this as a “hard core” repulsion for $L' = L'^{\text{MAX}}$. Effectively, the corresponding pseudopotential parameter, $V_{X^-X^-}(L'^{\text{MAX}})$ is infinite. In a similar way, $V_{e^-X^-}(L'^{\text{MAX}})$ is infinite for $L' = L'^{\text{MAX}} = 14$ and $V_{e^-X_2^-}(L'^{\text{MAX}})$ is infinite for $L' = L'^{\text{MAX}} = 13$.

Once the maximum allowed angular momenta for all four pairings AB are established, all four bands in Fig. 36 can be roughly approximated by the pseudopotentials of a pair of point charges with angular momentum ℓ_A and ℓ_B , shifted by the binding energies of appropriate composite particles. For example, the X^-X^- band is approximated by the e^-e^- pseudopotential for $\ell = \ell_{X^-} = Q - 1$ plus twice the X^- energy. The agreement is demonstrated in Fig. 36, where the squares, diamonds, and two kinds of triangles approximate the four bands in the four-electron-two-hole spectrum. The fit of the diamonds to the actual X^-X^- spectrum is quite good for $L' < 10$. The fit of the e^-X^- squares to the open circle

multiplicative states is reasonably good for $L' < 12$, and the $e^- - X_2^-$ triangles fit their solid circle non-multiplicative states rather well for $L' < 11$. At sufficiently large separation (low L'), the repulsion between ions is weaker than their binding, and the bands for distinct charge configurations do not overlap.

There are two important differences between the pseudopotentials $V_{AB}(L')$ involving composite particles and those involving point particles. The main difference is the hard core discussed above. If we define the relative angular momentum $\mathcal{R} = \ell_A + \ell_B - L'$ for a pair of particles with angular momentum ℓ_A and ℓ_B then the minimum allowed relative angular momentum (which avoids the hard core) is found to be given by

$$\mathcal{R}_{AB}^{\min} = 2 \min(k_A, k_B) + 1, \quad (36)$$

where $A = X_{k_A}^-$ and $B = X_{k_B}^-$. The other difference involves polarization of the composite particle. A dipole moment is induced on the composite particle by the electric field of the charged particles with which it is interacting. By associating an “ionic polarizability” with the excitonic ion X_k^- , the polarization contribution to the pseudopotential can easily be estimated. When a number of charges interact with a given composite particle, the polarization effect is reduced from that caused by a single charge, because the total electric field at the position of the excitonic ion is the vector sum of contributions from all the other charges, and there is usually some cancellation. We will ignore this effect in the present work and simply use the pseudopotential $V_{AB}(L')$ obtained from Fig. 36 to describe the effective interaction.

18.3. Generalized composite Fermion picture

The electron, X^- , X_2^- , \dots are different types of Fermions, all of which have the same charge. These Fermions belong to different classes a, b, c, \dots , distinguishable from one another. In a system containing N_α Fermions of type α ($\alpha \in a, b, \dots$) the energy of interaction of a Fermion pair as a function of pair angular momentum can be expressed as $V_{\alpha\beta}(L')$. Here $L' \equiv \hat{\ell}_i + \hat{\ell}_j$ is the sum of the angular momentum $\hat{\ell}_i$ of the i th particle of type α and $\hat{\ell}_j$ of the j th particle of type β , and α, β can be in the same class or in different classes. All of the pseudopotentials in Fig. 36 are superharmonic. Because of this, the lowest energy states in a system containing N_α Fermions of type α ($\alpha \in a, b, \dots$) will be Laughlin correlated. We can describe the Laughlin correlations by introducing an “effective monopole strength” $2Q_\alpha^*$ seen by Fermions of type α using the generalized CF picture introduced in Section 13F.

We write:

$$2Q_a^* = 2Q - \sum_b (m_{ab} - \delta_{ab})(N_b - \delta_{ab}). \quad (37)$$

What we have done here is to attach to all type a Fermions ($m_{aa} - 1$) flux quanta that couple only to the charges on all other type a Fermions and m_{ab} , flux quanta sensed only by charges on the type b Fermions. This is a straightforward generalization of what we did in making in Section 13F. The coefficients m_{ab} are the powers that occur in the generalized Laughlin wavefunction, $\prod_{(i,j)} (z_i^{(a)} - z_j^{(b)})^{m_{ab}}$ where $z_i^{(a)}$ is the complex coordinate of the i th Fermion of type a and the product is over all pairs (i, j) . For different multicomponent systems generalized Laughlin incompressible states are expected to occur when (i) all the hard-core pseudopotentials are avoided and (ii) each type of CFs (i.e., CF_{aS} , CF_{bS} , \dots) completely fills an integral number of their angular momentum shells. In other cases, low lying multiplets are expected to contain different kinds of CF quasiparticles (QE_{aS} , QE_{bS} , \dots , or QH_{aS} , QH_{bS} , \dots) of the incompressible generalized Laughlin states.

Correlations between different particles a and b result from adiabatically adding m_{ab} flux quanta (sensed by the charge q_a on particle a) to particle b . Because the charge q_i is the same for each of the negatively charged Fermions ($i = e, X^-, X_2^-, \dots$), $m_{ab} = m_{ba}$ produces the same $a - b$ correlations by flux attachment to particle a or to particle b . In Section 13 we discuss Fermions of different charge ($q_e = q_{FP}/2$). In that case $q_a m_{ab} = q_b m_{ba}$ is required for the same $a - b$ correlations. This is why $2\gamma N_e$ appeared in Eq. (22) and γN_p appeared in Eq. (23).

18.4. Low lying bands of N_e electron – N_h hole systems

18.4.1. Condensed states of charged excitons

Consider for a moment a system containing 12 electrons and six holes on a Haldane spherical surface at monopole strength $2Q = 17$. The charge configuration with the largest binding energy is that containing six X^- charged excitons. We will refer to it as (i); its total binding energy ε_i is equal to $6(\varepsilon_0 + \varepsilon_1)$. If we make a CF transformation on this system of $N_{X^-} = 6$ negatively charged excitons, we obtain $2Q_{X^-}^* = 2Q - 2(N_{X^-} - 1) = 7$. The angular momentum of the X^- is given by $\ell_{X^-} = Q - 1 = 15/2$ and that of the CF X^- by $\ell_{X^-}^* = Q_{X^-}^* - 1 = 5/2$. This means that the six CF X^- s completely fill the $\ell_{X^-}^* = 5/2$ shell giving a Laughlin $L = 0$ incompressible state at $\nu_{X^-} = 1/3$. Note that $2\ell = \nu^{-1}(N - 1)$ holds for the quantum liquid of X^- s just as it did in the case of electrons.

One point worth noting is that the generalized CF picture of a multicomponent plasma can be thought of in terms of fictitious CF fluxes and CF charges that have different “colors” as discussed in Section 13. For example, electrons could have a red Chern–Simons charge and X^- s a green charge. Then $m_{ee} - 1$ red and m_{eX^-} green Chern–Simons fluxes would be attached to each electron, while $(m_{X^-X^-} - 1)$ green and m_{X^-e} red Chern–Simons fluxes would be attached to each X^- .

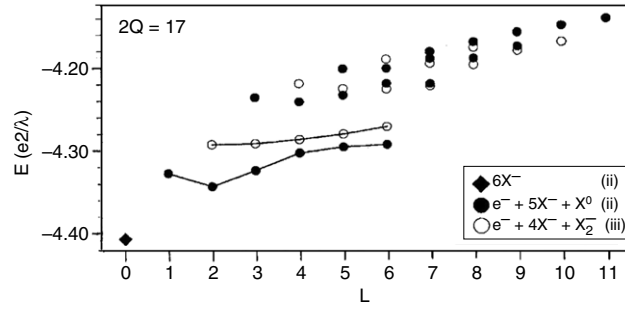


Fig. 37. Low energy spectra of different charge configurations of $12e + 6h$ on a Haldane sphere at $2Q = 17$: $6X^-$ (diamonds), $e^- + 5X^- + X$ (solid circles), and $e^- + 4X^- + X_2^-$ (open circles) (Wójs et al., 1999b).

Although X^- s have relatively long lifetimes for radiative recombination of an electron–hole pair, it seems unlikely that the Laughlin condensed state of negatively charged excitons can be observed by standard experimental techniques used in the case of condensed states of an electron liquid. However, the PL spectrum might give some indication of the correlations in the initial state. For example, if the ground state of a twelve electron–six hole system underwent e – h recombination, the initial state would be an $L = 0$ IQL state of six X^- excitons. Many different final states of the eleven electron–five hole system would be possible. Evaluating their eigenvalues and eigenfunction by numerical diagonalization would allow one to identify the energies and oscillator strength associated with different PL peaks. Selection rules would depend on sample properties like quantum well width, ratio of e^2/λ , Coulomb energy scale, to the LL separation, impurity concentration, etc. Such PL processes have not yet been studied in detail.

18.4.2. Other charge configurations

For the 12-electron–6-hole system, other charge configurations besides the six X^- s can occur as excited states. Among these are (ii) $e^- + 5X^- + X$ with total binding energy $\varepsilon_{ii} = 6\varepsilon_0 + 5\varepsilon_1$, and (iii) $e^- + 4X^- + X_2^-$ with total energy $\varepsilon_{iii} = 6\varepsilon_0 + 5\varepsilon_1 + \varepsilon_2$. The total energy of any state depends on the interaction energy of the constituent charged particles as well as the binding energy. The system of eighteen particles (12 electrons and 6 holes) at $2Q = 17$ is too large for us to diagonalize in terms of the electrons and holes and their interactions. However, we can obtain a reasonable approximation to the low lying energy spectrum by considering the different charge configurations denoted by (i) through (iii) each of which contains only six charged Fermions. We make use of our knowledge of the binding energies, angular momenta, and pseudopotentials $V_{AB}(L')$ where A and B can be e^- , X^- or X_2^- . The results of this simpler numerical calculation are presented in Fig. 37 (Wójs et al., 1999b). There is only one low lying state of the six X^- configurations, the $L = 0$ Laughlin $\nu_{X^-} = 1/3$ state. There are two bands of states in each of the charge configurations (ii) and (iii). The results presented in Fig. 37 can be understood from the generalized CF model. The CF predictions are: (i) for the system of $N_{X^-} = 6$, we take $m_{X^-X^-} = 3$ and obtain the Laughlin $\nu_{X^-} = 1/3$ state as discussed earlier. Because of the hard core of the $X^- - X^-$ pseudopotential, this is the only state of this charge configuration. (ii) For the $e^- + 5X^- + X$ configuration, we can take $m_{X^-X^-} = 3$ and $m_{eX^-} = 1, 2, \text{ or } 3$. For $m_{eX^-} = 1$ we obtain $L = 1 \oplus 2 \oplus 3^2 \oplus 4^2 \oplus 5^3 \oplus 6^3 \oplus 7^3 \oplus 8^2 \oplus 9^2 \oplus 10 \oplus 11$. For $m_{eX^-} = 2$ we obtain $L = 1 \oplus 2 \oplus 3 \oplus 4 \oplus 5 \oplus 6$ and for $m_{eX^-} = 3$ we obtain $L = 1$. (iii) For the grouping $e^- + 4X^- + X_2^-$, we set $m_{X^-X^-} = 3$, $m_{eX_2^-} = 1$, $m_{X^-X_2^-} = 3$ and $m_{eX^-} = 1, 2 \text{ or } 3$. For $m_{eX^-} = 1$, we obtain $L = 2 \oplus 3 \oplus 4^2 \oplus 5^2 \oplus 6^3 \oplus 7^2 \oplus 8^2 \oplus 9 \oplus 10$. For $m_{eX^-} = 2$, we obtain the multiplets $L = 2 \oplus 3 \oplus 4 \oplus 5 \oplus 6$, and for $m_{eX^-} = 3$, we have $L = 2$ (Quinn et al., 2003a). In the groupings (ii) and (iii) the sets of multiplets obtained for higher values of m_{eX^-} are subsets of those obtained for lower values of m_{eX^-} . We would expect them to form lower energy bands since they avoid additional \mathcal{R}_{eX^-} . However, note that the (ii) and (iii) states predicted for $m_{eX^-} = 3$ (at $L = 1$ and 2, respectively) do not form separate bands in Fig. 37. This is because the V_{eX^-} increases more slowly than linearly as a function of $L'(L' + 1)$ in the vicinity of $\mathcal{R}_{eX^-} = 3$. In such a case the CF picture fails (Wójs and Quinn, 1998b, 1999).

The agreement of our CF predictions with the data in Fig. 37 is really quite remarkable and strongly indicates that the multicomponent CF picture is correct. We were indeed able to confirm predicted Jastrow type correlations in the low lying states by calculating their coefficients of fractional parentage (de Shalit and Talmi, 1963). We have also verified the CF predictions for other systems that we were able to treat numerically. If exponents m_{ab} are chosen correctly, the CF picture works well in all cases.

18.5. Spectra of N_e electron–single hole system

In PL experiments the absorption of light creates a small number of electron–valence hole pairs in a quantum well that already has a concentration of conduction electrons. Because $N_h \ll N_e$, the valence holes are rather far apart, and the PL spectrum is not influenced by h – h interactions. One can evaluate the energies and wavefunctions for a single hole interacting with a gas of N_e electrons, investigate the allowed final states of $N_e - 1$ electrons, and calculate the energy and intensity of the PL spectrum lines. For this reason, it is useful to study the eigenstates of a N_e -electron–1-valence hole system. In order

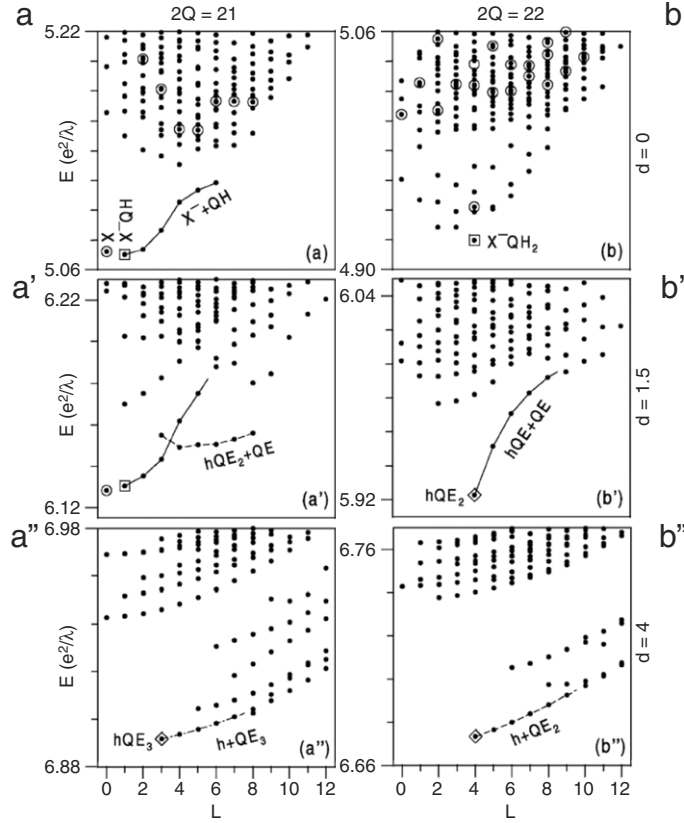


Fig. 38. Energy spectra of nine-electron-one-hole system for the monopole strength $2Q = 21, 22$ (from left to right), and for the interplane separation $d = 0, 1.5, 4$ (from top to bottom). Lines and open symbols mark the low states containing different bound excitonic complexes (Quinn et al., 2001b).

to remove the “hidden symmetry” that decouples the PL spectrum from the correlations in the underlying electron gas, we assume that the electrons and the hole reside on different 2D planes separated by a distance d between zero and four magnetic lengths, $\lambda = (\hbar c/eB)^{1/2}$. We take the cyclotron energies to be large compared to the Coulomb energy (e^2/λ) so that only a single LL for each kind of carrier is necessary.

In Fig. 38 we present the energy spectra for a system of 9 electrons and 1 valence band hole at three different values of separation d between the 2D layers and two different values of the monopole strength $2Q$ (Quinn et al., 2001b).

For $d \ll 1$ we have strong coupling between the electrons and the hole. Neutral (X) and charged excitons X^- are found. The multiplicative states at $d = 0$ are shown as solid dots surrounded by a small circle. Non-multiplicative states at $d = 0$ can have an X^- exciton interacting with the remaining $N - 2$ electrons. For $d \gg 1$ the valence hole interacts very weakly with the N -electron system, and the spectra can be described in terms of the eigenstates of the N -electron system multiplied by the eigenfunction of the hole with total angular momentum $\hat{L} = \hat{L}_e + \hat{L}_h$. For intermediate values of d ($d \simeq 2$) the e - h interaction is not a weak perturbation on the electronic eigenstates, but it is not always strong enough to bind a full electron to form an exciton.

For $d = 0$, X and X^- bound states occur. Due to the “hidden symmetry”, the multiplicative states containing an X have the same spectrum as the eight electron system shifted by the X binding energy. The CF model (Wójs and Quinn, 1998b, 1999; Wójs et al., 1999b) tells us the effective monopole strength seen by one CF in a system of $N' = N - 1 = 8$ electrons near $\nu = 1/3$ is $2Q^* = 2Q - 2(N' - 1)$. Q^* plays the role of the angular momentum of the lowest CF electron shell, therefore $Q^* = 7/2$ and 4 for the multiplicative states in frames (a) and (b) of Fig. 38, respectively. Since the lowest CF shell can accommodate $2Q^* + 1$ CFs, it is exactly filled in frame (a), but there is one empty state in the $\ell^* = 4$ CF level, or one QH of angular momentum $\ell_{QH} = 4$ in frame (b). Thus the lowest multiplicative states have $L = 0$ in frame (a) and $L = 4$ in frame (b). The magnetoroton band of multiplicative states in frame (a) is clearly marked. It has $2 \leq L \leq 8$, and it is contained within the quasicontinuum of non-multiplicative states.

For the non-multiplicative states we have one X^- and $N_e = N - 2$ remaining electrons. The generalized CF picture (Wójs et al., 1999b) allows us to predict the lowest energy band in the spectrum in the following way. The effective monopole strength seen by the electrons is $2Q^* = 2Q - 2(N_e - 1) - 2N_{X^-}$, while that seen by the X^- is $2Q_{X^-}^* = 2Q - 2N_e$. Here, we have attached to each Fermion (electron and X^-) two fictitious flux quanta and used the mean-field approximation to describe the effective monopole strength seen by each particle (note that a CF does not see its own flux). The angular

momentum of the lowest CF electron shell is $\ell_0^* = Q_e^*$, while that of the CF X^- shell is $\ell_{X^-} = Q_{X^-}^* - 1$ (Quinn et al., 2001b; Wójs et al., 1999b). For the system with $N_e = 7$ and $N_{X^-} = 1$ at $2Q = 21$ and 22 , the generalized CF picture leads to: one QH with $\ell_{QH} = 7/2$ and one X^- with $\ell_{X^-}^* = 5/2$, giving a band at $1 \leq L \leq 6$ for Fig. 38(a) and two QHs with $\ell_{QH} = 4$ and one X^- with $\ell_{X^-}^* = 3$ giving $L = 0 \oplus 1 \oplus 2^3 \oplus 3^3 \oplus 4^4 \oplus 5^3 \oplus 6^3 \oplus 7^2 \oplus 8^2 \oplus 9 \oplus 10$ for Fig. 38(b).

For $d \gg 1$, the electron–hole interaction is a weak perturbation on the energies obtained for the N -electron system. The numerical results can be understood by adding the angular momentum of a hole $\ell_h = Q$, to the electron angular momentum obtained from the simple CF model. The predictions are: for $2Q = 21$ there are three QEs each with $\ell_{QE} = 7/2$ and the hole has $\ell_h = 21/2$; for $2Q = 22$ two QEs each with $\ell_{QE} = 4$ and $\ell_h = 11$. Adding the angular momenta of the identical Fermion QEs gives L_e , the electron angular momenta of the lowest band; adding to L_e the angular momentum ℓ_h gives the allowed set of allowed multiplets appearing in the low energy sector. For example, in Fig. 38(b'') the allowed values of L_e are $1 \oplus 3 \oplus 5 \oplus 7$, and the multiplets at 7 and 3 have lower energy than at 1 and 5. Four low energy bands appear at $4 \leq L \leq 18$, $8 \leq L \leq 14$, $6 \leq L \leq 16$, and $10 \leq L \leq 12$, resulting from $L_e = 7, 3, 5$, and 1 , respectively.

For $d \approx 1$, the electron–hole interaction results in formation of bound states of a hole and one or more QEs. In the two-electron–one-hole system, the X and X^- unbind for $d \approx 1$, but interaction with the surrounding unbound electrons in a larger system can lead to persistence of these excitonic states beyond $d = 1$. For example, the band of states at $d = 0$ in Fig. 38(a) that we associated with an X^- interaction with a QH persists at $d = 1.5$ in Fig. 38(a'). However, it appears to cross another low energy band that extends from $L = 3$ to 8 . This latter band can be interpreted in terms of three QEs interacting with the hole as done in the weak-coupling limit shown in Fig. 38(a''). The other bands of the weak coupling regime (those beginning at $L = 5, 6, 7, 8$, and 9) have disappeared into the continuum of higher states as a result of the increase of V_{eh} .

For $2Q = 22$, the lowest band can be interpreted in terms of one X^- interacting with two QHs of the generalized CF picture. The X^- has $\ell_{X^-}^* = 3$ and each QH has $\ell_{QH} = 4$. The allowed values of L_{2QH} are $7, 5, 3$, and 1 , and the molecular state QH_2 which has the smallest average QH–QH distance would have $\ell_{QH_2} = 7$. This gives a band of $X^- + QH_2$ states going from $L = \ell_{QH_2} - \ell_{X^-}^* = 4$ to $L = \ell_{QH_2} + \ell_{X^-}^* = 10$. A higher band beginning at $L = 2$ might be associated with a $2QH$ state at $L_{2QH} = 5$ interacting with an X^- . The origin of the other bands is less certain.

It is worth noting that the X^- QH band in Fig. 38(a) resembles the neutral exciton band shown in the inset of Fig. 35. The latter band begins at $L = 0$ because $\ell_e = \ell_h = 5$ and $|\ell_e - \ell_h| \leq L \leq \ell_e + \ell_h$. For the X^- QH band $\ell_{X^-} = Q^* - 1 = 5/2$ and $\ell_{QH} = Q^* = 7/2$ giving a band starting at $L = \ell_{QE} - \ell_{X^-} = 1$ and ending at $L = \ell_{QE} + \ell_{QH} = 6$. The width of this band is smaller than that of the neutral X by at least an order of magnitude. This reflects the fact that the magnitude of the effective charges of the correlated X^- (and of the QH) is one third of the electron charge, and of the fact that the charge is spread over a wider region. This makes it clear that the correlated X^- can be thought as a quasi- X^- (QX^-), and just like the Laughlin QH it has an effective charge of magnitude $1/3$. This allows us to call the QH – QX^- band state a neutral quasiexciton QX^0 .

19. Photoluminescence

19.1. General considerations

Exact numerical diagonalization gives both the eigenvalues and the eigenfunctions. The low energy states $|i\rangle$ of the initial N -electron–one-hole system have just been discussed. The final states $|f\rangle$ contain $N' = N - 1$ electrons but no holes. The recombination of an electron–hole pair is proportional to the square of the matrix element of the photoluminescence operator $\hat{\mathcal{L}}$, where $\hat{\mathcal{L}} = \int d^3r \Psi_e(\vec{r}) \Psi_h(\vec{r})$ and $\Psi_e(\vec{r})$ (or $\Psi_h(\vec{r})$) annihilates an electron (or hole). We have evaluated $|\langle f | \hat{\mathcal{L}} | i \rangle|^2$ for all of the low-lying initial states and have found the following results (Wójs and Quinn, 2000b). (i) Conservation of the total angular momentum L is at most weakly violated through the scattering of spectator particles (electrons and quasiparticles) which do not participate directly in the recombination process if the filling factor ν is less than (approximately) $1/3$. (ii) In the strong coupling region, the neutral X line is the dominant feature of the PL spectrum. The X^- QH₂ state has very small oscillator strength for radiative recombination. (iii) For intermediate coupling, the hQE_2 and an excited state of the hQE (which we denote by hQE^*) are the only states with large oscillator strength for photoluminescence.

At zero temperature ($T = 0$), all initial states must be ground states of the N -electron–one-hole system. At finite but low temperatures, excited initial states contribute to the PL spectrum. The photoluminescence intensity is proportional to

$$w_{i \rightarrow f} = \frac{2\pi}{\hbar} \mathcal{Z}^{-1} \sum_{i,f} e^{-\beta E_i} |\langle f | \hat{\mathcal{L}} | i \rangle|^2 \delta(E_i - E_f - \hbar\omega), \quad (38)$$

where $\beta = (kT)^{-1}$ and $\mathcal{Z} = \sum_i e^{-\beta E_i}$.

19.2. Singlet and triplet charged excitons: photoluminescence for dilute ($\nu \ll 1$) systems

Only spin polarized charged excitons (with $S = 1$) are bound when the ratio $(\hbar\omega_C)/(e^2/\lambda)$ tends to infinity. In real systems at finite values of this parameter, both singlet ($S = 0$) and triplet ($S = 1$) charged excitons occur. According to the theory (Wójs and Quinn, 2000b) the singlet X_s^- is the ground state at low values of the magnetic field, while the triplet X_t^- is the ground state at very high magnetic fields. Numerical calculations of the ground states of both the singlet and triplet

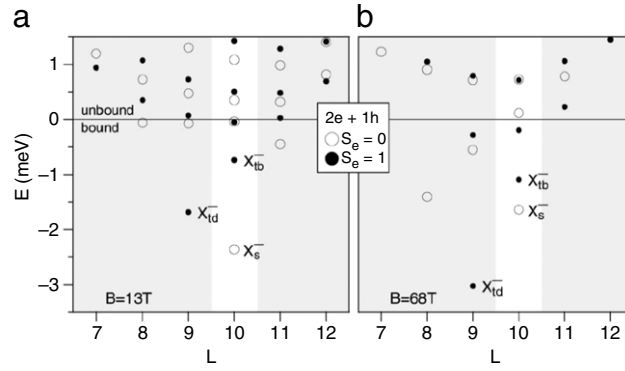


Fig. 39. Energy spectra (binding energies vs. angular momentum) of the two-electron-one-hole system on a Haldane sphere with the Landau level degeneracy $2Q + 1 = 21$. S_e denotes the total electron spin. The parameters are appropriate for the 11.5 nm GaAs quantum well (Wójs et al., 2000a).

charged excitons (Wójs and Quinn, 2000b) indicated a crossing at roughly $B \approx 30$ T for a symmetric GaAs quantum well, the width of which was about $w = 10$ nm. Observation of PL by Hayne et al. (1999) displaying three peaks that were interpreted as the X , X_t^- , and X_s^- , showed no crossing of the X_t^- and X_s^- up to the fields of 50 T. This led the experimenters to question the validity of variational calculations.

In this section we study very small systems (either two or three electrons and one valence band hole) in narrow ($w \sim 11.5$ nm) symmetric GaAs quantum wells. We include the effects of Landau level mixing caused by the interactions, and the effect of finite well width on the effective interaction. Only a single subband is used in the calculations, since the quantum well is relatively narrow. Both electrons and holes are described in the effective mass approximation, and interband coupling is partially accounted for by a magnetic field dependence of the cyclotron mass of the hole (taken from experimental data). The Zeeman energy depends on both the well width and the magnetic field B . Five Landau levels for both the electrons and holes were included in the calculation in order to obtain satisfactory convergence. The energies obtained for different values of the monopole strength $2Q$ were extrapolated to the large Q limit to eliminate finite-size effects.

The energy spectra of the two-electron-one-hole system calculated for $2Q = 20$ are shown in Fig. 39. Open and solid symbols mark singlet and triplet states (S_e is the total electron spin), and each state with $L > 0$ represents a degenerate L multiplet. Since the PL process (annihilation of an $e-h$ pair and emission of a photon) occurs with conservation of angular momentum, only states from the $L = Q$ channel are radiative (Wójs et al., 2000a). Recombination of other non-radiative states requires breaking rotational symmetry (e.g., by collisions with electrons). This result is independent of the chosen spherical geometry and holds also for a planar quantum well, except that the definition of the conserved momentum is different (Dzyubenko and Sivachenko, 1993, 2000; Dzyubenko et al., 1994).

The occurrence of a strict PL selection rule at finite B may seem surprising, since the hidden symmetry that forbids the X_{td}^- recombination in the lowest LL does not hold when the mixing with higher LLs is included. (The “d” in X_{td}^- means “dark” and X_{tb}^- is called the dark triplet because it is forbidden to decay radiatively.) However, it is both the hidden symmetry and the above-mentioned angular momentum conservation that independently forbid the X_{td}^- recombination, and the latter remains valid at finite B . Although the hidden symmetry and resulting N_X conservation law no longer hold at finite B , the X_{td}^- recombination remains strictly forbidden because of the independently conserved L .

We expect breaking of both symmetries for real experimental situations. The presence of impurities and defects, and $e-X_{td}^-$ scattering during recombination in the presence of excess electrons can relax the strict conservation of the X^- angular momentum in the radiative decay. However, for narrow and symmetric quantum wells containing a relatively small number of excess electrons, the symmetries may only be weakly broken and some remnant of the strict conservation laws may survive.

Three states marked in Fig. 39 are of particular importance: X_s^- and X_{tb}^- (“b” stands for “bright”) are the only strongly bound radiative states, while X_{td}^- has by far the lowest energy of all non-radiative states. The radiative triplet bound state X_{tb}^- was identified for the first time by Wójs et al. (2000a,b). The binding energies of all three X^- states are extrapolated to $\lambda/R \rightarrow 0$ and plotted in Fig. 40(a) as a function of B . For the X_s^- , the binding energy differs from the PL energy (indicated by a thin dotted line) by the Zeeman energy needed to flip one electron’s spin, and the cusp at $B \approx 42$ T is due to the change in sign of the electron g -factor. For the triplet states, the PL and binding energies are equal. The energies of X_s^- and X_{td}^- behave as expected: The binding of X_s^- weakens at higher B and eventually leads to its unbinding in the infinite field limit; the binding energy of X_{td}^- changes as $e^2/\lambda \propto \sqrt{B}$; and the predicted transition from the X_s^- to the X_{td}^- ground state at $B \approx 30$ T is confirmed. The new X_{tb}^- state remains an excited triplet state at all values of B , and its binding energy is smaller than that of X_s^- by about 1.5 meV. The oscillator strengths τ^{-1} of a neutral exciton X and the two radiative X^- states are plotted in Fig. 40 (b). In the two-electron-one-hole spectrum, the strongly bound X_s^- and X_{tb}^- states share a considerable fraction of the total oscillator strength of one X , with τ_{tb}^{-1} nearly twice larger than τ_s^{-1} .

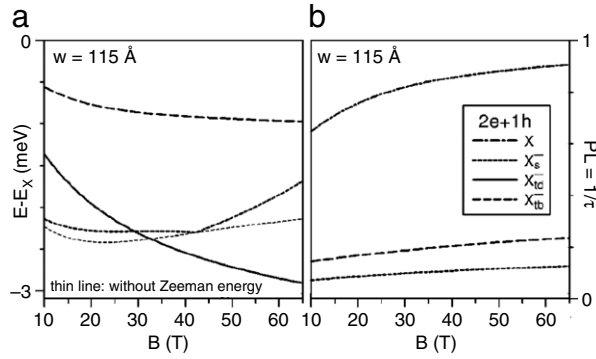


Fig. 40. The X^- energies (a) and oscillator strength (b) in the 11.5 nm GaAs quantum well plotted as a function of the magnetic field (Wójs et al., 2000b).

The comparison of calculated magnitude and magnetic field dependence of the X^- binding energies with the experimental PL spectra, as well as high oscillator strength of the X_{tb}^- , lead to the conclusion that the three peaks observed in PL are the X , X_s^- , and X_{tb}^- .

To understand why the X_{td}^- state remains optically inactive even in the presence of collisions, the $e-X^-$ interaction must be studied in greater detail. Our numerical results for a three-electron–one-hole system indicate that the lowest band of states consists of a triplet X^- and one unbound electron. Because the $X_{td}^- - e$ pseudopotential is superharmonic, in real experimental systems at a low electron concentration ($\nu \leq 1/3$) Laughlin correlations between the electron and X_{td}^- will effectively isolate the X_{td}^- from the surrounding 2D electron system. This prevents close collisions of the X_{td}^- and the spectator electron during the $e-h$ recombination. Although the X_{td}^- is no longer forbidden to decay radiatively since the spectator electron can change its angular momentum in the recombination process, this scattering process is weak for $\nu < 1/3$. The oscillator strength for radiative decay of the X_{td}^- is found to be more than an order of magnitude smaller than those of the X_s^- and X_{tb}^- . These results support the interpretation that the three peaks observed in many experiments correspond to the X , X_s^- , and X_{tb}^- . The X_{td}^- is not observed because of its small oscillator strength. The X_{td}^- recombination line has been observed (Yusa et al., 2001), when special care (very low temperatures and high quality samples) was taken to detect its weak signal. Even more convincing is the comparison with infrared absorption at very low temperature where only the X_{td}^- state is heavily occupied. Absorption spectra show only one strong peak in contrast to PL spectra which shows three, because the higher population of the X_{td}^- compensates for its lower oscillator strength for photon absorption compared to the X_s^- and X_{tb}^- (Schüller et al., 2002, 2003).

19.3. X^- in an incompressible quantum liquid of electrons: fractionally charged quasiexcitons

In Fig. 38(a) and (a') we observed both a low energy multiplicative state (consisting of a neutral exciton effectively decoupled from the remaining $N'_e = N_e - 1$ unbound electrons) at $L = 0$, and a band of non-multiplicative states extending from $L = 1$ to $L = 6$. This band could be identified (using a generalized CF picture) as a QH of the Laughlin IQL state coupled to the QX^- (which has Laughlin correlations with the $N'_e = N_e - 2$ unbound electrons). In Section 18 we discussed how it could be thought of as a neutral quasiexciton QX^0 . We will sometimes use the symbols (χ^-, χ, χ^+) for the three different possible quasiexcitons in place of (QX^-, QX, QX^+) . χ is the neutral QX (a bound state of χ^- and a QH), while χ^+ is a positively charged QX^+ (a bound state of χ and a QH).

In this subsection we review the many-body correlations associated with negatively charged excitons (or trions) immersed in a Laughlin IQL state, and predict a discontinuity of the PL spectrum at $\nu = 1/3$ (Byszewski et al., 2006; Goldberg et al., 1990; Wójs et al., 2006a) and for spin-polarized systems, we elucidate the earlier theory (Apalkov and Rashba, 1992, 1993; Zang and Birman, 1995) by identifying the “dressed exciton” with χ , its suppressed dispersion with the χ^- -QH pseudopotential of interaction among two Laughlin fractionally charged quanta, and the “magnetoroton-assisted emission” with the χ^- recombination.

Photoluminescence from systems containing a small number of quasiexcitons (χ^-, χ, χ^+) reflect the properties of these quasiexcitons in the initial state. The χ^- is formed when a valence band hole binds two electrons to form an X^- , which then becomes Laughlin correlated with the remaining unbound electrons (in, for example, an IQL $\nu = 1/3$ state). If several χ^- quasiexcitons are present, they repel one another. Then the radiative $e-h$ recombination is essentially that of an isolated χ^- in the IQL state of the remaining electrons. If the magnetic field is increased to values that make $\nu > 1/3$, Laughlin QHs will be present. The χ^- attracts the Laughlin QHs, and can form a neutral (χ^0) or positively charged (χ^+) quasiexciton. The resulting PL spectrum would be expected to reflect the properties of the initial χ^- or χ^+ for $\nu > 1/3$ and $\nu < 1/3$ respectively. For ν very close to the IQL value ($\nu = 1/3$) an initial χ^0 state might also be observed. The PL from different initial states could have different energies and different intensities, so observing a change in the PL spectrum as ν passes through an IQL value like $\nu = 1/3$ is not surprising (Goldberg et al., 1990; Schüller et al., 2002, 2003).

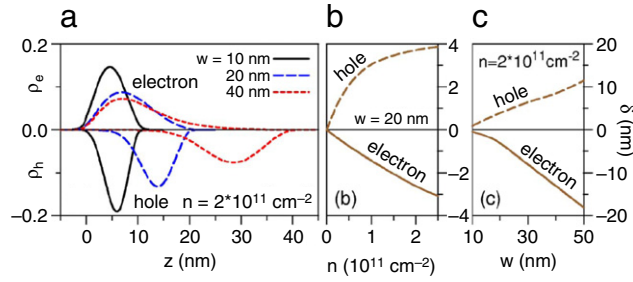


Fig. 41. (color online) (a) Lowest subband electron and heavy-hole charge density profiles in the normal direction $\rho(z)$ for one-sided doped GaAs quantum wells (b), (c) Displacements δ of the density maxima from the center of the quantum well as a function of electron concentration n and well width w (Wójs et al., 2006a).

We illustrate these concepts by use of exact numerical diagonalization for $N \leq 10$ electrons and one valence hole on a Haldane sphere (Haldane, 1983) with radius R , magnetic monopole strength $2Q = 4\pi R^2 Be/hc$, and magnetic length $\lambda = R/\sqrt{Q}$. The second-quantization Hamiltonian reads $H = \sum_i U_i c_i^\dagger c_i + \sum_{ijkl} V_{ijkl} c_i^\dagger c_j^\dagger c_k c_l$. Here, c_i^\dagger and c_i are operators creating and annihilating an electron in the conduction band or a hole in the valence band, in the state labeled by a composite index i containing all relevant single-particle quantum numbers (band, subband, and LL indices, angular momentum, and spin). The single-particle energies are measured from the ground states in conduction and valence bands, respectively. The Coulomb interaction matrix elements V were integrated in 3D by taking the actual electron and hole subband wavefunctions $\phi(z)$ calculated self-consistently (Tan et al., 1990) for $w = 10$ and 20 nm GaAs quantum wells, doped on one side to $n = 2 \times 10^{11} \text{ cm}^{-2}$ (yielding $\nu = 1/3$ at $B = 25$ T). The diagonalization was carried out in configuration–interaction basis, $|i_1, \dots, i_N; i_h\rangle = c_{i_1}^\dagger \cdots c_{i_N}^\dagger c_{i_h}^\dagger |vac\rangle$, where indices $i_1 \cdots i_N$ denote the occupied electron states, and i_h describes the hole. Finite size and surface curvature errors were minimized by extrapolation to the $\lambda/R \rightarrow 0$ limit. The combination of closed geometry, used as an alternative to periodic boundary conditions for modeling in-plane dynamics, with exact treatment of the single-particle motion in the normal direction allowed for quantitative estimates of binding energies characterizing extended experimental systems.

We begin with the calculation of X^- Coulomb binding energies Δ using $\phi(z)$, i.e., in the mean normal electric field due to a doping layer, but ignoring in-plane X^- –IQL coupling. We included five LLs and two ϕ -subbands for both e and (heavy) h . The lowest-subband e and h density profiles for $w = 10, 20$, and 40 nm are plotted in Fig. 41(a). The effect of charge separation in wider wells is evident. The shifts of the density maxima as a function of n and w are shown in Fig. 41(b) and 41(c). For the cyclotron energies ω_c (at $B = 25$ T; after the experiment of Cole et al. (1997)) and intersubband gaps Ω_s (from own calculations) we took $\omega_{ce} = 44.5$ meV, $\omega_{ch} = 7.7$ meV, $\Omega_{se} = 29.6$ meV; $\Omega_{sh} = 10.0$ meV for $w = 20$ nm, and $\omega_{ce} = 44.5$ meV, $\omega_{ch} = 8.1$ meV, $\Omega_{se} = 89.8$ meV; $\Omega_{sh} = 24.5$ meV for $w = 10$ nm. The valence subband mixing was neglected. The result for $w = 10$ nm is $\Delta_s = 2.3$ meV and $\Delta_t = 1.5$ meV, in qualitative agreement with earlier work. (Riva et al., 2001; Stebe and Ainane, 1989; Whittaker and Shields, 1997; Wójs et al., 2000b), which also predicted the X_s^- ground state. For $w = 20$ nm, neither symmetric-well nor lowest-subband approximation works well (e.g., the latter exaggerates charge separation in X/X^- which mostly affects the X_s^- and predicts its breakup at $B \geq 22$ T). Our best estimates are $\Delta_s = 1.5$ meV and $\Delta_t = 1.2$ meV. They are rather sensitive to the parameters, making prediction of the X^- ground state in real samples difficult and somewhat pointless. However, we expect that the X_t^- s, additionally favored by the Zeeman energy, could at least coexist with the X_s^- s at finite temperatures.

Consider a trion (either X_s^- or X_t^- , whichever state occurs at given w, n , and B) immersed in an IQL state. Effective e – X^- pseudopotentials are similar (Wójs et al., 2000b) to the e – e one (Haldane, 1987). In the lowest LL, this causes similar e – e and e – X^- correlations, described in a generalized two-component (Wójs et al., 1999a,b) CF picture (Jain, 1989). At Laughlin–Jain fillings $\nu_{\text{IQL}} = s/(2ps + 1)$, electrons converted to CF_e s fill the lowest s LLs in an effective magnetic field $B^* = B - 2pn(hc/e) = B/(2ps + 1)$. At $\nu \neq \nu_{\text{IQL}}$, QEs in the $(s + 1)$ st or QHs in the s th CF LL occur, carrying effective charge $\tilde{q} = \pm e/(2ps + 1)$. We find that, similarly, an X^- which is Laughlin correlated with surrounding electrons can be converted to a CF_{X^-} with charge $\mathcal{Q} = -\tilde{q}$.

This value can be obtained, e.g., by noting that when an X^- recombines, it leaves behind an indistinguishable electron which becomes a CF_e that either fills a QH in the s th CF_e LL or it appears as an additional QE in the $(s + 1)$ st CF_e LL. More importantly, partial screening of the trion’s charge is independent of either the particular X^- state or the filling factor, as long as correlations are described by the CF model. The same value $\mathcal{Q} = -\tilde{q}$ results for any other distinguishable charge $-e$ immersed in an IQL, if it induces Laughlin correlations around itself (e.g., an impurity (Haldane and Rezayi, 1985a) or a reversed-spin electron).

A trion coupled to an IQL and carrying reduced charge is a many-body excitation. To distinguish it from an isolated $2e + h$ state, we call it a charged QX and denote it by $\chi^- \equiv \chi^{-\tilde{q}}$. Being negatively charged, a χ^- interacts with IQL QPs. At $\nu < \nu_{\text{IQL}}$, the χ^- binds to a QH to become a neutral $\chi^- - \text{QH} = \chi$, with a binding energy called Δ_0 . Depending on sample parameters and spin of the trion, χ may bind an additional QH to form a positively charged $\chi^- - \text{QH}_2 = \chi^+$, with binding energy Δ^+ . At $\nu > \nu_{\text{IQL}}$, the χ^+ attracts and annihilates a QE: $\chi^+ + \text{QE} \rightarrow \chi$; this process releases energy $\Delta_{\text{IQL}} - \Delta^+$ (where

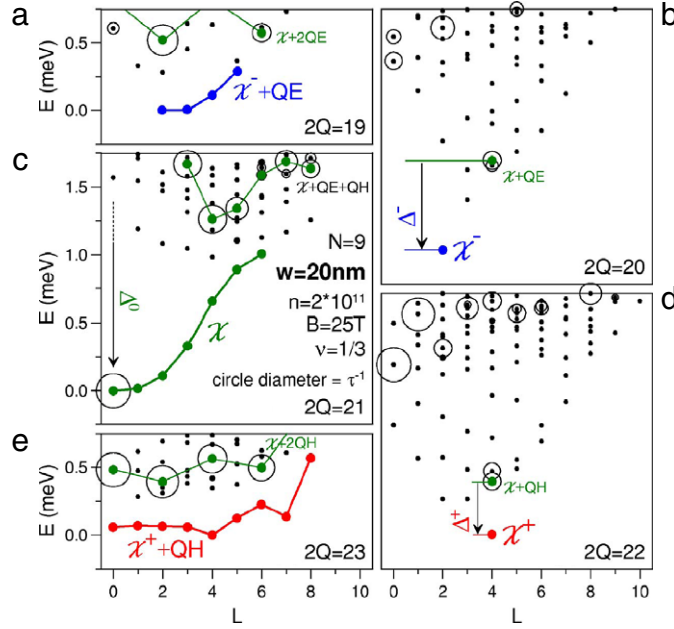


Fig. 42. (color online) Excitation energy spectra (energy E as a function of total angular momentum L) of $9e + h$ systems on a sphere, with up to two QEs or QHs in Laughlin $\nu = 1/3$ IQL. Oscillator strengths τ^{-1} are indicated by the area of the open circles (Wójs et al., 2006a).

$\Delta_{\text{IQL}} = \varepsilon_{\text{QE}} + \varepsilon_{\text{QH}}$ is the IQL gap). The χ may annihilate another QE: $\chi + \text{QE} \rightarrow \chi^-$, with energy gain

$$\Delta^- = \Delta_{\text{IQL}} - \Delta^0 \quad (39)$$

that can be interpreted as χ – binding energy. The χ and χ^\pm are different states in which a hole can exist in an IQL. If $\Delta^\pm > 0$, then depending on ν , either χ^- or χ^+ is the most strongly bound state. If $\Delta^- \neq \Delta^+$, the PL spectrum will be discontinuous at ν_{IQL} . For long-lived χ^\pm (made of a dark X_t^\pm), recombination of the χ is also possible, especially at $\nu \approx \nu_{\text{IQL}}$ (within a Hall plateau), when QP localization impedes χ^\pm formation. The QXs resemble normal excitons in n - or p -type systems, except that the concentration of their constituent QPs can be varied (in the same sample) by a magnetic field. Also, their kinetics ($\chi \leftrightarrow \chi^\pm$) are more complicated because of the involved QE–QH annihilation.

We have tested the QX idea numerically for Laughlin $\nu = 1/3$ IQL. First, we calculated spin-polarized $Ne + h$ energy spectra for $w = 20$ nm, in search of the QX_t s. The X_t^- has 94% squared projection onto the lowest LL, so we ignored LL mixing in the $Ne + h$ calculation (direct tests confirmed that it is negligible). The low-lying states in Fig. 42 are understood using the CF picture (Jain, 1989; Wójs et al., 1999a,b) and addition rules for angular momentum. On a sphere, the CF transformation introduces an effective monopole strength $2Q^* = 2Q - 2(K - 1)$, where $K = N - 1$ is the total number of free electrons and X^- s. The angular momenta of constituent QPs are $\ell_{\text{QH}} = Q^*$, $\ell_{\text{QE}} = Q^* + 1$, and $\ell_{\chi^-} = Q^* - 1$. The χ^- is a dark ground state in (b) at $L = \ell_{\chi^-} = 2$, and χ^+ is found in (d) at $L = \ell_{\chi^+} = |(2\ell_{\text{QH}} - 1) - \ell_{\chi^-}| = 4$. Bands of χ^- –QE and χ^+ –QH pairs are marked in (a) and (e). In (c) the radiative $L = 0$ ground state is a multiplicative state, opening a $X = X^-$ –QH band (Chen and Quinn, 1993; Wójs and Quinn, 2000b,c), earlier called a “dressed exciton” and identified (Apalkov and Rashba, 1992, 1993; Zang and Birman, 1995) as responsible for the doublet structure in PL. The continuous χ dispersion shown in Fig. 43(a) results (Apalkov and Rashba, 1992, 1993; Zang and Birman, 1995) from the in-plane dipole moment being proportional to the wave vector $k = \ell/R$. It is suppressed (compared to X) because of the reduced charge of the χ constituents, χ_t^- and QH. In the absence of an IQL the center of mass of the two charges are separated and the cyclotron motion of each charge together with their Coulomb attraction causes them to move with a momentum proportional to their separation ($d \propto k$). In an IQL, the charge quantum is reduced to \tilde{q} . This has no consequence at $k = 0$, and the χ is equivalent to an X decoupled from the remaining electrons. A moving χ has a dipole moment proportional to its wave vector but it is smaller because the charges are $\pm\tilde{q} = \pm e/3$. The χ and X dispersions become similar in size, when χ acquires dipole moment in a different way than X , by splitting into χ^- and QH, each carrying only one small quantum $\pm\tilde{q}$. Indeed, the χ and X dispersions become similar when energy and length scales are rescaled on account of the $\tilde{q} \rightarrow e$ charge reduction. Note that we also explain the emission from χ at $k\lambda \sim 1.5$, proposed (Apalkov and Rashba, 1992, 1993; Zang and Birman, 1995) for the lower peak in PL, as the $\chi^- \rightarrow \text{QE}$ recombination assisted by QH scattering. However, a small dV/dk and a large τ^{-1} at $k\lambda \sim 1.5$ needed for this emission requires significant well widths, $w > 20$ nm.

By identifying the multiplicative states containing an χ with $k = 0$, one can estimate Δ^\pm and Δ^0 as marked in Fig. 42 (b) and (d). More accurate values were obtained by comparing the appropriate energies identified in the spectra obtained at different values of $2Q$, in which either χ^\pm , χ , or QP is alone in the IQL, followed by extrapolation to $N \rightarrow \infty$. Our best estimates, whose reasonable accuracy of under 0.05 meV is confirmed by Eq. (39), are $\varepsilon_{\text{QH}} = 0.73$ meV, $\varepsilon_{\text{QE}} = 1.05$ meV,

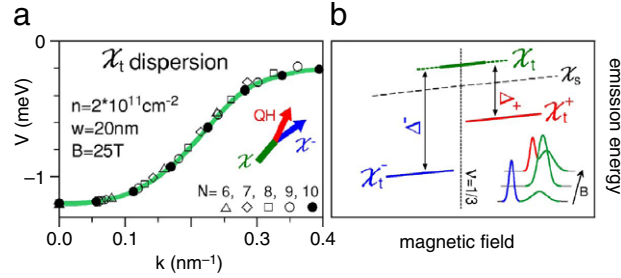


Fig. 43. (color online) Dispersion of neutral quasiexciton χ_t in Laughlin $\nu = 1/3$ IQL; χ_t splits into χ_t^- and QH at $k > 0$. (b) Schematic PL discontinuity due to χ_t^\pm emissions (Wójs et al., 2006a).

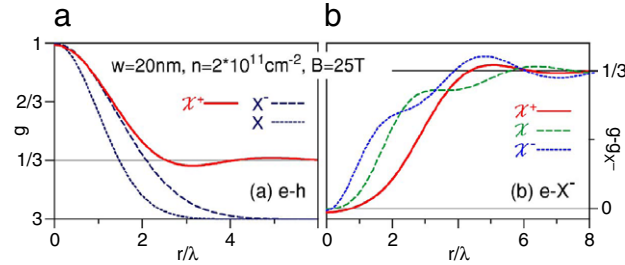


Fig. 44. (color online) (a) The e - h pair-distribution function (PDF) of quasiexciton χ_t^+ and isolated χ_t^- and X , normalized to measure the local filling factor. (b) The e - X^- PDF for different QXs; curve for χ^+ resembles e - e PDF of Laughlin liquid; shoulders for χ and χ^+ reflect additional charge quanta pushed onto the hole (Wójs et al., 2006a).

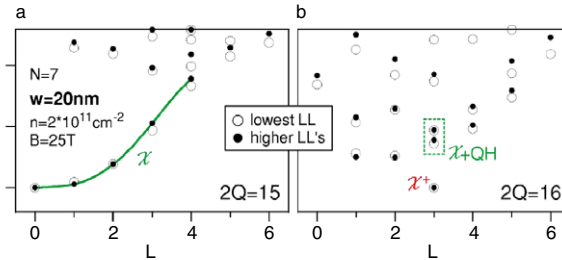


Fig. 45. (color online) Excitation spectra similar to Fig. 42, but for $7e + h$ system with and without LL mixing (Wójs et al., 2006a).

$\Delta^0 = 1.20$ meV, $\Delta^- = 0.52$ meV, and $\Delta^+ = 0.27$ meV. Depending on χ^0/χ^\pm kinetics, either $\Delta^+ \neq \Delta^-$ or $\Delta^0 \neq \Delta^\pm$ asymmetry will make PL energy jump at $\nu = 1/3$, as sketched in Fig. 43(b). Similar behavior has been observed (Byszewski et al., 2006; Goldberg et al., 1990). The χ^\pm discontinuity is different from that due to anyon excitons (Chen and Quinn, 1994b; Parfitt and Portnoi, 2003; Portnoi and Rashba, 1996; Rashba and Portnoi, 1993; Wójs and Quinn, 2000b,c) anticipated in much wider wells (e.g., for $w \geq 40$ nm at $n = 2 \times 10^{11}$ cm $^{-2}$). The two effects can be distinguished by different magnitude ($\sim \Delta_{\text{IQL}}$ vs Δ^\pm) and opposite direction of the jump of emission energy when passing through $\nu = 1/3$. In the present case, the small ratio of χ^\pm and X^\pm binding energies is the signature of the fractional charge of the IQL excitations—directly observable as splittings in PL. The QXs are defined through a sequence of gedanken processes: (i) trion binding: $2e + h \rightarrow X^-$, (ii) Laughlin correlation: $X^- \rightarrow \chi^-$, (iii) QH capture: $\chi^- \rightarrow \chi/\chi^+$. Hence, χ and χ^\pm are in fact the same X^- , only differently separated from the surrounding electrons.

This is evident in the e - h pair-distribution functions $g(r)$ shown in Fig. 44(a) and normalized so as to measure electron concentration near the hole in units of ν . The χ^+ curve calculated for $N = 10$ is compared with $g_{X^-}(r) = \exp(-r^2/4)$ which accurately describes an X_t^- . The similarity at short range proves that the χ^+ is an X^- well separated from the 2D electron gas. In Fig. 44(b) we plotted $\delta g = g - g_{X^-}$ which measures the $e - X^-$ correlations in different QX states. Clearly, δg_{χ^+} resembles the e - e pair-distribution function of a Laughlin $\nu = 1/3$ liquid, while shoulders in δg_χ and δg_{χ^-} reflect additional charge quanta pushed onto the hole in χ and χ^- . Let us add that integration of $[g(r) - 1/3]$ directly confirms fractional electron charge of $-(4/3)e$, $-e$, and $-(2/3)e$ bound to the hole in the χ^- , χ , and χ^+ states.

The accuracy of the lowest LL approximation is demonstrated in Fig. 45, in which we compare the excitation energy spectra similar to Fig. 42(a) and (d), but calculated for the $7e + h$ systems, with and without inclusion of one higher e and h LL. Evidently, neither the χ dispersion nor the χ^+ binding energy appear sensitive to the LL mixing. This is in contrast

to the behavior of X or X^- , and the difference obviously reflects weaker interactions among the fractional QX constituents (compared to the same cyclotron energy scale).

The quasiexcitons formed by the singlet X_s^- have been studied numerically for a quantum well of width $w = 10$ nm by considering an $8e + h$ system with spin $S = 3$ (i.e., one spin flipped). In contrast to the results for the quasiparticles formed by the triplet X_t^- , the χ_s^\pm charged singlet quasiexcitons are excited states. The X_s^- charge distribution is more compact than that of X_t^- , leading to stronger dispersion of neutral χ_s^0 and a different coupling of the X_s^- to the Laughlin quasiparticles. The neutral χ_s^0 is the most strongly bound state regardless of the presence of Laughlin QEs and QHs. This may result in a continuous PL peak for χ_s^0 , but precludes PL discontinuity in narrow wells with a strong X_s^- ground state. The χ_s peak splits into a σ_\pm doublet due to spin \downarrow and \uparrow recombination involving either QEs or “reversed-spin” QERs (Rezayi, 1987), but temperature-activated emission at $k > 0$ is not expected. The QX idea can be extended to other IQLs (e.g., $\nu = 2/3$ or $2/5$). However, different behavior of QX_t s and QX_s s at $\nu = 1/3$ is an example that PL discontinuity is not guaranteed. Via Eq. (39), it is governed by sample and ν -dependent Δ_{IQL} and Δ^0 which must be recalculated.

20. Summary and conclusions

The fractional quantum Hall effect is a paradigm for all strongly interacting systems, containing, at high magnetic field B , only a single energy scale, the Coulomb scale e^2/λ , where λ is the magnetic length. Understanding all of the observed IQL states may well give insight into a number of strongly interacting systems of great current interest.

In this paper we have reviewed exact numerical diagonalization of small systems within the Hilbert subspace of a single partially occupied LL. The numerical results are thought of as “numerical experiments”, and simple intuitive models fitting the numerical data are sought, to better understand the underlying correlations. We describe calculations for N electrons confined to a Haldane spherical surface, and present simple results at different values of the LL degeneracy $g = 2\ell + 1$. We demonstrate that Jain’s remarkable CF picture predicts not only the values of 2ℓ at which IQL ground states occur for different values of N , but also predicts the angular momenta L of the lowest band of multiplets for any value of 2ℓ in a very simple way. We emphasize that Jain’s CF picture is valid, not because of some magical cancellations of Coulomb and Chern–Simons gauge interactions beyond mean-field, but because it introduces Laughlin correlations by avoiding pair states with the lowest allowed relative angular momentum $\mathcal{R} = 2\ell - L'$. The allowed angular momentum multiplets which avoid pair states with $\mathcal{R} = 1$ form a subset of the set of multiplets $G_{N\ell}(L)$ that can be formed from N Fermions in a shell of angular momentum ℓ . This subset avoids the largest repulsion and has the lowest energy. Our adiabatic addition of Chern–Simons flux introduces Laughlin correlations without the necessity of introducing an irrelevant mean-field energy scale $\hbar\omega_c^* = \nu\hbar\omega_c$.

Jain’s sequence of filled CF shells does not require an interaction between CF quasiparticles. The incompressibility results from the energy required to create a QE–QH pair in the integrally filled CF state. Haldane’s hierarchy of IQL states was based on the implicit assumption that the residual interaction between QPs was sufficiently similar to the Coulomb interaction between electrons in LLO that the QPs would form their own Laughlin correlated daughter states.

The experiment of Pan et al. showed that neither Jain’s CF picture nor Haldane’s hierarchy was the whole story. Residual pair interactions between QPs had been determined (Sitko et al., 1996) up to an overall constant (unimportant for QP correlations). This pseudopotential $V_{\text{QP}}(L')$ could be used to determine the spectrum of daughter states containing N_{QP} quasiparticles in a partially filled QP shell. Qualitatively correct results can be expected when $V_{\text{QP}}(L')$ is small compared to the energy necessary to create a QE–QH pair in the IQL state. When the CF picture was reapplied to the QPs, the Haldane hierarchy of all odd denominator fractions resulted (Sitko et al., 1997). Numerical calculations demonstrates that this CF hierarchy scheme of Laughlin correlated QPs at each level didn’t always work, probably because $V_{\text{QP}}(L')$ was not sufficiently similar to $V_0(L')$, the pseudopotential for electrons in LLO.

The energy of a multiplet $|\ell^N; L\alpha\rangle$ formed from N electrons in a shell of angular momentum ℓ is given by Eq. (5). Wójs and Quinn proved a simple theorem, Eq. (10) that led to the conclusion that a pseudopotential of the form $V_H(\hat{L}') = A + B\hat{L}'^2$ (referred to as a “harmonic” pseudopotential) failed to lift the degeneracy of the multiplets α that had the same total angular momentum L . Correlations (removal of this degeneracy) were caused only by the anharmonic part of $V(L')$, i.e. by $\Delta V(L') = V(L') - V_H(L')$. For $\Delta V(L') = k\delta(\mathcal{R}, 1)$ ($\mathcal{R} = 2\ell - L'$ is referred to as the relative pair angular momentum), where $k > 0$, the lowest energy state for each value of L is the multiplet for which $P_{L\alpha}(\mathcal{R} = 1)$ is a minimum. Here $P_{L\alpha}(\mathcal{R} = 1)$ is the probability that $|\ell^N; L\alpha\rangle$ has pairs with pair angular momentum $L' = 2\ell - 1$. This is exactly the condition for Laughlin correlations at $\nu = (2\mathcal{R} + 1)^{-1} = 1/3$. If the anharmonic part of $V(L')$ is negative (i.e. $k < 0$), then the lowest energy for each angular momentum L occurs for the multiplet with $P_{L\alpha}(\mathcal{R} = 1)$ equal to a maximum, indicating a tendency to form pairs with $\mathcal{R} = 1$.

Because the pseudopotentials for electrons in LLO and LL1 are well-known, and for QEs and QHs of the Laughlin $\nu = 1/3$ (and other IQL states) can be evaluated, we can attempt to interpret the numerical diagonalization results in terms of simple intuitive pictures of the correlations expected from $V_0(\mathcal{R})$, $V_1(\mathcal{R})$, and $V_{\text{QP}}(\mathcal{R})$.

For LLO Laughlin correlations among the electrons are expected and found. For LL1, pairing correlations are found for $1/2 \geq \nu_1 > 1/3$, and Laughlin correlation are found $1/3 > \nu_1 \geq 1/5$ ($\nu_1 = \nu - 2$). The strongest IQL states are found at $\nu_1 = 1/2$, $1/3$, and their e – h conjugate states. Laughlin correlations with four Chern–Simons fluxes (CF^4) are expected for $1/3 \geq \nu_1 > 1/5$. The $N_p = N/2$ pairs are Laughlin correlated and give an IQL state at $2\ell = 2N + 1$ and its conjugate at $2\ell = 2N - 3$. The elementary excitations can also be interpreted in terms of a generalized CF picture described by Eqs. (22)

and (23). The $\nu_1 = 1/3$ state is found at $2\ell = 3N - 7$, not at $2\ell = 3N - 3$ of the Laughlin state in LL0. We do not completely understand correlations at $\nu_1 = 1/3$, but they could arise from triplets or from forming pairs of pairs.

We investigate the possibility of a spin phase transition in the $\nu = 4/11$ IQL state observed by Pan et al. The two spin states are daughter states of the Laughlin $\nu = 1/3$ IQL state, each of which has a QE filling factor $\nu_{\text{QE}} = 1/3$. For the fully spin polarized state, the QEs partially fill CFL1 and have the same spin as the filled CFL0 \uparrow . For the partially spin polarized state the quasiparticles are QERs, and they partially fill CFL0 \downarrow .

By numerical diagonalization of N electron systems with different values of the total electronic spin, we determine the QP energies ϵ_{QP} and their interactions $V_{\text{QP}}(\mathcal{R})$ (for QP = QE and QER) as a function of the width w of the quantum well. The total energy is the sum of the QP energies, their interaction energy, and the Zeeman energy. Wide wells weaken electron–electron interactions and favor partially spin polarized states. Large Zeeman energy favors fully spin polarized states. We sketch a phase diagram in the well width vs. Zeeman energy plane and show a rough estimate of the phase boundary between the two states.

Finally, a system containing electrons and valence band holes is studied. Neutral excitons $X = (eh)$, and charged excitonic complexes $X^- = e(eh)$, $X_2^- = e(eh)^2$, etc. are found and their angular momenta, binding energies and interactions with one another are evaluated. In dilute systems with $\nu \ll 1/3$, the singlet X_s^- and triplet X_t^- electron spin states are the ground states at low and high magnetic field respectively. The X_s^- ground state and an excited triplet state are shown to be the only strongly radiative states. The latter state is called the bright triplet X_{tb}^- , while the triplet ground state is called the dark triplet X_{td}^- .

For systems with filling factor ν close to an IQL value (e.g. $\nu \simeq 1/3$), the X^- becomes Laughlin correlated with the electrons and has effective charge $-e/3$, the same as that of Laughlin QEs. This QX^- can bind one or two Laughlin QHs to form a QX^0 or a QX^- . The spectra of these systems and their PL intensities can be evaluated numerically, and they agree quite well with the predictions of the CF picture.

The unified thread connecting the work included in this manuscript is the generalized CF picture. By knowing the behavior of the appropriate electron or QP pseudopotential, one can make an educated guess at the nature of the ground state correlations. Laughlin correlations in LL0 are the simplest type. Pairing or formation of larger clusters when $V(\mathcal{R})$ is subharmonic is more complicated. However, the generalized CF picture (built on the ideas of Laughlin, Haldane, Halperin and Jain) can be applied to pairs of electrons in LL1 or to pairs of QHs in CFL0 and pairs of QEs in CFL1. This simple model seems to give qualitatively correct results not just for when an IQL ground state occurs, but often for the spectrum of low energy excitations. We don't totally understand the correlations in every case (e.g. at $\nu = 7/3$ and at $\nu_{\text{QE}} = 1/3$ for spin polarized systems). However, we are certain that the full hierarchy of FQH states involves other types of correlations in addition to Laughlin. The nature of the correlations at each level of the hierarchy will depend on the appropriate pseudopotential, as will the path through the hierarchy levels that result.

Acknowledgments

The authors acknowledge the important contributions of Jennifer J. Quinn, Piotr Sitko, X. M. Chen, Daniel Wodzinski, Isabela Szlufarska, Anna Gładysiewicz and Pawel Hawrylak to parts of the work presented in this paper. JQ and GS acknowledge the partial support from Basic Science Program of DOE and KS from KRF-2006-005-J02804.

References

- Aharonov, Y., Bohm, D., 1959. Phys. Rev. 115 (3), 485.
- Apalkov, V.M., Rashba, E.I., 1992. Phys. Rev. B 46 (3), 1628.
- Apalkov, V.M., Rashba, E.I., 1993. Phys. Rev. B 48 (24), 18312.
- Balatsky, A., Fradkin, E., 1991. Phys. Rev. B 43 (13), 10622.
- Bardeen, J., Cooper, L.N., Schrieffer, J.R., 1957. Phys. Rev. 108 (5), 1175.
- Benjamin, A.T., Quinn, J.J., Quinn, J.J., Wójs, A., 2001. J. Combin. Theory, Series A 95 (2), 390.
- Béran, P., Morf, R., 1991. Phys. Rev. B 43 (15), 12654.
- Bloch, F., 1928. Z. Phys. 52, 555.
- Byszewski, M., Chwalisz, B., Maude, D.K., Sadowski, M.L., Potemski, M., Saku, T., Hirayama, Y., Studenikin, S., Austing, D.G., Sachrajda, A.S., Hawrylak, P., 2006. Nature (London) 2.
- Cage, M.E., 1987. Experimental aspects and metrological applications of the integer quantum hall effect. In: Prange, R.E., Girvin, S.M. (Eds.), The Quantum Hall Effect. In: Graduate Texts in Contemporary Physics, Springer-Verlag, New York, pp. 37–68 (Chapter 2).
- Cage, M.E., Dziuba, R.F., Field, B.F., 1985. IEEE Trans. Instrum. Meas. (ISSN: 0018-9456) 34 (2), 301.
- Chakraborty, T., Pietiläinen, P., Zhang, F.C., 1986. Phys. Rev. Lett. 57 (1), 130.
- Chang, A.M., Berglund, P., Tsui, D.C., Stormer, H.L., Hwang, J.C.M., 1984. Phys. Rev. Lett. 10, 997.
- Chang, C.-C., Jain, J.K., 2004. Phys. Rev. Lett. 92 (19), 196806.
- Chen, X.M., Quinn, J.J., 1993. Phys. Rev. B 47 (7), 3999.
- Chen, X.M., Quinn, J.J., 1994a. Solid State Commun. 92 (11), 865.
- Chen, X.M., Quinn, J.J., 1994b. Phys. Rev. B 50 (4), 2354.
- Choi, H.C., Kang, W., Das Sarma, S., Pfeiffer, L.N., West, K.W., 2008. Phys. Rev. B 77 (8), 081301(R).
- Cole, B.E., Chamberlain, J.M., Henini, M., Cheng, T., Batty, W., Wittlin, A., Perenboom, J.A.A.J., Ardavan, A., Polisski, A., Singleton, J., 1997. Phys. Rev. B 55 (4), 2503.
- Du, R.R., Stormer, H.L., Tsui, D.C., Pfeiffer, L.N., West, K.W., 1993. Phys. Rev. Lett. 70 (19), 2944.
- Dzyubenko, A.B., Lozovik, Y.E., 1983. Sov. Phys. - Solid State 25 (5), 874.
- Dzyubenko, A.B., Mandray, A., Huan, S., Sivachenko, A.Y., Etienne, B., 1994. Phys. Rev. B 50 (7), 4687.

- Dzyubenko, A.B., Sivachenko, A.Y., 1993. *Phys. Rev. B* 48 (19), 14690.
- Dzyubenko, A.B., Sivachenko, A.Y., 2000. *Phys. Rev. Lett.* 84 (19), 4429.
- Eisenstein, J.P., Cooper, K.B., Pfeiffer, L.N., West, K.W., 2002. *Phys. Rev. Lett.* 88 (7), 076801.
- Fano, G., Ortolani, F., Colombo, E., 1986. *Phys. Rev. B* 34 (4), 2670.
- Fertig, H.A., Brey, L., Côté, R., MacDonald, A.H., 1996. *Phys. Rev. Lett.* 77 (8), 1572.
- Fradkin, E., Schaposnik, F.A., 1991. *Phys. Rev. Lett.* 66 (3), 276.
- Gallais, Y., Kirschenmann, T.H., Dujovne, I., Hirjibehedin, C.F., Pinczuk, A., Dennis, B.S., Pfeiffer, L.N., West, K.W., 2006. *Phys. Rev. Lett.* 97 (3), 036804.
- Giuliani, G.F., Quinn, J.J., 1985. *Phys. Rev. B* 31 (6), 3451.
- Goerbig, M., Lederer, P., Smith, C.M., 2006. *Physica E* 34 (1–2).
- Goerbig, M.O., Lederer, P., Smith, C.M., 2004. *Phys. Rev. B* 69 (15), 155324.
- Goldberg, B.B., Heiman, D., Pinczuk, A., Pfeiffer, L., West, K., 1990. *Phys. Rev. Lett.* 65 (5), 641.
- Greiter, M., Wen, X.-G., Wilczek, F., 1991. *Phys. Rev. Lett.* 66 (24), 3205.
- Greiter, M., Wen, X.-G., Wilczek, F., 1992. *Nucl. Phys. B* 374 (3), 567.
- Haldane, F., 1987. In: Prange, R.E., Girvin, S.M. (Eds.), *The Quantum Hall Effect*. Springer-Verlag, New York, pp. 303–352 (Chapter 8).
- Haldane, F.D.M., 1983. *Phys. Rev. Lett.* 51 (7), 605.
- Haldane, F.D.M., Rezayi, E.H., 1985a. *Phys. Rev. Lett.* 54 (3), 237.
- Haldane, F.D.M., Rezayi, E.H., 1985b. *Phys. Rev. B* 31 (4), 2529.
- Halperin, B.I., 1983. *Helv. Phys. Acta* 56 (1–3), 75.
- Halperin, B.I., 1984. *Phys. Rev. Lett.* 52 (18), 1583.
- Halperin, B.I., Lee, P.A., Read, N., 1993. *Phys. Rev. B* 47 (12), 7312.
- Hayne, M., Jones, C.L., Bogaerts, R., Riva, C., Usher, A., Peeters, F.M., Herlach, F., Moshchalkov, V.V., Henini, M., 1999. *Phys. Rev. B* 59 (4), 2927.
- He, S., Zhang, F.C., Xie, X.C., Das Sarma, S., 1990. *Phys. Rev. B* 42 (17), 11376.
- Heiman, D., Goldberg, B.B., Pinczuk, A., Tu, C.W., Gossard, A.C., English, J.H., 1988. *Phys. Rev. Lett.* 61 (5), 605.
- Jain, J.K., 1989. *Phys. Rev. Lett.* 63 (2), 199.
- Jain, J.K., 1990. *Phys. Rev. B* 41 (11), 7653.
- Kallin, C., Halperin, B.I., 1984. *Phys. Rev. B* 30 (10), 5655.
- Kamilla, R.K., Wu, X.G., Jain, J.K., 1996. *Solid State Commun.* 99, 289.
- von Klitzing, K., 1986. *Rev. Mod. Phys.* 58 (3), 519.
- von Klitzing, K., Dorda, G., Pepper, M., 1980. *Phys. Rev. Lett.* 45 (6), 494.
- Kukushkin, I.V., Haug, R.J., von Klitzing, K., Ploog, K., 1994. *Phys. Rev. Lett.* 72 (5), 736.
- Landau, L.D., 1956. *Zh. Eksp. Teor. Fiz.* 30, 1058. (*Sov. Phys.-JETP* 3, 920 (1957)).
- Landau, L.D., 1957. *Zh. Eksp. Teor. Fiz.* 32, 59. (*Sov. Phys.-JETP* 5, 101 (1957)).
- Landau, L.D., Lifshitz, L.M., 1977. *Quantum Mechanics: Non-Relativistic Theory*, 3 ed. Elsevier Science, Oxford.
- Laughlin, R.B., 1983. *Phys. Rev. Lett.* 50 (18), 1395.
- Laughlin, R.B., 1984. *Surf. Sci.* 142 (1–3), 163.
- Laughlin, R.B., 1988. *Phys. Rev. Lett.* 61 (3), 379.
- Leadley, D.R., Nicholas, R.J., Maude, D.K., Utjuzh, A.N., Portal, J.C., Harris, J.J., Foxon, C.T., 1997. *Phys. Rev. Lett.* 79 (21), 4246.
- Lee, S.-Y., Scarola, V.W., Jain, J.K., 2001. *Phys. Rev. Lett.* 87 (25), 256803.
- Lee, S.-Y., Scarola, V.W., Jain, J.K., 2002. *Phys. Rev. B* 66 (8), 085336.
- Leinaas, J.M., Myrheim, J., 1977. *Nuovo Cimento* B37, 1.
- Lerner, I.V., Lozovik, Y.E., 1981. *Sov. Phys. - JETP* 53 (4), 763.
- Lopez, A., Fradkin, E., 1991. *Phys. Rev. B* 44 (10), 5246.
- Lopez, A., Fradkin, E., 1992. *Phys. Rev. Lett.* 69 (14), 2126.
- Lopez, A., Fradkin, E., 1993. *Phys. Rev. B* 47 (12), 7080.
- Lopez, A., Fradkin, E., 1995. *Phys. Rev. B* 51 (7), 4347.
- López, A., Fradkin, E., 2004. *Phys. Rev. B* 69 (15), 155322.
- MacDonald, A.H., Palacios, J.J., 1998. *Phys. Rev. B* 58 (16), R10171.
- MacDonald, A.H., Rezayi, E.H., 1990. *Phys. Rev. B* 42 (5), 3224.
- MacDonald, A.H., Rezayi, E.H., Keller, D., 1992. *Phys. Rev. Lett.* 68 (12), 1939.
- Mancoff, F.B., Zielinski, L.J., Marcus, C.M., Campman, K., Gossard, A.C., 1996. *Phys. Rev. B* 53 (12), R7599.
- Mandal, S.S., Jain, J.K., 2002. *Phys. Rev. B* 66 (15), 155302.
- Moore, G., Read, N., 1991. *Nucl. Phys. B* 360 (2–3), 362.
- Morf, R., d'Ambrumenil, N., 1995. *Phys. Rev. Lett.* 74 (25), 5116.
- Morf, R.H., 1998. *Phys. Rev. Lett.* 80 (7), 1505.
- Morf, R.H., d'Ambrumenil, N., Das Sarma, S., 2002. *Phys. Rev. B* 66 (7), 075408.
- Murthy, G., Shankar, R., 1999. *Phys. Rev. B* 59 (19), 12260.
- Murthy, G., Shankar, R., 2002. *Phys. Rev. B* 65 (24), 245309.
- Murthy, G., Shankar, R., 2003. *Rev. Mod. Phys.* 75 (4), 1101.
- Pan, W., Stormer, H.L., Tsui, D.C., Pfeiffer, L.N., Baldwin, K.W., West, K.W., 2003. *Phys. Rev. Lett.* 90 (1), 016801.
- Pan, W., Xia, J.-S., Shvarts, V., Adams, D.E., Stormer, H.L., Tsui, D.C., Pfeiffer, L.N., Baldwin, K.W., West, K.W., 1999. *Phys. Rev. Lett.* 83 (17), 3530.
- Paquet, D., Rice, T.M., Ueda, K., 1985. *Phys. Rev. B* 32 (8), 5208.
- Parfitt, D.G.W., Portnoi, M.E., 2003. *Phys. Rev. B* 68 (3), 035306.
- Park, K., Jain, J.K., 2000. *Phys. Rev. B* 62 (20), R13274.
- Pauli, W., 1925. *Z. Phys.* 31, 765.
- Peterson, M.R., Das Sarma, S., 2008. [arXiv:0801.4819v1](https://arxiv.org/abs/0801.4819v1).
- Pinczuk, A., Dennis, B.S., Pfeiffer, L.N., West, K., 1993. *Phys. Rev. Lett.* 70 (25), 3983.
- Portnoi, M.E., Rashba, E.I., 1996. *Phys. Rev. B* 54 (19), 13791.
- Quinn, J.J., Quinn, J.J., 2003. *Phys. Rev. B* 68 (15), 153310.
- Quinn, J.J., Quinn, J.J., 2006. *Solid State Commun.* 140 (2), 52.
- Quinn, J.J., Wójs, A., 2000a. *J. Phys.: Condens. Matter* 12, R265.
- Quinn, J.J., Wójs, A., 2000b. *Physica E* 6 (1–4), 1.
- Quinn, J.J., Wójs, A., Quinn, J.J., 2001a. *Physica E* 9 (4), 701.
- Quinn, J.J., Wójs, A., Yi, K.-S., 2003a. *Recent Res. Devel. Physics* 4, 749.
- Quinn, J.J., Wójs, A., Yi, K.-S., 2003b. *Phys. Lett. A* 318 (1–2), 152.
- Quinn, J.J., Wójs, A., Yi, K.-S., 2004a. *J. Korean Phys. Soc.* 45, S491.
- Quinn, J.J., Wójs, A., Yi, K.-S., Quinn, J.J., 2004b. *The Electron Liquid Paradigm in Condensed Matter Physics*. IOS Press, Amsterdam, pp. 469–497.
- Quinn, J.J., Wójs, A., Yi, K.-S., Szlufarska, I., 2001b. *Physica E* 11 (2–3), 209.
- Rashba, E.I., Portnoi, M.E., 1993. *Phys. Rev. Lett.* 70 (21), 3315.
- Read, N., Rezayi, E., 1999. *Phys. Rev. B* 59 (12), 8084.
- Rezayi, E.H., 1987. *Phys. Rev. B* 35 (6), 3032.
- Rezayi, E.H., 1991. *Phys. Rev. B* 43 (7), 5944.

- Rezayi, E.H., Haldane, F.D.M., 2000. *Phys. Rev. Lett.* 84 (20), 4685.
- Riva, C., Peeters, F.M., Varga, K., 2001. *Phys. Rev. B* 63 (11), 115302.
- Schüller, C., Broocks, K.-B., Heyn, C., Heitmann, D., 2002. *Phys. Rev. B* 65 (8), 081301(R).
- Schüller, C., Broocks, K.-B., Schröter, P., Heyn, C., Heitmann, D., Bichler, M., Wegscheider, W., Chakraborty, T., Apalkov, V.M., 2003. *Phys. Rev. Lett.* 91 (11), 116403.
- de Shalit, A., Talmi, I., 1963. *Nuclear Shell Theory*. Academic Press, New York.
- Shankar, R., Murthy, G., 1997. *Phys. Rev. Lett.* 79 (22), 4437.
- Silin, V.P., 1957. *Zh. Eksp. Teor. Fiz.* 33, 495. (*Sov. Phys.-JETP* 6, 387 (1958)).
- Simion, G.E., Quinn, J.J., 2008. *Physica E* 41 (1), 1.
- Simon, S.H., Halperin, B.I., 1993. *Phys. Rev. B* 48 (23), 17368.
- Simon, S.H., Rezayi, E.H., Cooper, N.R., 2007. *Phys. Rev. B* 75 (7), 075318.
- Sitko, P., Yi, K.-S., Quinn, J.J., 1997. *Phys. Rev. B* 56 (19), 12417.
- Sitko, P., Yi, S.N., Yi, K.S., Quinn, J.J., 1996. *Phys. Rev. Lett.* 76 (18), 3396.
- Smet, J.H., 2003. *Nature* 422, 391.
- Sommerfeld, A., 1928. *Z. Phys.* 47 (1).
- Sondhi, S.L., Karlhede, A., Kivelson, S.A., Rezayi, E.H., 1993. *Phys. Rev. B* 47 (24), 16419.
- Stebe, B., Ainane, A., 1989. *Superlatt. Microstruct.* 5 (4), 545.
- Szlufarska, I., Wójs, A., Quinn, J.J., 2001. *Phys. Rev. B* 64 (16), 165318.
- Tan, I.-H., Snider, G.L., Chang, L.D., Hu, E.L., 1990. *J. Appl. Phys.* 68 (8), 4071.
- Töke, C., Jain, J.K., 2006. *Phys. Rev. Lett.* 96 (24), 246805.
- Töke, C., Regnault, N., Jain, J.K., 2007. *Phys. Rev. Lett.* 98 (3), 036806.
- Tsui, D.C., Stormer, H.L., Gossard, A.C., 1982. *Phys. Rev. Lett.* 48 (22), 1559.
- Whittaker, D.M., Shields, A.J., 1997. *Phys. Rev. B* 56 (23), 15185.
- Wigner, E., Seitz, F., 1933. *Solid State : Adv. Res. Appl.* 1, 97.
- Wilczek, F., 1982a. *Phys. Rev. Lett.* 48 (17), 1144.
- Wilczek, F., 1982b. *Phys. Rev. Lett.* 49 (14), 957.
- Wilczek, F., 1990. *Fractional Statistics and Anyon Superconductivity*. World Scientific, Singapore.
- Willett, R., Eisenstein, J.P., Störmer, H.L., Tsui, D.C., Gossard, A.C., English, J.H., 1987. *Phys. Rev. Lett.* 59 (15), 1776.
- Wilson, A., 1931. *Proc. R. Soc. London A* 133, 458.
- Wójs, A., 2001a. *Phys. Rev. B* 63 (12), 125312.
- Wójs, A., 2001b. *Phys. Rev. B* 63 (23), 235322.
- Wójs, A., Gladysiewicz, A., Quinn, J.J., 2006a. *Phys. Rev. B* 73 (23), 235338.
- Wójs, A., Hawrylak, P., Quinn, J.J., 1999a. *Phys. Rev. B* 60 (16), 11661.
- Wójs, A., Hawrylak, P., Quinn, J.J., 2000a. *Physica E* 8 (3), 254.
- Wójs, A., Quinn, J.J., 1998a. *Physica E* 3 (4), 181.
- Wójs, A., Quinn, J.J., 1998b. *Solid State Commun.* 108 (7), 493.
- Wójs, A., Quinn, J.J., 1999. *Solid State Commun.* 110 (1), 45.
- Wójs, A., Quinn, J.J., 2000a. *Philos. Mag.* B 80, 1405.
- Wójs, A., Quinn, J.J., 2000b. *Phys. Rev. B* 63 (4), 045303.
- Wójs, A., Quinn, J.J., 2000c. *Phys. Rev. B* 63 (4), 045304.
- Wójs, A., Quinn, J.J., 2000d. *Phys. Rev. B* 61 (4), 2846.
- Wójs, A., Quinn, J.J., 2002a. *Physica E* 12 (1–4), 63.
- Wójs, A., Quinn, J.J., 2002b. *Solid State Commun.* 122 (7–8), 407.
- Wójs, A., Quinn, J.J., 2002c. *Phys. Rev. B* 66 (4), 045323.
- Wójs, A., Quinn, J.J., 2002d. *Phys. Rev. B* 65 (20), 201301(R).
- Wójs, A., Quinn, J.J., 2005. *Phys. Rev. B* 71 (4), 045324.
- Wójs, A., Quinn, J.J., 2006. *Phys. Rev. B* 74 (23), 235319.
- Wójs, A., Quinn, J.J., 2007. *Phys. Rev. B* 75 (8), 085318.
- Wójs, A., Quinn, J.J., Hawrylak, P., 2000b. *Phys. Rev. B* 62 (7), 4630.
- Wójs, A., Simion, G., Quinn, J.J., 2007. *Phys. Rev. B* 75 (15), 155318.
- Wójs, A., Szlufarska, I., Yi, K.-S., Quinn, J.J., 1999b. *Phys. Rev. B* 60 (16), R11273.
- Wójs, A., Wodziński, D., Quinn, J.J., 2005. *Phys. Rev. B* 71 (24), 245331.
- Wójs, A., Wodziński, D., Quinn, J.J., 2006b. *Phys. Rev. B* 74 (3), 035315.
- Wójs, A., Yi, K.-S., Quinn, J.J., 2003. *Acta Phys. Pol. A* 103, 517.
- Wójs, A., Yi, K.-S., Quinn, J.J., 2004. *Phys. Rev. B* 69 (20), 205322.
- Wu, T.T., Yang, C.N., 1976. *Nucl. Phys. B* 107 (3), 365.
- Wu, T.T., Yang, C.N., 1977. *Phys. Rev. D* 16 (4), 1018.
- Wu, X.G., Jain, J.K., 1994. *Phys. Rev. B* 49 (11), 7515.
- Xia, J.S., Pan, W., Vincente, C.L., Adams, E.D., Sullivan, N.S., Stormer, H.L., Tsui, D.C., Pfeiffer, L.N., Baldwin, K.W., West, K.W., 2004. *Phys. Rev. Lett.* 93 (17), 176809.
- Xie, X.C., Das Sarma, S., He, S., 1993. *Phys. Rev. B* 47 (23), 15942.
- Xie, X.C., He, S., Das Sarma, S., 1991. *Phys. Rev. Lett.* 66 (3), 389.
- Yi, K., Quinn, J.J., 1997. *Solid State Commun.* 102 (11), 775.
- Yi, K.S., Sitko, P., Khurana, A., Quinn, J.J., 1996. *Phys. Rev. B* 54 (23), 16432.
- Yusa, G., Shtrikman, H., Bar-Joseph, I., 2001. *Phys. Rev. Lett.* 87 (21), 216402.
- Zang, J., Birman, J.L., 1995. *Phys. Rev. B* 51 (8), 5574.